

POSSIBILITIES AND LIMITATIONS

OF

ROTARY DRILLING IN HARD ROCK

Thesis presented for

the Degree of

Doctor of Philosophy

by

C. FAIRHURST, B.ENG. (Hons.)

Department of Mining,

University of Sheffield.

MAY, 1955.

AD MAJOREM DEI GLORIA

LIST OF CONTENTS.

	<u>Page</u>
SECTION I - <u>Introduction.</u>	
Investigations and results obtained by previous workers.	2
Drillability.	6
Methods of Reducing Resistance to Penetration	
1. Chemical Softeners.	9
2. Rotary Percussive Drilling.	10
Increase of Mechanical Strength of Bits.	11
Theories of the rock cutting action in rotary drilling.	12
Merchants Analysis of Metal Cutting.	16
Orthogonal Cutting.	16
Relationship between Shear Angle & Rake Angle.	18
The Particular Case of Discontinuous Cutting.	19
Oblique Cutting.	20
Application of Shear Theory to Rock Cutting.	22
SECTION II - <u>Planing Tests.</u>	23
Initial Experiments.	24
Initial Milling Machine Experiments.	25
Investigations using Cine-Camera and Tool Dynamometer.	28
Single Camera Arrangement.	29
Two-Camera Arrangement.	30
Investigation of Rock Cutting Action.	32
Analysis of Major Fractures	34
Basic Mechanism of Rock Cutting Action.	36
Effect of Abrasive Wear.	38
Effect of Rake Angle.	38
Summary of Rock Cutting Theory.	38
Practical Implications of Cutting Theory.	39
Investigation of Effect of Variation in Conditions of Cutting.	40
Variation in Rake Angle.	41
" " Depth of Cut	41
Width	42
Number of Free Faces	42
Angle of Obliquity	43
Wear	44
Speed of Cutting	45
General Conclusions.	45
SECTION III - <u>Rock Drilling Tests.</u>	47
Apparatus.	47
Torque and Rotary Speed Determinations.	48

	<u>Page</u>
Brake Characteristics of $1\frac{1}{2}$ H.P. Drill Motor.	48
Brake Characteristics of 5 H.P. Motor.	50
Test Procedure.	50
Results.	51
Comparison of Performance of Standard Concentric and Eccentric Bits.	52
Spearhead Bits.	54
Oblique Bits.	55
Carbide Failure in Rotary Drilling.	56
Method of Attachment of Bit to Rod.	57
Modified Bit Designs	58
Choice of Carbide Grade.	60
Conclusions.	60
Notes on Tests II.	61
Analysis and Examination of Rock Cuttings.	62
Determination of Instantaneous Torsional Fluctuation during Rock Drilling.	64
Arrangement of Strain Gauges.	64
Static Calibration of Gauges.	66
Results of Strain Gauge Tests.	67
1. Magnitude of Force Oscillation.	67
2. Frequency of Impact.	67
Conclusions.	68
Tests to Determine Principal Sources of Pressure Loss in Flush Water Supply Circuit.	69
Conclusions.	71
SECTION IV - (Summary of Main Conclusions.	72
{ Brief Suggestions for Further Research.	75
{ Acknowledgements.	77

SECTION V. TABLES OF RESULTS.

Table 1.	Analysis of Major Fractures.
Table 2.	Effect of Variation in Rake Angle.
Table 3.	" " " " Depth of Cut.
Table 4.	" " " " Width of Cut.
Table 5.	" " " " Number of Free Faces.
Table 6.	" " " " Obliquity Angle.
Table 7.	" " " " Speed of Cutting.
Table 8.	" " " " State of Wear.
Table 9.	Brake Characteristics of $1\frac{1}{2}$ H.P. Drill Motor
Table 10.	" " " 5 H.P. " "
Table 11.	Results of Drilling Tests (included in Section III)
Table 12.	Sieve Analysis of Cuttings' Samples.
Table 13.	Flush Water Flow Test Results.
Table 14.	Rocks Used in Planing Tests.

SECTION VI. APPENDICES.

Appendix 1.	Definition of Terms Used in Rotary Drillings
2.	Eccentric Bit Cutting Action.
3.	Theory of Oblique Cutting in Rotary Drilling.
4.	Effect of Variation of Point Angle on Effective Wedge Angle.
5.	Deflection and Stresses of Bit Leg under Load.
6.	Determination of Ideal Profile for Cutting Edge of Rotary Bit.

Brief Summaries of Papers Mentioned in Thesis.

Appendix 7.	Basic Mechanics of Metal Cutting Process, M.E. Merchant.
8.	Mechanics of Three-Dimensional Cutting Operation. Shaw, Cook, Smith.
9.	Shear Angle Relationship in Metal Cutting. Shaw, Cook, Finnie.
10.	Derivation of Besisk & Kuhne Formula.

List of References.

LIST OF ILLUSTRATIONS.

- Fig. 1.) Characteristic Curves of Rotary Drilling.
2.)
3. Besigk and Kuhne Penetration Theories.
 4. To Illustrate Coeuillets Assumptions.
 5. Merchants force analysis.
 6. Shear Fractures in Discontinuous Cutting.
 7. Stabler's observation on Chip Flow.
 8. Initial Planing Apparatus.
 9. Early Milling Machine Apparatus.
 10. Tool Dyanamometer.
 11. Rock Planing Apparatus with Cine-Cameras.
 12. Microscope-Camera Assembly.
 13. Rock Cutting Action of + 20° Rake Tool.
 14. " " " " 0° " "
 15. " " " " - 20° " "
 16. Typical Major Fractures.
 17. Merchants force diagram.
 18. Photoelastic stress patterns.
 19. Forces at point of Tool Tip.
 20. Effect of Variation in Rake Angle.
 21. " " " " Depth.
 22. " " " " "
 23. " " " " Width.
 24. To illustrate Free Faces, Obliquity.
 25. Effect of Variation in No. of Free Faces.
 26. " " " " Obliquity.
 27. Wear Measuring Set Up.
 28. Effect of Wear.
 29. Drilling Control Panel.
 30. Characteristics of 1½ H.P. Motor.
 31. Full Scale Drilling Rig.
 32. Eccentric & Concentric Bits.
 33. Cutting Action of Eccentric & Rotary Bits.
 34. Bit Types used in Tests.
 35. Oblique Bits.
 36. Modified Bits.

LIST OF ILLUSTRATIONS, Cont'd

- Fig. 37. Typical Rock Cutting Sample.
38. Large Cuttings.
39. Strain Gauge Layout.
40. Slip Ring Assembly.
41. Strain-Gauge-Oscilloscope Set Up.
42. " " " " "
43. Oscilloscope Camera Combination.
44. Typical Traces.
45. Modified Wet Drilling Attachment.
46. Pressure Losses in Water Flow Systems.

SECTION 1.

INTRODUCTION

A critical account of previous research and existing views held in relation to those aspects of the rotary drilling problem relevant to the research carried out by the writer.

INTRODUCTION

Rock drilling forms an important part of operations in many fields of engineering and may be a major item in the capital cost of any enterprise. In mining, increased mechanisation, large reorganisation schemes, and the adoption of the horizon system, have resulted in an enormous increase in the amount of drilling taking place. It soon becomes apparent that drilling speeds would have to be speeded up considerably if the desired rates of tunnel drivage and reorganisation were to be attained. This led to the development of interest in the adoption of rotary drilling, already successful in coal and soft rocks, to replace percussive drilling in even harder rock. The rotary technique had long been recognised to be inherently capable of higher drilling rates together with several other important advantages, viz.

1. Electrical power may be used instead of the highly inefficient compressed-air systems.
2. Concentrations of small dust sizes is much lower, thus reducing the health hazard.
3. Less noise is produced.

Balanced against this however were two main disadvantages:-

1. The applied thrusts required are considerably higher, necessitating power-feeds and rig-mounted machines.
2. The continuous rotation of the bit in contact with the rock results in rapid wear and consequent rapid fall in drilling rate.

Of these, the second disadvantage was the more serious until the introduction of rotary bits tipped with a highly wear resistant alloy metal, tungsten carbide. This has resulted in the successful application of rotary drilling to all but the hardest and most abrasive of rocks. Drill-rigs have been designed capable of supporting high-powered

drilling machines and of exerting thrusts often of several thousands of pounds.

1

Inett has quoted figures for a hard sandstone which illustrate the improvements obtained:-

Depth of hole: - $6\frac{1}{2}$ feet

Method of Drilling	Drilling Speed in hole	Overall time/hole (Including withdrawal and changing from hole to hole).
Percussive	6"/min	20 mins.
Rotary	19"/min	8 mins. *

* includes 3 mins. changing bit after each hole.

Successful application to rocks of medium hardness and abrasiveness naturally encouraged the application of rotary drilling to still more difficult propositions, but it was quickly realised that existing equipment was unsuitable. The incidence of bit failures increased sharply and wear again became excessive. Thus it was that the research project suggested to the writer was:-

"An investigation into the possibilities and limitations of rotary drilling in hard and abrasive rocks, using high axial thrusts and low rotary speeds".

Investigations and results obtained by previous research workers.

Academic research into the factors governing the successful application of rotary drilling has unfortunately been limited, and it soon becomes apparent when commencing investigations that the process is controlled by a large number of variables, the individual effect of each often being unknown. The writer was somewhat dismayed when first introduced to the problem to discover an amazing lack of knowledge of the fundamental nature of the operative rock breakdown process. Investigation of fundamentals, it is thought, is essential to the correct interpretation of drilling test results and to allow reliable predictions to

be made.

It is indeed fortunate that the problem of rotary drilling is important at a time when a similar problem is engaging the attention of scientists and engineers in the field of metal cutting, and the results of research into the metal machining problem will be shown to be of great value towards an understanding of rock breakdown. It is nevertheless necessary to study the particular problem in rock experimentally since there are many differences, if not in principle, at least in degree. Equipped with this fundamental knowledge it is possible to review the information already available and thus substantiate conclusions already arrived at, explain and harmonise results previously thought to be contradictory, and, it is hoped, obtain a much more accurate picture of the rotary drilling process.

Early research quickly established that the principle employed in rotary drilling differed from that in percussive drilling, the former depending for efficient penetration upon a steadily applied axial force combined with a rotary torque, whereas the latter is characterised by rapid direct impact blows driving the bit into the rock. Consequently rotary drills require much heavier thrusts than the percussive type. The combined action of the thrust force and torque cause the bit to penetrate into the rock along a helical path, removing a flake of rock ahead of it equal in thickness to the depth of penetration per revolution.

The two main characteristic curves, i.e.

(a) Drilling Rate - Axial Thrust curve.

(b) Drilling Rate - R.P.M.

were established, from which several interesting points emerge:-

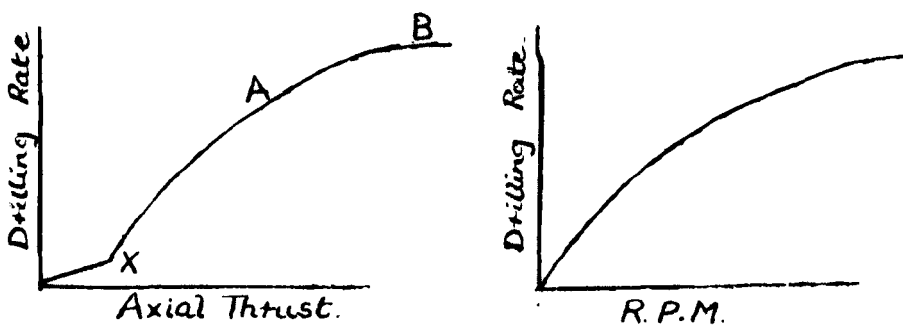


Fig.1. Characteristic curves of Rotary Drilling.

(i) The drilling rate/thrust curve shows a distinct gradient change at X. This is well recognised by most workers and has been termed the Critical Drilling Point. It marks the point at which the applied thrust is sufficient to overcome the elasticity of the rock, penetration commences, and grinding ends. From X - A the increase is almost uniform and beyond A the gradient begins to fall until it becomes almost horizontal. Beyond this point the drill motor stalls.

(ii) The drilling rate/R.P.M. curve shows a somewhat similar characteristic form except that there is no initial critical point.

These curves suggest that there is a limit both in thrust and R.P.M., probably different for various rocks, beyond which no appreciable increase in drilling rate is obtained; and various views have been put forward to explain them.

Alpan ² has termed point B in Fig.(a) "the maximum efficiency point", (mainly because the drilling rate is highest) beyond which stalling of the electric motor occurs.

Inett ¹ also regards the region A - B to mark the onset of stalling. Shepherd's ³ tests have not confirmed the "stalling region" and he considers the relationship between drilling rate and thrust to be linear beyond X.

Others have attributed the fall from A to the onset of "binding" of the cuttings at high penetration rates. Alpan makes several interesting observations relating to the

"maximum efficiency point". He states

- (a) that "the harder the bit tips, the lower the thrust required for the maximum efficiency point". Here hardness presumably indicates wear resistance.
- (b) Eccentric-type bits reach the maximum efficiency point at lower thrusts than concentric bits of the same hardness.

It is interesting to note that the 'harder' the tip the less will be the rate of wear, in which case the 'bit-rock' contact pressure for a given thrust will be higher. This is also the case for the second observation, i.e. the contact pressure will be higher when using the eccentric bit at a given thrust. Since it is the contact pressure which determines the depth of cut per revolution (and hence the drilling rate) it seems to indicate that the so called "maximum efficiency point" in a given rock is dependent more on the drilling rate than on the actual thrust. A third observation made by the same worker is that "the maximum efficiency point" is reached at a lower value of thrust when using a high rotational speed than when using a low one.

These indications that the peak of the curve is dependent on the depth of cut and the rotational speed, confirm the view held by the writer, and developed later in this thesis, that the fall in rate of increase of drilling rate is due mainly to the increased severity of impact at high rotational speeds and high flake thickness/revolution.

Thus it can be seen that there does appear to be a limit both with thrust and rotary speed beyond which no further benefit may be obtained. The writer believes it is possible to raise these limits somewhat by methods described later but, in practice, other limits may be imposed. The most frequent of these is failure of the rock drilling equipment due to inadequate mechanical strength. The problem then is how to overcome the two limits:-

1. Resistance of the rock to penetration.
2. Mechanical strength of the rock drilling equipment.

This classification suggests two broad lines along which the investigations may proceed.

- (i) Reduction of the rock resistance to penetration i.e. determining ways in which the necessary applied forces may be reduced.
- (ii) Increased mechanical strength, i.e. study of design features, with a view to strengthening the bit wherever possible, or reducing the stresses on vulnerable parts of the system.

It is first essential to determine what ~~physical~~ properties of the rock influence its resistance to penetration or, as it has been called, its Drillability; and, further, to obtain some understanding of the ways in which failure occurs and the nature of the stresses causing failure. This again emphasises the necessity to study the fundamental nature of the drilling process.

Drillability.

Considerable attention has been paid to the assessment of those ~~physical~~ properties of rock which determine its resistance to penetration.

Shepherd ³ has presented a comprehensive survey of methods used by various authorities and, from tests conducted with a Shore Scleroscope, produced "work hardening" values for various rocks. The value is a measure of the percentage increase in Shore number after a series of readings taken on the same part of the rock. He has observed that the height of rebound, ^{or} "Shore Number", of the small impacting weight increases from an initial value with repeated drops to a maximum value beyond which it remains constant. This is considered a measure of the degree of compaction of the rock grains under impact, which, it is claimed, is a more reliable indication of the resistance to drilling than the initial Shore value. The shear and

tensile strengths of the rock will undoubtedly be affected by the percentage of voids between the grains and thus the foregoing method would appear to measure a factor of importance. A second factor, the Abrasion Coefficient, is measured by rotating a brass bar of a given diameter under a fixed load on a flat surface of the rock for a known time. The loss in weight of the brass bar per unit time gives the Abrasion Factor $\times 10^{-3}$. The final drillability index is then obtained by subtracting the Abrasion Factor from the Work Hardening Factor. This method of summation appears arbitrary and assumes that both factors are equal in importance.

Bergrad and Sievers ⁴ have developed a formula by which they claim to be able to predict the drilling rate in any rock. The formula involves the use of two known constants for the rock, termed "C" and "J" factors. "C" is the wear constant, measured by the loss in weight of metal pins rotating on a test fork on the rock under a known contact pressure. "J" is the "drilling constant" and is determined by rotating an octagonal spear-point bit on the rock under a known load and measuring the penetration after one minute. The use of an actual drilling test seems to be the most reliable indication of drilling resistance, but it is unfortunate that Sievers has used (a) the spear-point bit, (b) a contact pressure generally below the critical pressure, since the bit is then not cutting as in practice, but grinding. If the ~~bit~~^{test} was designed such that no grinding occurred (as it must at the centre of a spear-point bit) it would appear that tests similar to those described by Sievers will give a reliable indication of Drillability. Besigt and Kühne ⁵ have incorporated the results obtained from the "penetration" of a small diameter, loaded pin into the polished surface of a rock specimen into a general formula for drilling, the derivation of which is shown in ~~the~~ Appendix. (D).

$$S = 0.0157 \frac{n}{b} (D + D_k) \log A_1 \frac{Q}{K_k F}$$

where S = Drilling rate (in cm/min)

n = R.P.M. of bit

b = Effective thickness of hardmetal insert.

D = bit diameter (in cm)

D_k = core diameter (in cm)

$\log A_1$ = Experimentally determined constant 100
for tungsten carbide tipped
bits.

Q = Drilling Thrust (in Kg)

K_k = Critical drilling pressure (kg / cm²) *

F = Area of contact between effective hardmetal
layer and face of bore-hole (in cm²).

* K_k is determined from a value obtained by tests
using a loaded pin on a smooth specimen of the rock.

This formula also contains values obtained by measuring properties not considered by the writer to be ~~involved~~ ~~important~~ in rotary drilling and hence the formula must be invalid. The stress system set up when a rock specimen is loaded over a small area in the manner described is totally different from that set up in rotary drilling. In the former the rock immediately beneath the loaded pin is in a state of almost hydrostatic stress and penetration may only be effected by compaction of the rock grains, whereas in actual drilling the rock is free to shear off to a free surface (see next section).

A further error in the formula is that the thickness of carbide insert is assumed to have a marked effect on the drilling rate. The thrust force is considered to be distributed all across the under face of the insert which is incorrect, and, in fact, generally impossible since the cutting path varies in inclination for each element of cutting edge whereas generally the bit clearance angle is constant.

Fettweis has re-presented some of the conclusions of Besigk and Kühne which are equally invalid.

Shore hardness determinations appear to be

favoured by Continental authorities, sometimes combined with values for "Toughness", which has been defined ³ as "the ability of the rock to resist rupture by the tearing apart of its minerals or parts of the same mineral". Another definition given ³ is "the ability of the rock to withstand the shock of an applied force or thrust". Toughness thus appears to be similar to impact strength and is, in fact, measured by the number of drops of a small hammer from a fixed height which the rock can sustain before fracture.

Alpan ² states that "each rock has characteristic properties of hardness, toughness, abrasion and texture, each of which affects the penetration speed", but does not in his paper indicate the manner or degree of the effect.

Most of the above tests appear to be very empirical and do not even simulate the actual conditions of drilling. The Shore Scleroscope appears to be favoured by many although Shepherd ³ states that alone the Shore number is not a reliable indication of drillability. This confirms the writer's opinion that such tests do not appear to measure ~~physical~~ properties of the rock important in rotary drilling, and it would appear that in addition to the wear constant, some more fundamental physical constants such as Youngs Modulus of Elasticity may be a more reliable indication. Further observations are included in Section II of this thesis.

Methods of reducing resistance to penetration.

1. Chemical Softeners.

Work has recently been published ^{6,7} on the use of chemical "softening" agents as a means of reducing the rock drilling resistance. Small concentrations of chemical compounds, so far mainly metallic chlorides, have been used in the flush water during drilling. Increased drilling rates, sometimes as much as 100% higher, have been obtained without increased thrust or rotational speed. The effect

is not fully understood although Reh binder⁶ and his colleagues consider that the solution penetrates into the many inherent and induced micro-cracks in the rock reducing the surface attraction across the cracks and hence effectively reducing the rock strength. The action is complex and has received little attention except by the above mentioned authors. It appears that considerable improvements in drilling rates, of the order of 50% - 100%⁷ may be obtained in certain rocks tested, although the concentration of softening agent is extremely critical.

2. Rotary-percussive drilling.

Rotary-percussive drilling is a new technique of drilling in which the rotary and percussive operations occur together. Whilst it is not strictly accurate to say that the rock's drilling resistance is reduced, since the actual power of the drills is increased, to obtain the higher drilling rates, the rock is actually weakened in relation to its "rotary drilling resistance". This is accomplished by subjecting the rock to rapid, severe, impact blows whilst rotation is taking place. Proctor¹⁹ has demonstrated that such percussive blows on rock result in pulverisation for a considerable depth below the rock surface (up to six times the depth of imprint in a hard limestone), and it is to be expected that crack systems are further developed around this zone and the point of impact. This results in the rock being effectively weakened so that, as Inett¹ states "the combined rotary and percussive machine can reach, at medium thrusts, drilling speeds equal to those produced by rotary methods at high thrusts". Figures quoted show that wear is reduced and overall drilling speeds are higher than for pure rotary drilling. Comparative figures taken from the same information as the earlier table show:-

Depth of holes:- $6\frac{1}{2}$ ft.

Method of Drilling	Drilling Speed in the Hole	Overall time/hole (including changing from hole to hole, etc.)
Rotary	19" /min	3 mins.
Rotary-Percussive	40-60" /min	4 mins.

The rotary-percussive technique is still undergoing development but appears to have considerable possibilities.

The above two techniques seem to be those most worthy of note in relation to reducing rock resistance.

3. Increased Mechanical Strength.

The second aspect of the general problem, namely attention to strength considerations, is perhaps the more important inasmuch as it is always advisable to ensure that the system is as mechanically robust as possible commensurate with high drilling rates, independent of whether the rock is difficult to drill or not. Most failures have been located at the bit, undoubtedly the weak link at the present stage of development of drilling equipment. Before the causes of failure could be diagnosed it was first essential to understand the manner in which stresses were imposed on the bit and further, to determine the magnitude of such stresses. This necessitated a detailed investigation of the nature of the cutting action, an account of which forms an important part of the next section of this thesis. Other workers had attempted to describe the cutting action although it appears no detailed experimental observations had been made.

Theories advanced relating to the nature of the rock cutting action in rotary drilling.

Besigk and Kühne consider that the bit penetrates into the rock by the application of axial thrust which overcomes the resistance of the rock, the depth of penetration being dependent on the magnitude and time of

application (as determined by the speed of rotation) of the thrust, the torque supplied by the drill motor serving to break off the rock to the free surface. The bit is thus said to penetrate by a series of 'steps' or 'jumps', (see Fig.3) the width of the steps being dependent on the thickness of the carbide insert.

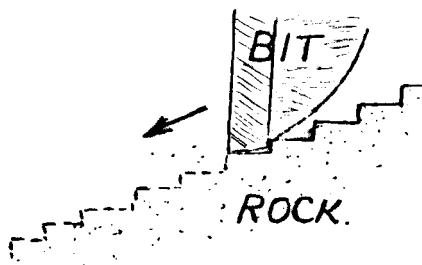


Fig.3 (a) Besigk & Kühne idea of penetration.

If it is admitted that this does happen it is then possible to explain the influence of thrust and rotational speed. From the "load penetration" curves (Fig. 3(b)), obtained by applying loads to a small circular hardmetal pin resting on a flat polished surface of rock, it can be seen that the penetration does not increase uniformly with depth

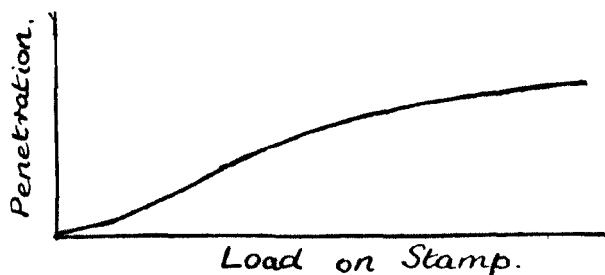


Fig. 3(b) Load - Penetration curve obtained by Besigk & Kühne.

but has a similar characteristic form as the thrust/drilling rate curve (Fig.1(a)). It is also well known that the time of application is important when determining the resistance of a material to applied stresses. A heavy load applied for a short length of time may not cause failure where a lighter load applied for a longer time will do so. (This is so important that standard rates of loading are laid down for the determination of the physical properties of materials). Thus, say Besigk and Kühne, the higher the rotary speed the shorter the time of load application over a given part of the hole, and consequently the effect is reduced and hence also the penetration for a given thrust.

Accepting the first premise, i.e. that the thrust in rotary drilling causes penetration in a similar manner to that of the "loaded-pin" test described, this is seen to be a convincing explanation of the shape of the drilling rate/thrust and drilling rate/rotary speed curves. However, as the writer hopes to show from experimental work described in the following section of this thesis, this first assumption is, in fact, erroneous.

Both Shepherd and Coeuillet⁹ have presented theories which assume that the resultant force (combination of thrust and torsional forces) acting on the rock will have the same inclination as the path along which the bit travels. Whilst this may appear reasonable it is not in fact the case as can be seen immediately if wear is taken into account. Frictional wear can only occur if there is contact pressure between the sliding surfaces, where the resultant force lies along the line of advance then no such pressure can exist and consequently no wear will result. In actual practice, however, wear always takes place and one is led to the conclusion that the resultant force must lie below the helical path of cutting. The force distribution has been determined by the writer and confirms the above conclusion.

Coeuillet has applied his theoretical analysis of the force distribution to the design of drill bits but makes several assumptions which are incorrect, as reference to the next section of this thesis will show. He assumes:-

(1) That the line of shear^{fracture} is in a direction perpendicular to the front face of the bit.

This is not necessarily so.

(2) The force required to cause fracture is proportional to the area of the triangle formed by the line of shear, the rock surface, and the front face of the bit, i.e. ΔABC in Figure 4. This is

incorrect; the force required is dependent on the length of the shear plane AB.

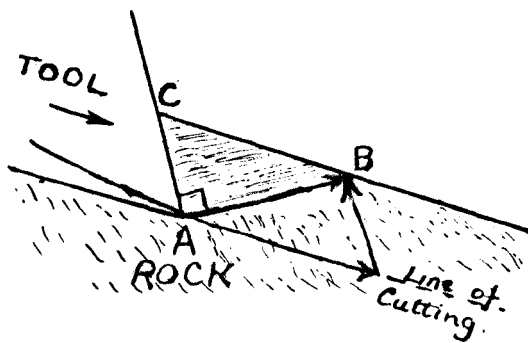


Fig. 4. To illustrate Coeillet's assumption relating to forces at bit tip.

- (3) That failure always occurs in shear along a line inclined upwards towards the free surface. (In actual fact failure is often first developed in tension.)

The weakness of the theory is demonstrated by the fact that negative rake cutting demands a new theory:- if the shear plane was perpendicular to the front face then it would be directed downwards into the rock, i.e. away from the free surface.

Shepherd has also stated that the speed of penetration of rotary drill bits is proportional to the square of the bit diameter. This appears somewhat surprising since it contradicts to some extent the view held by Schultz¹⁰ and others, that the penetration rate is governed by the bit-rock contact pressure. As the bit diameter is increased whilst maintaining constant axial thrust, the contact pressure will fall proportionately with increase in length of cutting edge; the rotational speed of the motor may fall slightly due to increased torque, (although it is possible that the reduced depth of cut may result in approximately the same torque even with increased diameter). These two effects would combine to result in a reduction in penetration rate slightly more than proportionately with increase in diameter but, it is thought, not proportional to the square of the diameter. It is unfortunate that measurements of torque and instantaneous rotary speeds were not made so that the penetration per

revolution could have been determined.

Further investigations by the same worker have demonstrated that increased leg rake angle (i.e. increased forward tilt of the front cutting face) does result in increased penetration rate. Using standard eccentric type bits he states that the most satisfactory performance was derived from bits having a positive rake of 8° - 10° on the leading leg and a smaller positive rake (about 3°) on the core-braker leg. If account is taken of the fact that the path of that part of the leading ^{leg} engaged in cutting travels on a less inclined helical path than the part cutting on the core-braker leg, it can be shown from a simple calculation that the effective rake angle is approximately the same on both legs and hence loading on each leg would be the same. The relationship between penetration rate (S) and leading leg rake angle (α) is stated to be:-

$$S = E \sec^m \alpha.$$

where E is the penetration rate for a similar bit having zero rake on the leading leg, and "m" is a variable number.

Alpan ² has demonstrated that the use of legs inclined back about 3° - 6° from the direction of cutting (termed negative leg rake bits) helps to prevent flaking and chipping of the carbide. Thus, whilst positive leg rake increases drilling rates for a given thrust, negative rake increases bit strength.

Much of the fundamental theory of cutting has been developed in relation to metal cutting. Even in this field there are many problems that remain to be solved and some of the theories will undoubtedly be modified. However, there appears to be considerable agreement over many points which the writer believes to hold for diverse types of cutting including the process operative in rotary drilling.

Merchant, a pioneer in metal cutting research, has stated "the analyses made apply equally well to any type of cutting process where the geometrical conditions are similar."

Early research on metal cutting¹¹ appears to have been inconclusive and it was not until the work of Merchant¹² was published that academic interest was once more aroused in this complex problem. Merchant's theories, although modified by later workers, still form the ground work of cutting theory.

Merchant's Analysis of Cutting.

Merchant has classified cutting into three main types:

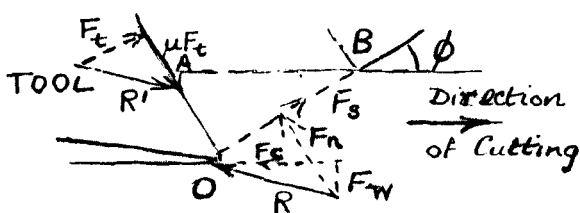
- (1) Continuous cutting.
- (2) Continuous cutting with built-up edge.
- (3) Discontinuous cutting.

In types (1) and (2) the material is removed in a continuous ribbon whereas the latter is characterised by a chipping process in which the material is intermittently broken off in chips. Typical of type (3) is the fracture observed when machining cast iron, and it is this latter type which most simulates rock cutting.

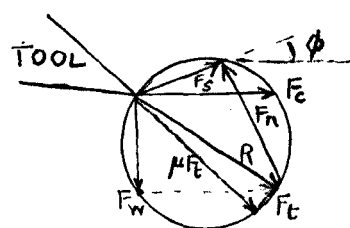
Orthogonal Cutting.

Orthogonal cutting is the more usual and simple condition in which the cutting edge is perpendicular to the direction of cutting. The system is essentially two-dimensional and the forces acting may be represented as in

Fig. 5 (a)



(a)



(b)

Fig. 5. Merchant's analysis of force system in orthogonal cutting.

in which the tool point is engaged in the material to be cut. Experimental observations have shown that the material generally fails in shear along what approximates to a plane defined by the line OB inclined at an angle ϕ to the direction of cutting. This angle is termed the Shear Angle and it is along this shear plane that plastic

deformation occurs without fracture in the case of ductile materials and with fracture in the case of non-ductile or brittle materials. With rock, generally very brittle, little or no plastic deformation takes place and in fact failure often occurs in tension before shearing. This is, however, dealt with more fully later in this thesis. Factors which appear to determine the direction of the shear plane are:-

- (1) The rake angle α :- ϕ is known to increase with increase of α although the exact nature of the relationship is much in dispute.
- (2) The coefficient of friction between the material and the front face of the cutting tool.

As is seen in Fig. 5 (a) the system is in equilibrium under the action of equal and opposite forces R and R^1 . R is the resultant force exerted by the material of the stressed portion above OB .

R^1 is the force which the tool exerts on the stressed portion.

R is composed of forces F_w and F_c , respectively the reactions to the applied thrust force and cutting force. It (R) can be alternatively separated into components F_s , the shear force acting along the shear plane; and F_n , a compressive force exerted on the shear plane.

R^1 can be separated into components as shown:-
 μF_t , a friction force acting along the tool face, and
 F_t , the normal reaction acting perpendicular to the tool face.

The above division of the forces into their principal components represents the most satisfactory analysis presented to explain the theory of planing and is one which appears to satisfy most experimental observations. Since R and R^1 are equal and opposite it is most convenient to represent all the forces as if acting at the tool point,

when the various components can be deduced from the circle diagram shown in Fig.5(b). The only inaccuracy involved by this representation is that the couple due to actual slight non-collinearity of R and R¹ is neglected. This, however, has been shown by Merchant to be insignificant. It is hoped to show that this analysis is very helpful as a means of understanding the nature of rock break down in rotary drilling. The more important mathematical derivations of basic formulae for cutting have been included in the Appendix ^{to} of this thesis but it is perhaps advisable here to comment briefly on the nature of disagreements existing between various authorities relating to the conditions of metal cutting, since these also serve to throw light upon the conditions of rock cutting.

1. The Relationship between Shear Angle (ϕ) and Rake Angle (α)

It has been well proved for both metal and rock that variation in the tool rake angle affects the force distribution and the force necessary to cause failure. The first analysis by Merchant led to the equation:-

$$\phi = \frac{\alpha}{2} + \frac{\pi}{4}$$

but this he later found to be in disagreement with experimental data so he accordingly introduced a "machining constant", a function of the compressive stress acting on the shear plane, this apparently bringing the theory more into agreement with experimental data. Phillips¹³ has also described the effect of the compressive stress across the shear plane in modifying the line of failure when carrying out compression tests on rock specimens. The shear stress is considered to be reduced by the effect of "internal frictional resistance". The force acting across the shear plane OB is reduced by a factor $K.F_n$. (K is analagous to a coefficient of friction) and it can be shown that, by taking this factor into account, the most effective shear stress is not along the direction of the usual maximum shear stress but at some other inclination.

Theories such as the above are numerous and in a

recent well-written article, Shaw, Cook and Finnie¹⁴ have discussed the assumptions underlying each, pointing out their inadequacies, and presenting a further theory which does apparently present a view closer to the truth. In this the authors criticise the Merchant theory for assuming that the direction of the shear plane is unaffected by the direction of the resultant force on the tool and that the coefficient of friction on the front face of the tool in contact with the rock is independent of the rake angle. By consideration of the fundamental processes of friction they deduce that the coefficient of friction is in fact significantly affected by rake angle and incorporate this into a theory which takes account of the discrepancies previously obtained between theoretically predicted and experimentally observed values. A more detailed explanation of this theory is given in ~~the~~ Appendix⁹ to this thesis.

The Particular Case of Discontinuous Cutting.

Merchant's analysis for the particular case of discontinuous cutting appears to be in some agreement with the phenomena observed by the writer in rock planing. Discontinuous cutting is characteristic of brittle materials, and whereas in continuous cutting the plastic flow along the shear plane is insufficient to cause fracture (the material being simply continuously deformed), in this special case the slight deformation that occurs results in complete separation of the material from the main body across the shear plane.

The analysis demonstrates that the fundamental mechanics is much the same as for discontinuous cutting. Observations made when cutting cast iron revealed that fracture occurs from the tool point along the principal shear plane to the surface of the material. This is followed by numerous subsidiary ^{shear failures} ~~fractures~~ ^{without complete fracture,} occurring from the tool point along shear planes at higher inclinations (to the direction of cutting) terminating at the inclined surface of the previous fracture (See Fig. 6) until once more a further major fracture occurs to the main surface of the material.

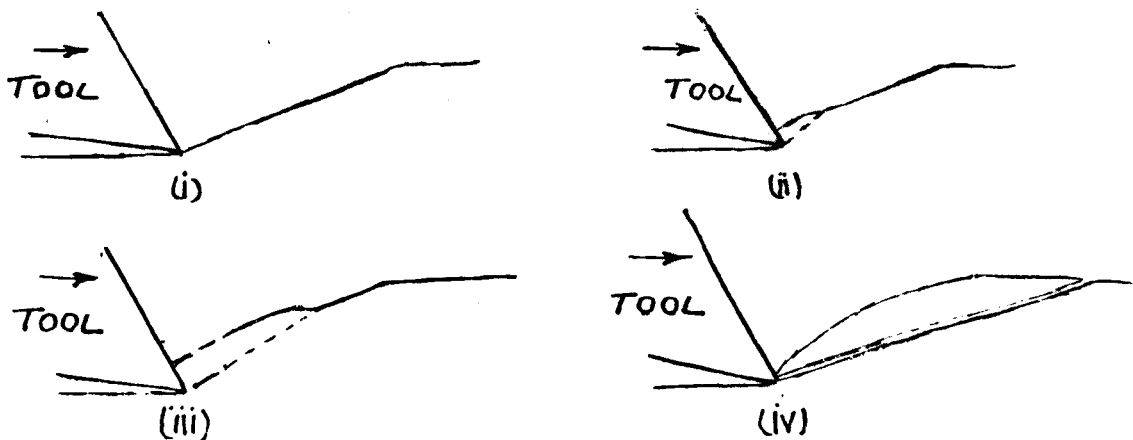


Fig.6. Shear Fractures in Discontinuous Cutting

It is argued that subsidiary fracture occurs when the stress in the direction of the subsidiary ~~fracture~~ ^{plane} is greater than in any other direction. It should be noticed that although the force component in the direction of major fracture is higher than in the "subsidiary" directions, the area of shear is also greater than the area of the subsidiary planes, so that the actual stress is not always a maximum along the major shear plane. ~~A fuller explanation of this theory is given in the Appendix.~~

Oblique Cutting.

The above brief description of cutting theory has been confined to the more simple case of orthogonal, or "two-dimensional" cutting. However, there appear to be some properties of general three-dimensional theory of cutting which may be important in rotary drilling. This type of cutting has been termed "Oblique Cutting", differing from orthogonal cutting in that the cutting edge is not perpendicular to the direction of cutting but inclined at some angle from the perpendicular, this angle being termed the Angle of Obliquity. The manner of cutting is of interest insofar as it presents certain possibilities of improved design, some of which have been investigated by the author.

At first ¹⁵ it appeared advantageous from a purely geometrical viewpoint, since turning the tool at some angle other than 90° to the direction of cutting increased the effective rake angle, whilst at the same time maintaining tip strength, the relationship being simply:-

$$\tan \alpha_e = \tan \alpha_a \sec \lambda$$

where α_e is the effective rake angle

α_a is the rake angle if the bit was cutting orthogonally

λ is the angle of obliquity.

Work by Stabler¹⁶ on metal, later confirmed by Shaw, Cook and Finnie¹⁷ suggests however that the beneficial effect may be even greater than suggested by the formula just given.

Although unable to suggest a reason, Stabler observed that the direction of flow of the continuous chip across the tool face was not in the direction of cutting as would be expected (and assumed in above formula), but at a direction deviating from this, the angle of deviation being approximately equal to the angle of obliquity (See Fig.6(a)). This Stabler

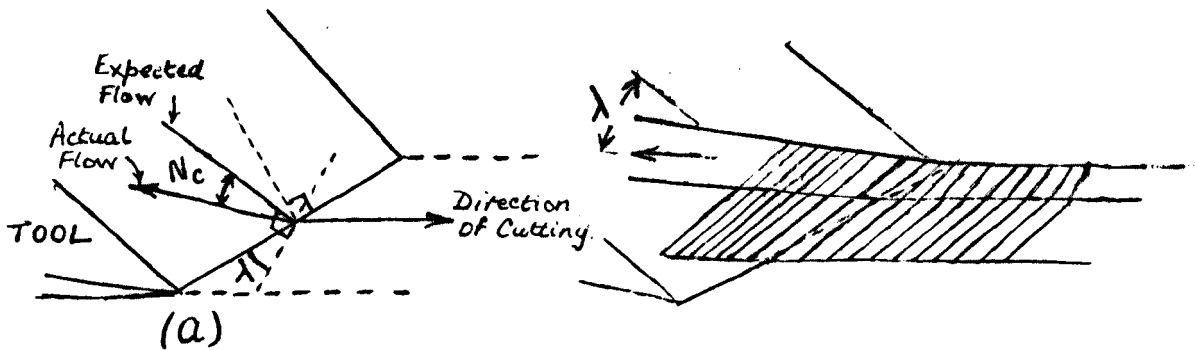


Fig. 6. To illustrate Stabler's observation on chip flow in Oblique Cutting.

has confirmed with models observing the flow of stacked plates when "cut" by a wedge Fig.6(b). Assuming that the deviation (N_c) equals the angle of obliquity he has derived the following relationship for the effective, or true, rake angle. (α_e)

$$\sin \alpha_e = \sin^2 \lambda + \cos^2 \lambda \sin \alpha_a$$

which gives a greater value for ' α_e ' than the previous formula. Shaw, Cook and Finnie have attempted to explain this deviation

as being due to the influence of the coefficient of friction between the material and the cutting tool face, (Their detailed explanation is given in the Appendix) and that Stabler's Rule ($N_c = \lambda$) is only an approximation in most cases being most nearly correct where the coefficient of friction is high.

A further point to note is that the resultant force on the rock acts in the direction towards which the tool is inclined. The directing of stress in this matter, it is felt, could be important in drill bit design, e.g. to ensure good

breakage of the core formed between the bit legs, and is referred to in the next section of this thesis.

The above brief summary presents some of the more acceptable of the existing theories of cutting which the writer has attempted to relate to rock drilling.

Application of Shear Theory to Rock Cutting.

Whilst it appears reasonable that the explanation of cutting just presented has much that is true with the cutting process in rotary drilling, it is nevertheless essential that the particular case of rock be studied experimentally and hence determine whether in fact the reasoning is valid; and further to examine certain aspects which are of especial importance, e.g. effect of depth of cut, speed of cutting and wear.

In the next section of this thesis an account is given of the experiments carried out with the above aim in view. Several aspects have been considered in both small-scale and full-scale tests from which a theory of rock cutting is developed and applied to suggest the possibilities and limitations of rotary drilling in rock. Some considerations which may be of importance in limiting the method and which are not related to cutting theory, e.g. flush water supply, have also been studied and the results embodied in the thesis.

SECTION II.

PLANING TESTS.

Rock Planing Tests.

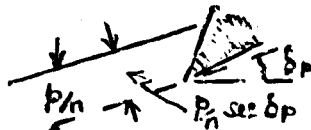
The justification for the use of planing tests as a means of studying phenomena in rotary drilling may be appreciated by considering the manner in which a hole is bored by a rotary bit.

The bit penetrates into the rock along a helical path under the action of an axial thrust force and a rotary torque. The inclination (δ_p) of this path at a given point "P" on the cutting edge, distance "r" from the axis of rotation, will be

$$\delta_p = \tan^{-1} \frac{p}{2\pi r} \dots\dots\dots(i)$$

where "p" is the bit penetration/revolution.

Thus the path of the bit element P may be represented as ~~in a helical path~~ ^{below} in which the element is planing off the rock ahead of it to a depth of $\frac{p}{n} \sec \delta_p$



where "n" is the number of bit legs or wings.

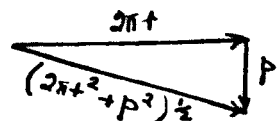
It should further be noted that

(a) Effective Leg Rake Angle = Nominal Leg Rake Angle
 + Inclination of Cutting Path
 i.e. $\alpha_e = \alpha_a + \delta_p \dots\dots\dots(ii)$

(b) Effective Clearance Angle = Nominal Clearance Angle
 - Inclination of Cutting Path.
 i.e. $C_e = C_a + \delta_p \dots\dots\dots(iii)$

Whilst the angular velocity of a rotary bit is constant, the peripheral velocity (V_p) at a given point P. ~~is given by~~ is given by

$$V_p = \frac{[(2\pi r)^2 + p^2]^{1/2}}{N} = \frac{2\pi r}{N} (1 + \tan^2 \delta_p)^{1/2} \dots\dots(iv)$$



where "N" is the rotary speed. (R.P.M.)

Since $\tan^2 \delta_p$ is generally much less than unity, the linear velocity is approximately proportional to the radius to that point.

Thus it can be seen that:-

- (a) the linear cutting speed varies across the cutting edge.
- (b) the effective leg rake angle " " " " "
- (c) the effective clearance angle " " " " "

and further, any variation in thrust will automatically cause a variation in all three factors.

The nett result, therefore, of any rock drilling test is affected by several variables which combine to complicate the analysis. However, the action remains one of planing (with a variable cutting rate across the tool face) and it was decided to eliminate the complications introduced by rotation by studying simple planing across a rock surface in which a close control of variables can be maintained. These tests can be considered to indicate the conditions of cutting at a thin element of the cutting edge of a rotary bit, the total effect under actual drilling conditions being the integration of individual elemental effects.

Initial experiments.

Apparatus.

Early experiments were carried out using the apparatus shown diagrammatically in Fig. 9. This was made up of a "Dexion" slotted angle framework in which was mounted a variable height steel table to which smooth rectangular rock specimens could be clamped. The cutting tool was attached to the end of the ram of a Holman air-leg cylinder fitted horizontally in the framework. The table consisted of a steel plate 36" wide x 30" long x $\frac{1}{8}$ " thick (A) on which rested a similar plate 18" wide (B). The rock specimen was placed in position on the latter plate and clamped (Clamps C) to it. Two screwed rods (D) enabled the rock to be traversed across plate A, the two plates being then bolted together through the slots (E). The whole could then be raised to the desired depth of cut by means of three adjusting screwed rods (H) placed concentrically (120° apart for ease of levelling) under plate A. When finally positioned, the table was rigidly bolted to the framework through the angles at F.

A pressure gauge (G) mounted on the air-leg indicated cutting force. Maximum travel of the piston was approximately 4 feet, thus allowing cuts to be taken completely across the rock sample.

Aims of experiments.

By use of this apparatus it was hoped to measure the

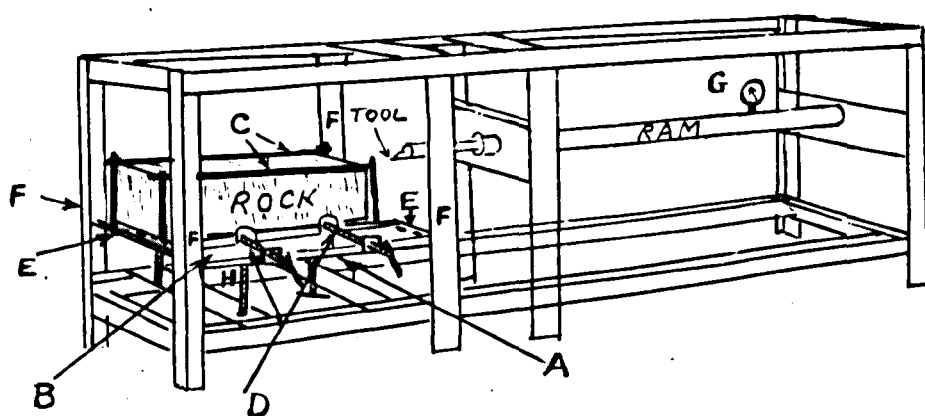


FIG 8. INITIAL ROCK PLANING APPARATUS.

cutting force required for various conditions of cutting viz.

- (a) Variable bit angles.
- (b) " depth of cut.
- (c) " width of cut.
- (d) " speed of cutting.

Several tests were attempted which quickly revealed that the apparatus was unsuitable, the main reasons being:

Reasons for failure of experiments.

1. Tendency for the depth of cut to vary considerably due to whip of the projecting rod of the ram.. Occasionally the tool would rise out of the cut and shoot dangerously across the rock surface.

Steel guides were later introduced above the ram but these did not eliminate whip completely.

2. Inadequacy of the ram force, except for very light cuts, when depth fluctuations assume maximum importance, and narrow cuts.
3. Lack of control over cutting speed.
4. Difficulty and expense involved in obtaining sufficiently smooth samples of rock of the dimensions required. Concrete samples were used for some trials but the earlier objections to the apparatus precluded any detailed work with them.

The tests were therefore abandoned and attention turned to the possibility of using a metal milling machine for similar tests. It is considered, however, that apparatus of the type designed could be very much improved by the provision of a screw-feed drive for the cutting tool to replace the ram. The feed-screw would be driven through gears by a suitable electric motor (variable speed A.C.) thus allowing a wide range of cutting speeds.

By this means the apparatus could be considerably reduced in size and its rigidity increased. The power consumed by the motor would then indicate the mean cutting force.

Initial milling machine investigations.

Early investigations using the milling machine (seen in detail in Fig 9) were intended to obtain information relating to the rock breakdown process in the vicinity of the cutting tool tip.

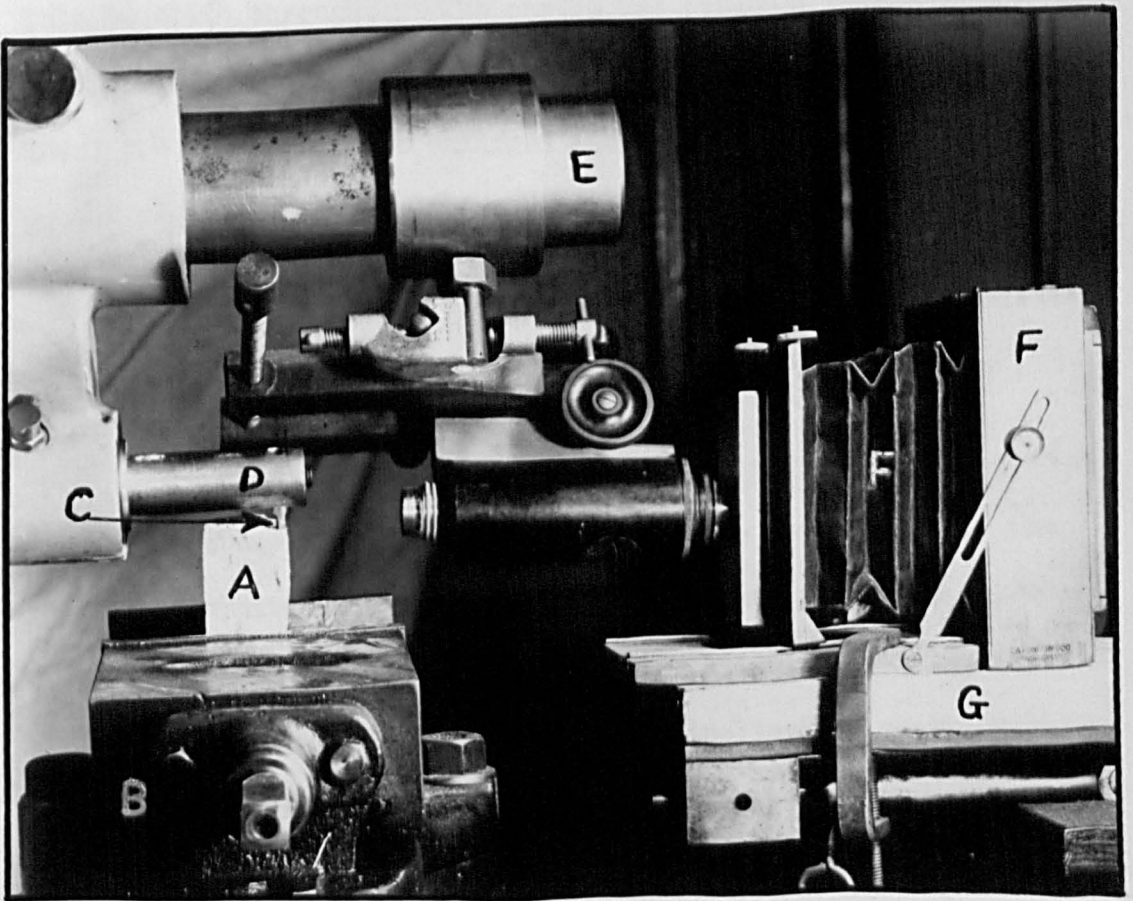
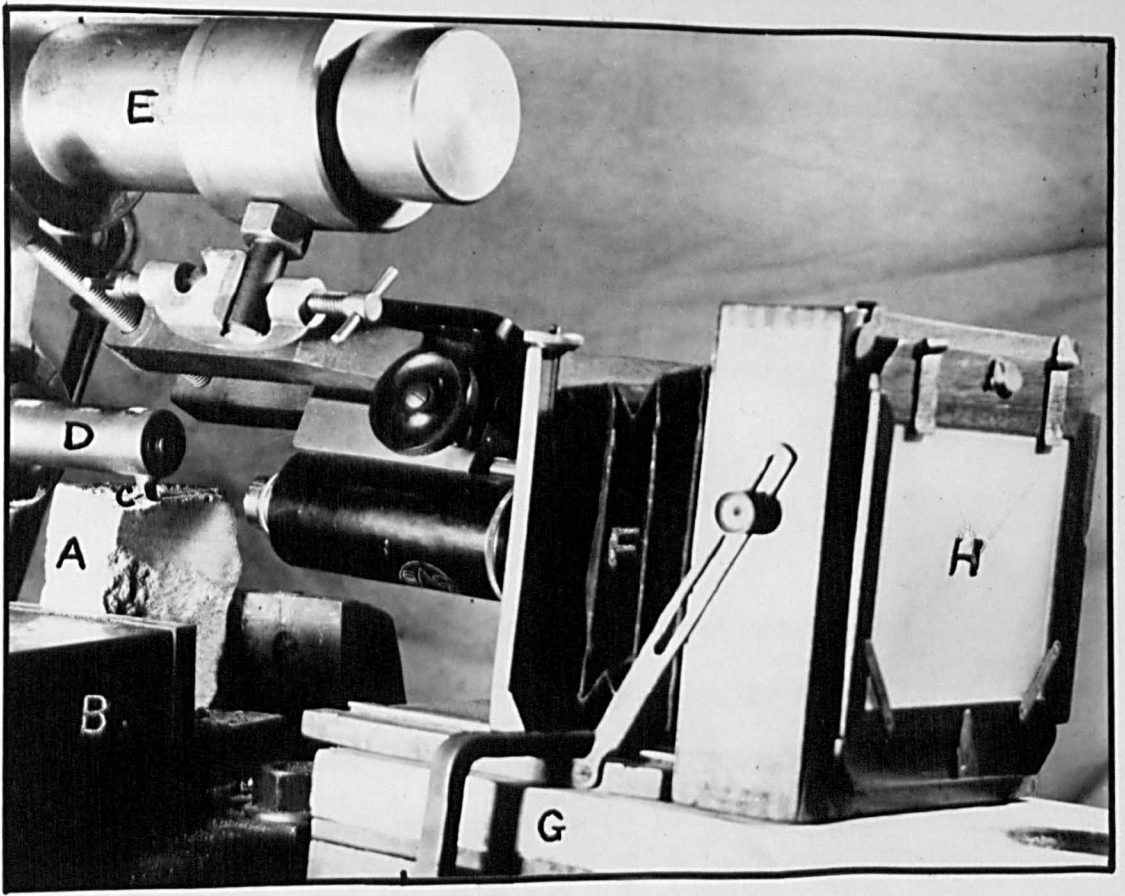


FIG 9. EARLY MILLING MACHINE APPARATUS.

Apparatus. (See Figs.9(a) and 9(b).)

A small rectangular specimen of rock (A), approximately a 2½" cube, was clamped into the vice (B) on the travelling table of a milling machine. The tool (C), a short length of ½" diameter High Speed Steel, was fitted into the milling arm D. This arrangement enabled the tool rake angle to be varied simply by rotating the milling arm, which was, however, rigidly fixed during cutting. Variation in depth of cut could be obtained readily by altering the height setting of the milling table. (All controls on the milling table are graduated such that depths of cut, distance cut, etc. can be read accurately to 0.0005").

The front face of the rock was set exactly in line with the outer edge of the cutting tip to enable the cutting tip region to be accurately focussed through the microscope-camera arrangement. This consisted of a 32 mm objective (x 10 eyepiece) microscope attached to the arbor (E) with the eyepiece projecting inside the bellows of a small plate-camera (F). The bellows were made light-proof by replacing the camera lens and holder by a brass plate with a circular aperture just large enough to allow the microscope tube to slide through. The camera was attached to a sliding board (G) screwed onto a tripod, thus allowing the whole arrangement to be moved for focussing, the enlarged image being projected onto the ground glass screen (H). Progress of the fracture was observed on the screen and the cut stopped at interesting stages to allow the event to be photographed.

Results.

Typical photographs obtained using various rake angles on a soft sandstone are shown in Fig.9C. These suggested that the rock is intermittently broken ahead of the cutting tip by a process of shear along a line inclined to the direction of cutting. It also appears to suggest the the angle of inclination of the fracture line is related to the rake angle (as can be seen by comparing Fig.9C(b) - positive rake angle and Fig.9C(f) - negative rake angle). No definite conclusions could be formed at this stage, however, since

1. Only a limited number of fractures could be photographed in

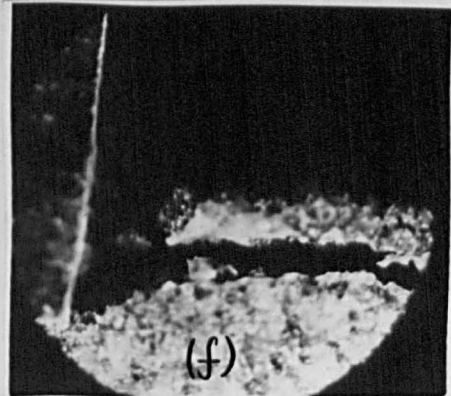
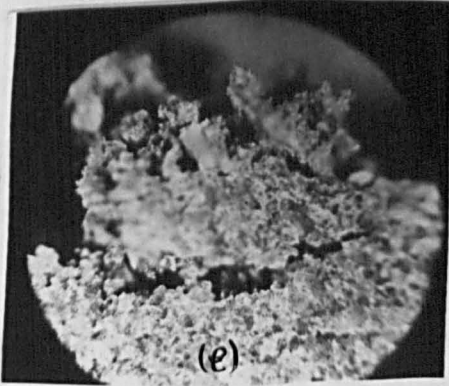
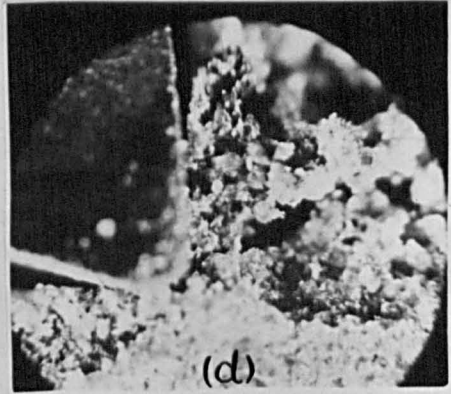
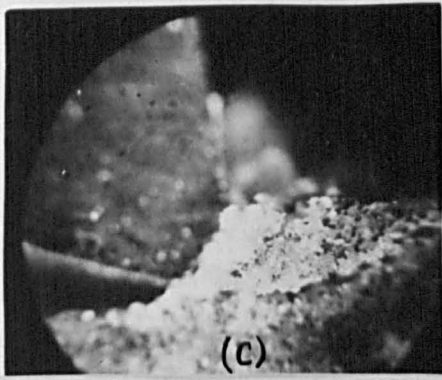
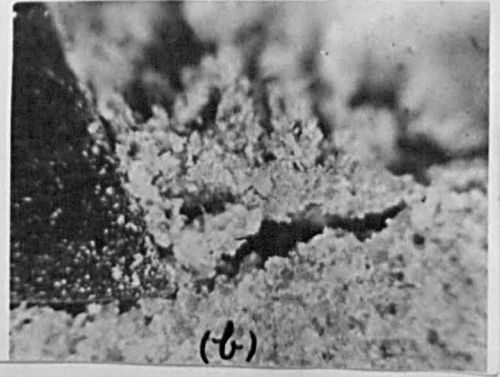
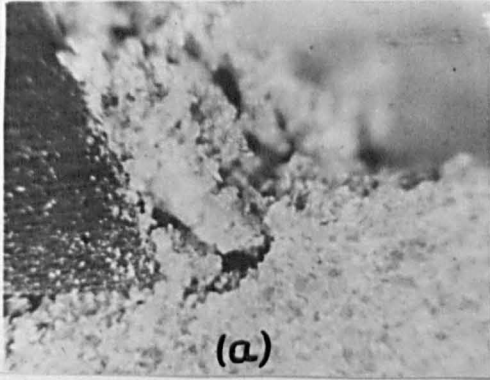


FIG 9C. OBSERVED FRACTURES.

view of the cost of photographic plates.

2. All photographs were made with the tool stationary and no continuous record of the development of fractures could be obtained.
3. The method gave no indication of the operative force system causing fracture.

Attempts were made to overcome the second objection by dispensing with the microscope arrangement and taking repeated photographs with a 35 m.m. camera fitted with lens extension pieces, in conjunction with an electronic flash unit. The short tool was replaced by one 3" long rotating continuously in the milling arm D, the rock being raised continuously to engage with the rotating tool. It was hoped that by taking sufficient photographs a comprehensive idea of the development of a fracture could be built up. This also proved unsuccessful mainly due to:

1. Difficulty of synchronising operation of the camera with the time during which the tool was cutting.
2. Variation in fracture angle such that the development of each was different.

As one of the main defects of the milling machine is the low speed ~~at~~ ^{of} cut, the method of using a rotating tool allows high peripheral speeds to be obtained. Variation in tool length is also a means of varying tool rigidity, a factor of importance as will be shown later.

The above tests led to the conclusion that a detailed analysis of the fracture process was impossible without

- (a) a continuous record of the development of fracture.
- (b) some method to determine the instantaneous operative force system.

The former requirement could be met by use of a high-speed cine-camera, whilst the second necessitated some form of force dynamometer. The writer was in the process of designing a single-component dynamometer when he was fortunate in being able to obtain on loan a three-component machine lathe model, as used for metal cutting, by which the complete force system on the cutting tool

could be determined. Accordingly the existing apparatus was modified to incorporate this equipment.

Investigations using Cine-cameras and Tool Dynamometer.

The investigations may conveniently be divided into two series:-

1. Investigation of rock fracture process.

This necessitated using two cine-cameras, one to take continuous photo-micrographs of fracture development, the other to record the instantaneous force values indicated on the dynamometer dial gauges. The apparatus is shown in Fig.11(a).

2. Investigation of Effect of Varying Cutting Conditions on Force System.

In this series dial readings alone were recorded hence one camera only was required. The apparatus is shown in Fig.11(b).

Description of Apparatus.

Lathe Tool Dynamometer. Figs 10(a) and 10(b)

The dynamometer is a robust instrument designed for use in metal cutting lathes. The principle of operation is very simple as reference to Fig.10(a) will reveal. The tool (A), usually $\frac{3}{4}$ " diameter H.S.S. 4" long (or less) slides into a steel cylinder (B) clamped in position by two Allan screws (C) which are not in contact with the outer case. The outer surface of the cylinder is accurately ground at D such that it is free to move in any direction under the action of forces applied to it via the tool. The geometrical form of the surface to which D is ground, ensures that the movement of the cylinder in any of the three principal directions is directly proportional to the force in that direction with no interaction of forces under complex loads. Movement of the cylinder is restrained by steel diaphragms (E) ground from $\frac{1}{8}$ " plate. Thus any load will cause a deflection of the diaphragms proportional to the component of the load acting on the diaphragm. Use of various diaphragm thicknesses enables the load range to be varied depending on the loads expected and the sensitivity required. Deflection of the diaphragms is indicated by three dial gauges (F) (1 dial division

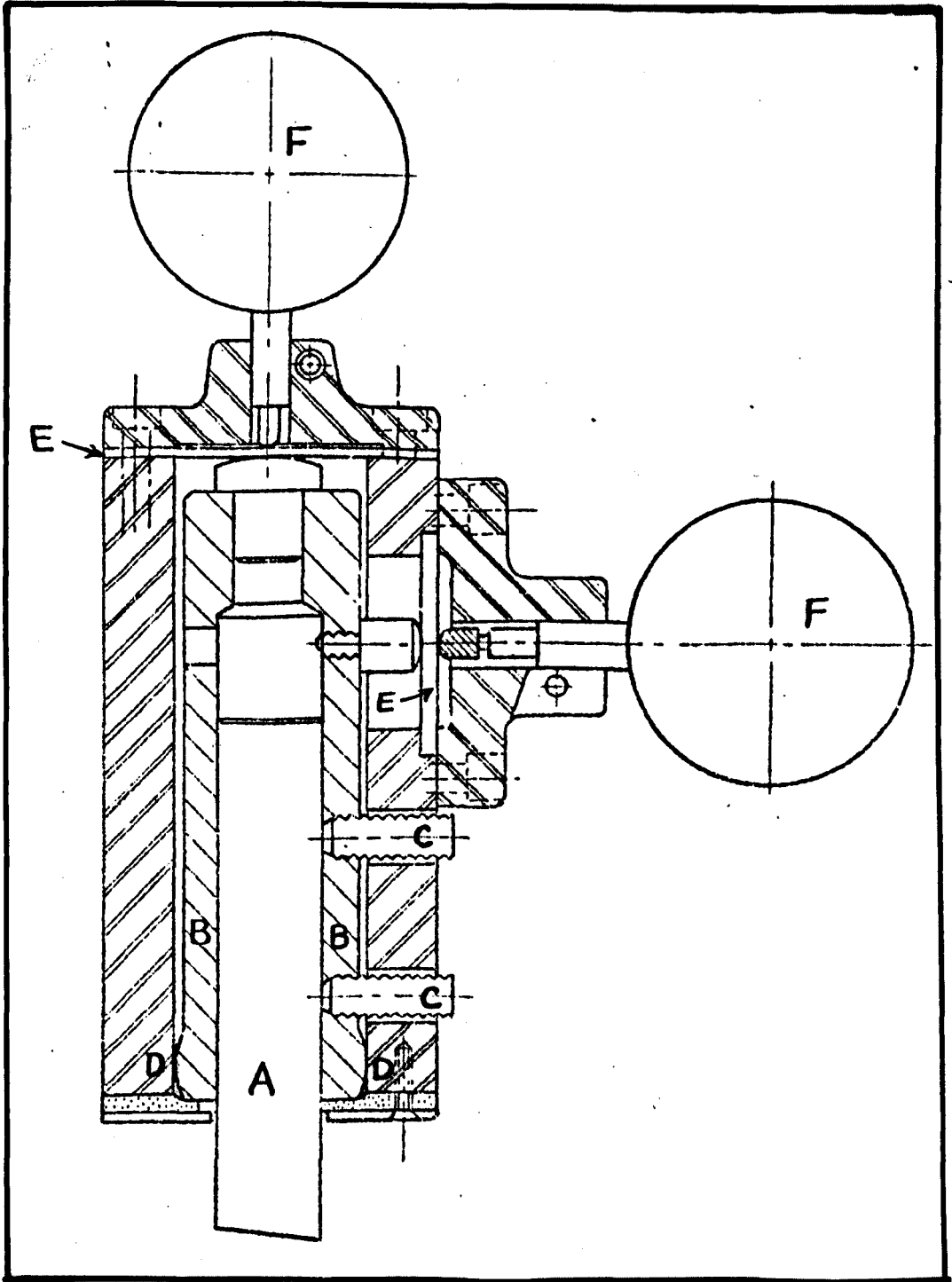


FIG.10A. SECTION OF TOOL DYNAMOMETER

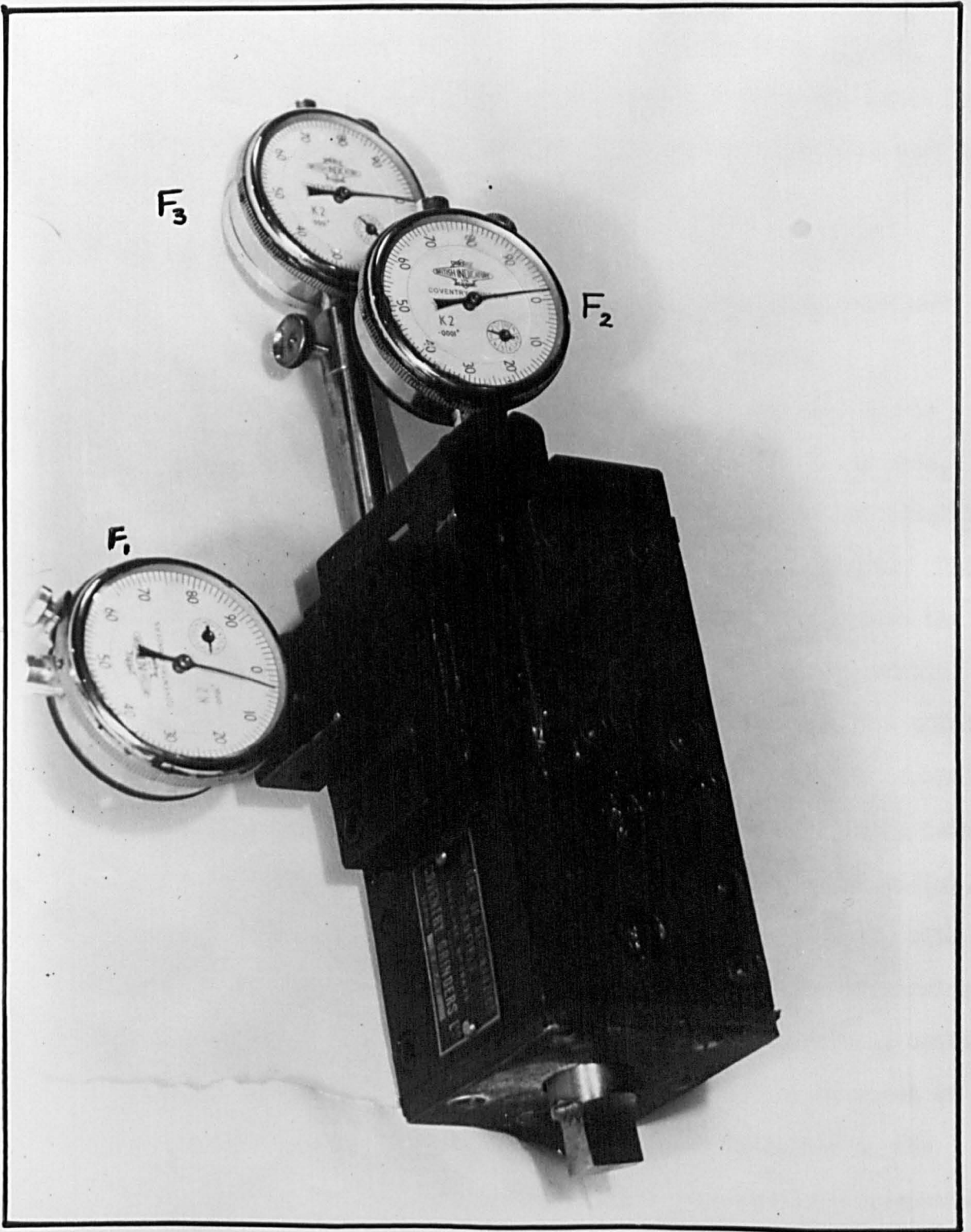


FIG. 10 B. TOOL DYNAMOMETER

= 0.0001" deflection). Deflection of the side force diaphragm (F3) is transmitted to the gauge via a lever ~~assembly~~ to enable the gauge to be fixed vertically. Each set of diaphragms is calibrated by direct loading of a special tool-piece fitted in the cylinder and a calibration chart supplied with the instrument. As will be observed from the diagram this calibration is correct only for one setting of the tool. Where required, the sensitivity may be increased by allowing greater projection of the tool, thereby increasing the moment of side and horizontal forces, and hence the deflection. In this case the necessary moment correction must be applied.

Single-Camera arrangement.

Although used in the reverse order the "single-camera" arrangement is described first for the sake of clarity.

In order to set up the dynamometer as required in the milling machine a special attachment (A in Fig. 11(b)) was made, countersunk on the back face to allow free rotation of the slightly projecting vertical milling spindle over which it was fixed. This spindle is geared directly to the motor (B) which also drives the traversing table (C), and had previously prevented the use of the mechanical drive to the table. By this means, however, the spindle was free to rotate without interference to cutting and the mechanical drive could therefore be used. On the front face of A was a lathe type tool clamp to which the dynamometer was attached as shown (D). The rock specimen (E), approximately a 2½" cube, was clamped, with the top surface level, in the vice rigidly fixed to the traversing table (F). The table was raised until the rock was just in contact with the tool point, this position being indicated by movement of the vertical dial. The reading of the height indicator on the handle (H) was noted. (One revolution of each handle corresponded exactly to a movement of 0.200", with 100 graduations per revolution). The rock was then traversed across the rock surface to ensure that the latter was level and, when clear of the tool, raised by the desired amount in preparation for cutting. For re-setting after a cut the rock could be moved sideways in front of the tool by handle S.

The Paillard Dolor camera P₁ was set upon a tripod,

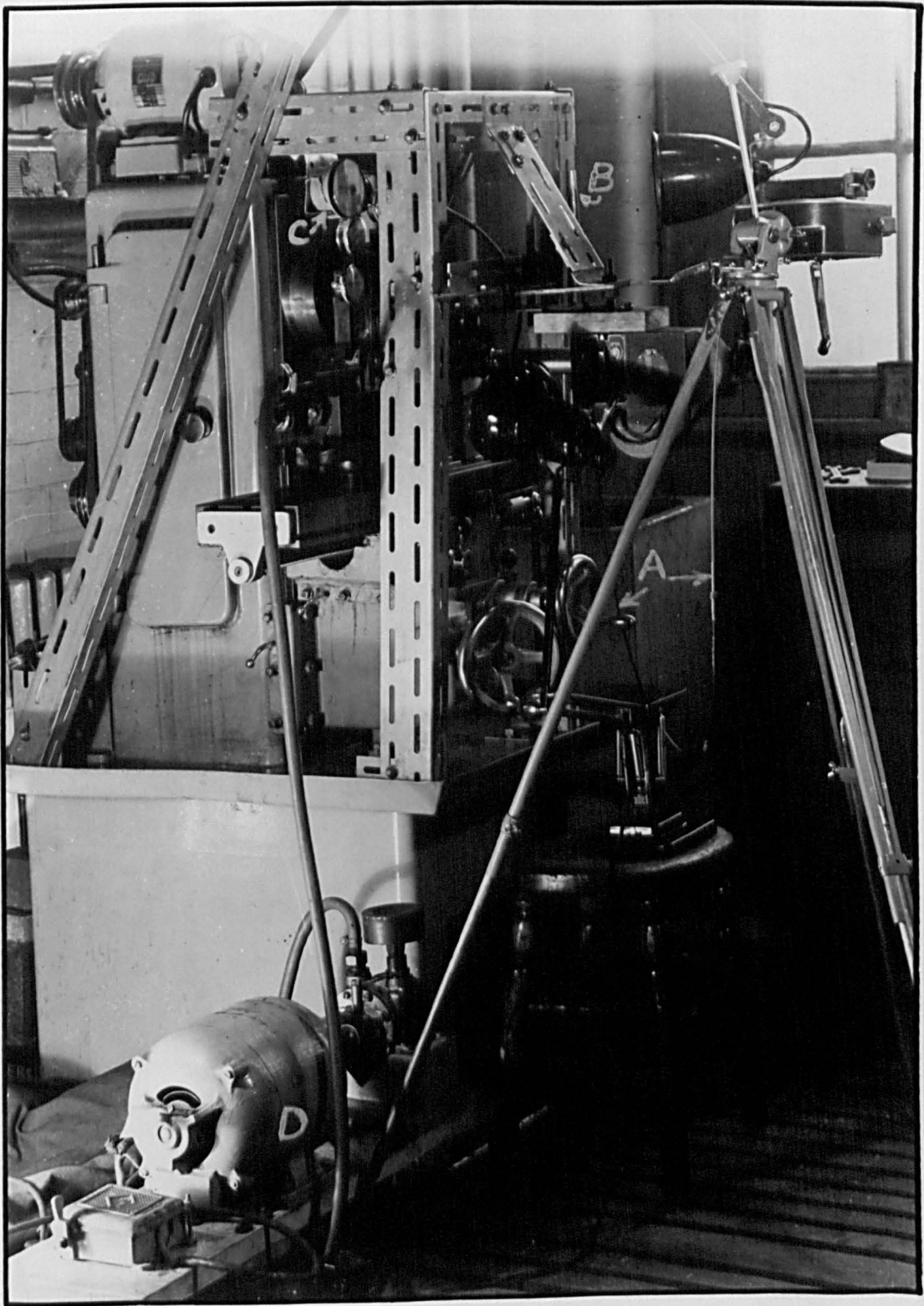


FIG. II A. ROCK PLANING APPARATUS
(TWO CAMERAS)

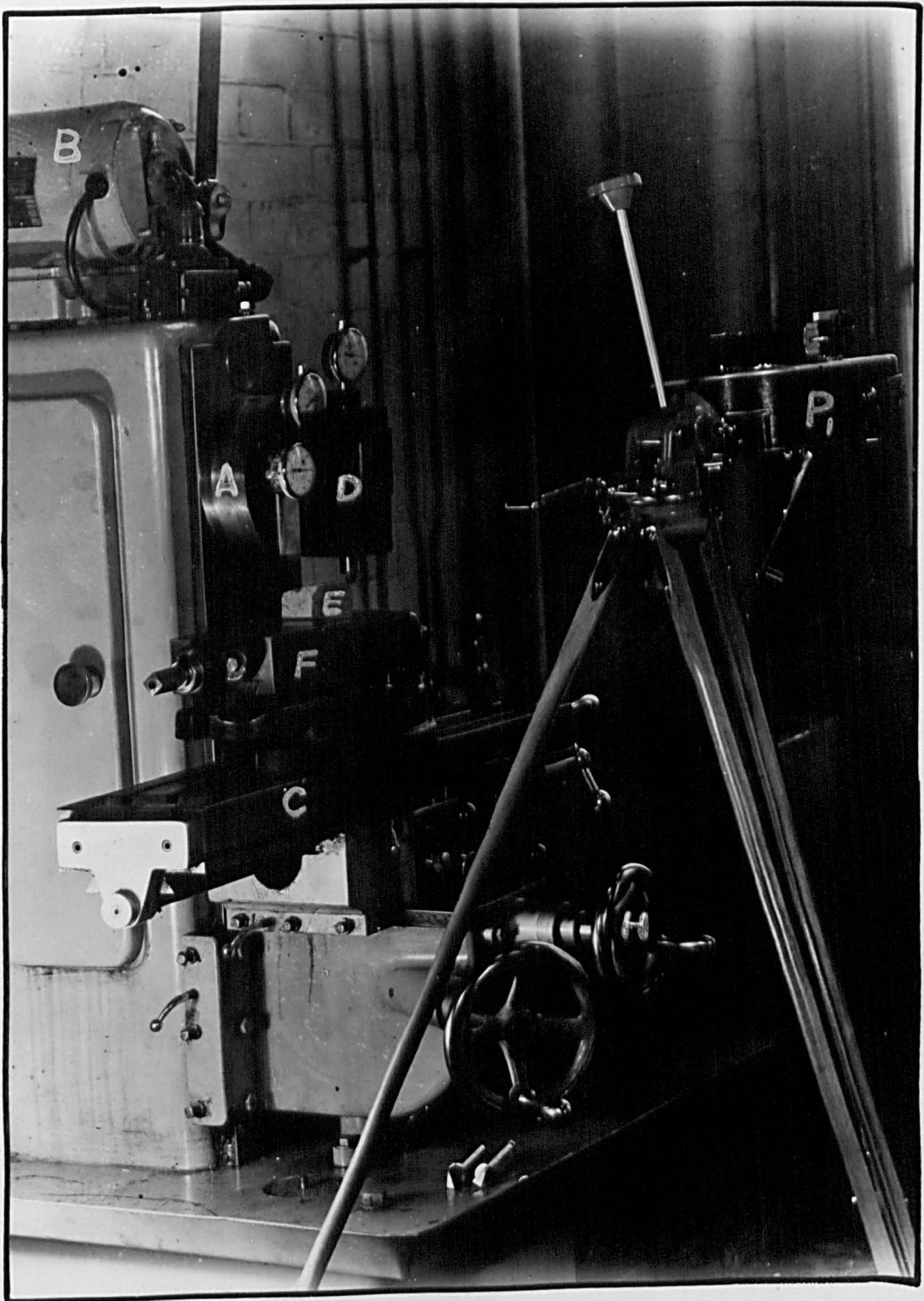


FIG. II B. ROCK PLANING APPARATUS
(ONE CAMERA.)

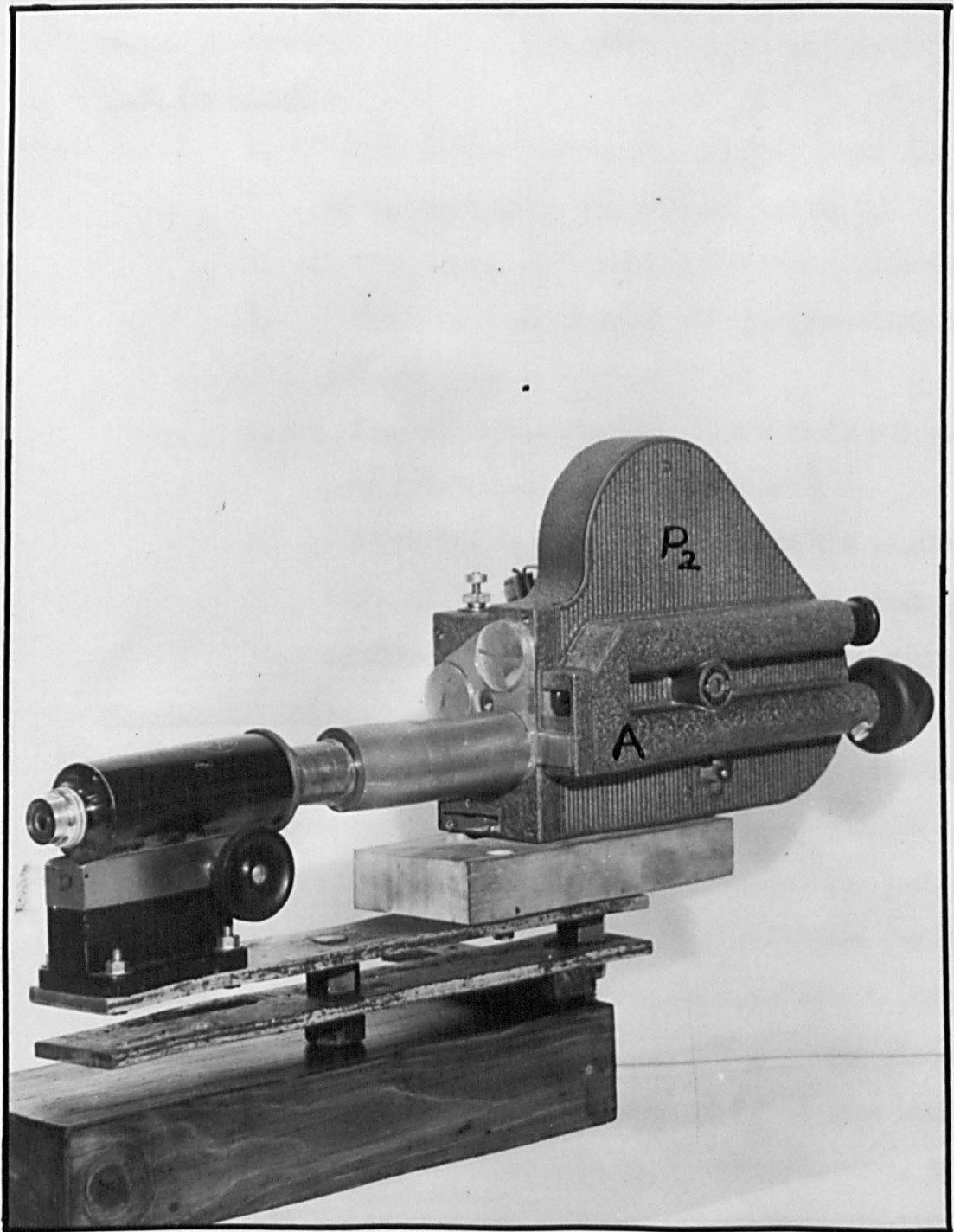


FIG.12.

MICROSCOPE-CINE CAMERA
ASSEMBLY

focussed on the dial gauges. Lighting for the dials was provided by a single Photo-flood light placed immediately above the camera and shining slightly downwards. Tests were identified by taking a single frame picture of the test number chalked on a blackboard placed in front of the dials just prior to starting the test.

Test Procedure.

1. The rock was set at the required depth and brought up to the tool by the traverse handle T.
2. The camera was wound and the test number recorded.
3. The camera was started and the traversing table put into gear.
4. The camera was stopped and the table put out of gear immediately the cut was completed.
5. Depending on the abrasiveness of the sample under test, the rock was either immediately reset for a further test or the tool removed for re-sharpening.

"Two-Camera" arrangement.

In order to observe the rock cutting action together with the instantaneous force system, it was necessary to add the microscope-camera combination (Fig.12) to the apparatus just described. The Pathe-Webb cine-camera (F₂) was chosen for its suitability for microscopic work of this nature since it was provided with a direct view-finder (A) which, by means of prisms placed in front of the shutter, diverted 10% of the light and thus enabled the actual field projected onto the film to be observed, even, if desired, whilst cutting was in progress. Focussing was thus simplified and no film or time was wasted through incorrect "aiming" of the microscope. The microscope (32 mm objective x 4 Huygens eyepiece) was connected via a 2½" brass extension tube to the camera, as shown, projecting an image of unit magnification onto the cine-film. Additional lengths of tube could be added if higher magnifications were desired but it was generally necessary to use unit magnification in order to obtain a field of view large enough to observe the full extent of fractures.

This combination was held by a rigid Dexion angle framework and fixed in the correct position by means of slots and bolts. Slight

adjustment was occasionally required since the position of the tool tip in the field of view varied for different rake angle tools. The provision of a dual release cable (A) (Fig. 11(a)) attached to the starting button of each camera enabled both cameras to be started and stopped simultaneously by depressing the cable plunger (B).

Further additions include:-

1. A tachometer (C), driven through a flexible cable from the final drive spindle to the table. This was placed in the plane of the dial gauges and photographed with them, thus indicating any table speed fluctuations that might occur during drilling.
2. A small air-blower (D) by which a jet of air was directed at the tool tip to prevent build up of any fractured rock particles which otherwise tended to accumulate and obscure details of the fracture process.

Lighting for both dials and rock was provided by No. 1. Photo-flood bulbs fed down from a common supply in order that it could be cut off for an instant from both films simultaneously. This periodic "black-out" (of approximately $\frac{1}{4}$ second duration) on the developed films served to correlate the two records and check the running speeds of the two cameras set as accurately as possible to run at the same speed. Tests carried out earlier had indicated that, with care, the cameras could be set to run at speeds within 4% of each other. This, together with the periodic checks, was considered acceptable.

Two Camera Test Procedure.

1. The cutting tool, sharpened to the correct angles, was accurately set in the dynamometer. This setting was $1'' + \frac{1}{2}$ (depth of cut) from the under face of the dynamometer casing, the position for which the calibration had been made.
2. The rock was set to the required depth and brought up to the tool by the traverse handle.
3. The cameras were wound and the test numbers recorded as described previously.
4. A check was made to ensure that the fields of view

of the cameras were accurate and in focus.

5. The milling table drive was set to the desired speed by varying the belt drive gears and the drive motor then started.
6. Lighting for the two fields of view was switched on together with the air blower, all being connected to a common supply.
7. Both cameras were started together by depressing the dual-release cable plunger, and the table drive then immediately thrown into gear.
8. Lighting was interrupted for an instant by rapidly flicking the light switch off and on.
9. The cable plunger was released to stop both cameras, and the table put out of gear, as soon as it was observed that the cut was completed.
10. The dynamometer was removed and the tool replaced ready for the next test.

Investigation of the Back Cutting Action.

Fig. 13(a) shows selected frames from a cine record of a $\pm 20^\circ$ rake tool of High Speed Steel, $\frac{1}{4}$ " wide taking a cut $1/200$ " deep across a sample of Darley Dale Sandstone, a medium size grain, abrasive rock. Fig. 14(b) shows the corresponding two dimensional force system, together with the variation in direction of the resultant force on the tool. Figs. 14(a), 14(b) and 15(a), 15(b) are similar records obtained when using similar tools having 0° and -20° rake respectively on the same rock. Examination of the record in Fig. 13 shows that the following sequence of events takes place:- (N.B. The tool travels from right to left relative to the rock).

Frame 3.

The tool is in contact with the edge of the rock. The forces begin to build up in both the direction of cutting and perpendicular to it. It should be noted that no vertical force is applied - it is induced by the cutting action.

Frame 5.

Fracture has occurred to the rock surface, starting initially in approximately the direction of cutting, later swinging up to the surface. The force curve

shows a sudden drop.

Frame 22.

The tool has travelled across the fractured surface with little build up of force until it once more engages with the rock at the base of the inclined fracture line. The force builds up until fracture occurs to the horizontal surface accompanied by a further drop in force. Comparison of this fracture with that shown in Frame 5 shows that there is again a change in direction of the fracture line although it does not commence in the same direction.

Frame 27.

Further fracture has occurred in a line inclined upwards from the tool up to the surface. Frame 26 shows the fracture line immediately after removal of the rock chip.

Frame 36.

The tool has advanced from the stage in Frame 28 intermittently fracturing rock ahead of it along planes of high upward inclination from the tool tip to the inclined surface of the previous fracture, resulting in minor drops in the force build up. This intermediate action between major fractures may also be observed to have taken place between Frames 37 and 52; 61 and 63.

Frame 96.

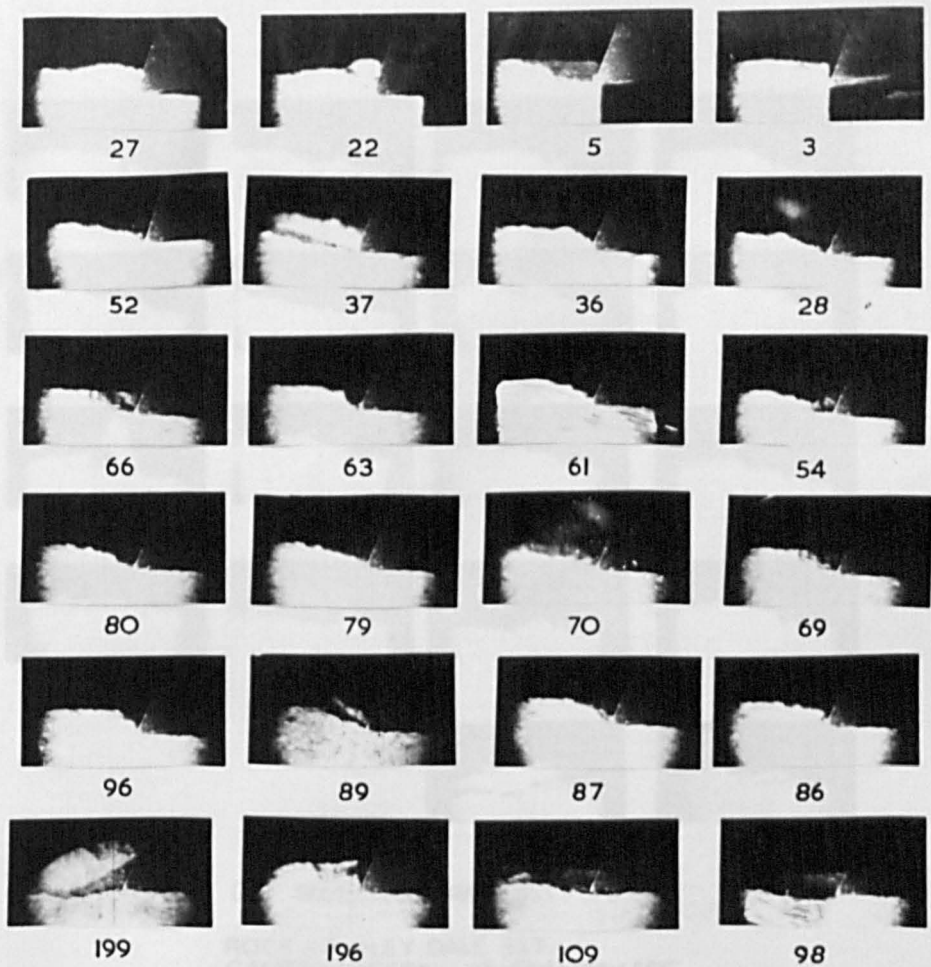
Fracture has been initiated in a direction inclined downwards into the rock. This may also be observed in Frame 199.

Frame 109.

The tool is completely out of contact with the rock.

Examination of Figs. 14 and 15 reveals that the characteristic action is basically unaltered. This may thus be summarised as:-

- (i) Tool in contact with previously fractured surface.
- (ii) Force builds up, minor fractures occurring to the previous fracture line with resultant small drops in force.
- (iii) The force continues to increase until a value is reached sufficient to cause fracture to the



SELECTED FRAMES.

ROCK:- DARLEY DALE SST.
 CAMERA SPEED:- 9 FRAMES/SEC
 CUTTING SPEED:- 9"/MIN

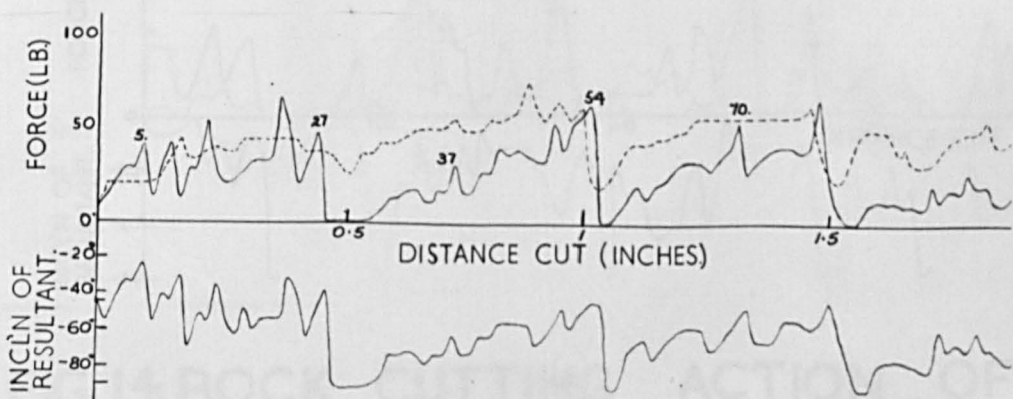
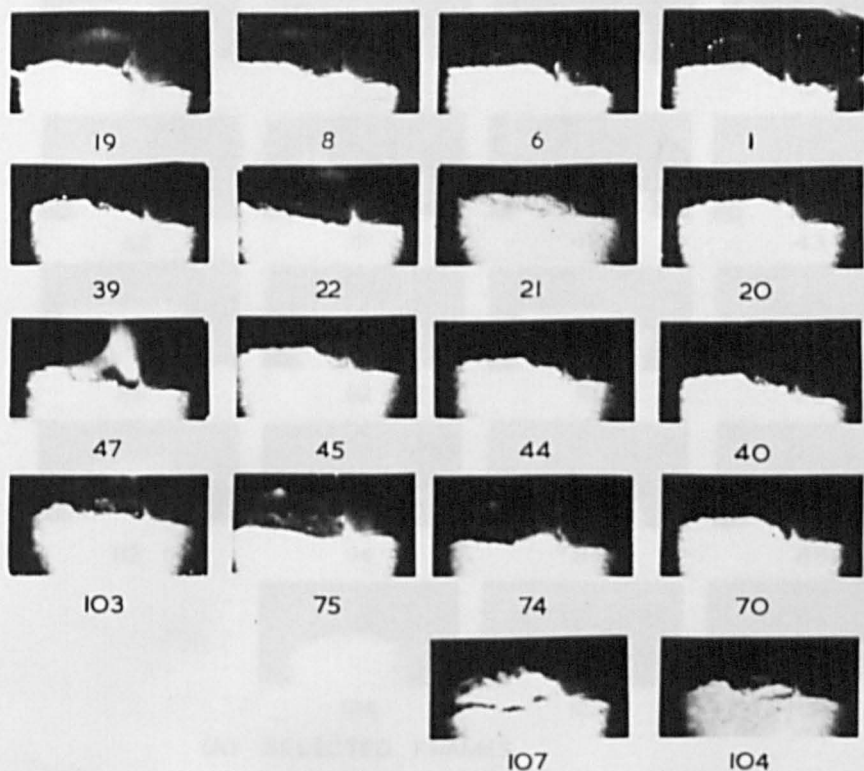


FIG.13 ROCK CUTTING ACTION OF

+20° RAKE TOOL



(A). SELECTED FRAMES.

ROCK :- DARLEY DALE SST.
 CAMERA SPEED :- 9 FRAMES / SEC
 CUTTING SPEED :- 9" / MIN

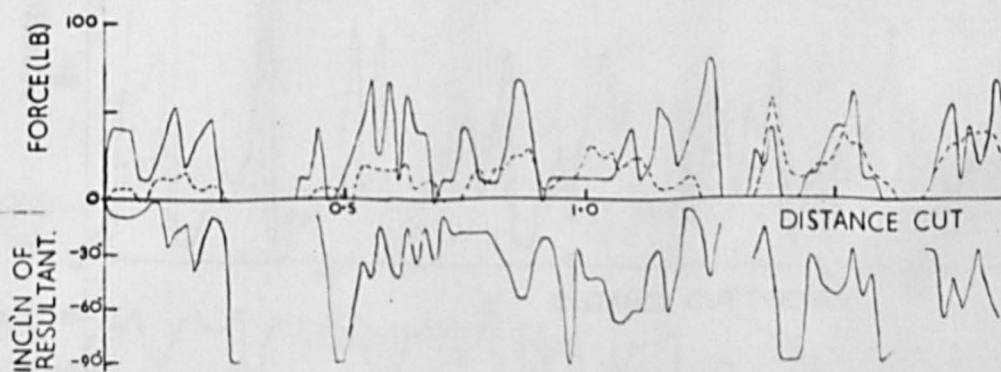
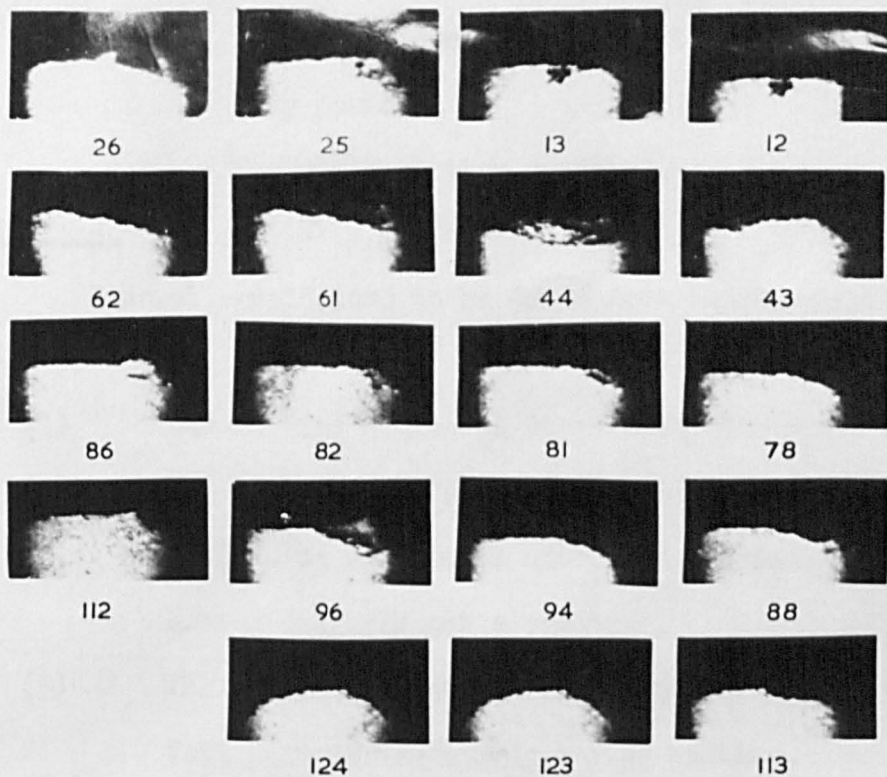


FIG. 14. ROCK CUTTING ACTION OF
 0° RAKE TOOL



(A) SELECTED FRAMES.

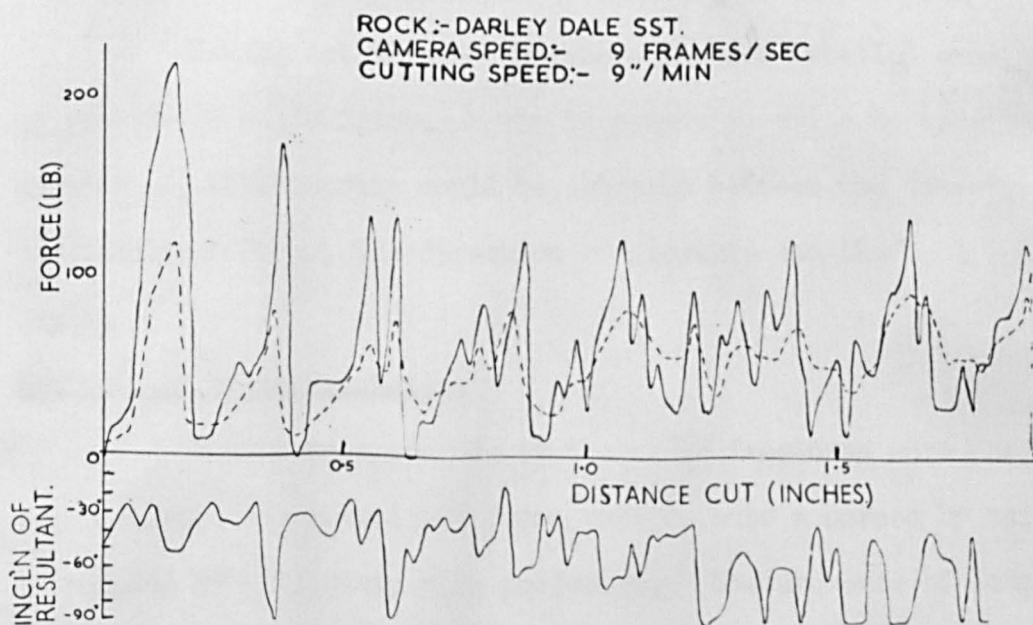


FIG. 15. ROCK CUTTING ACTION OF
 -20° RAKE TOOL

horizontal surface. The force drops suddenly. Energy stored in deflection of the tool is released, driving it forward at a speed determined by its inertia. Depending on the direction of fracture the tool may lose contact with the rock, in which case the force falls to zero, or re-engage immediately with it when the fall is only partial. The cycle is then repeated.

Conclusions.

General conclusions to be drawn from this analysis are:-

- (1) The cutting action is essentially discontinuous.
- (2) The direction of fracture is very variable and the peak force associated with such fracture is correspondingly not a constant.
- (3) The inclination of the resultant force below the tool path varies widely during cutting.
- (4) The drop in force on fracture is very rapid.

Having established the above facts a detailed examination of records of major fractures was then made in order to ascertain whether any relationship could be obtained between the direction of the resultant force, the direction of fracture and the tool rake angle.

Analysis of Major Fractures.

Cine-camera records of the major fractures were projected, together with the associated force record, onto a screen by using an adapted 35 m.m. strip film projector. Measurements of length and direction of each fracture were taken from the magnified image and scaled down to the correct value. The accuracy of measurement of angles cannot be guaranteed within $\pm 3^\circ$ since many of the fractures changed slightly in direction around grain boundaries, etc.

Results.

Results are shown in Tables 1 A and 1 B from which it is immediately apparent that no quantitative measurements can be made. There would appear to be no relationship between the fracture angle

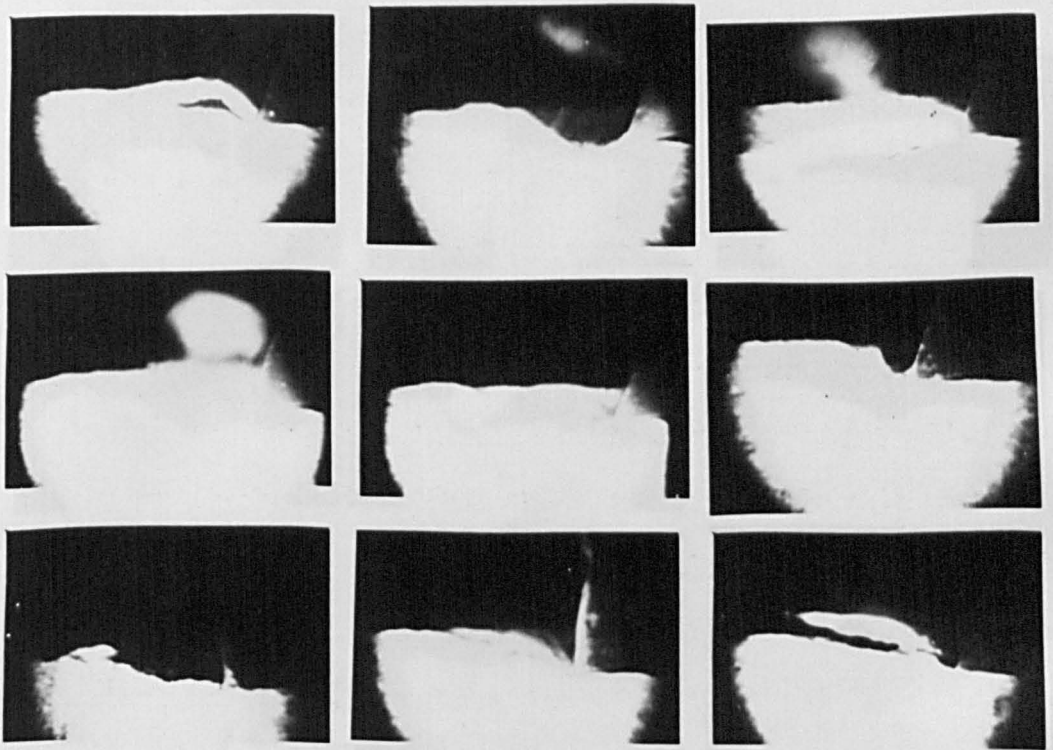


FIG.16 A. TYPICAL FRACTURES.

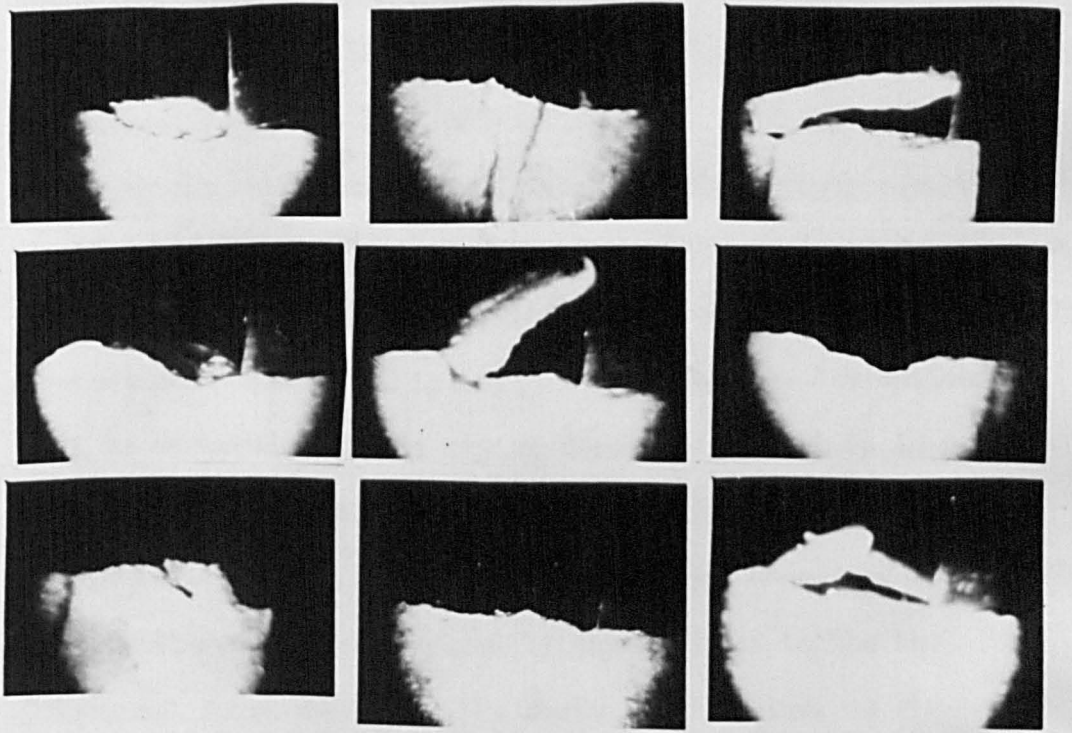
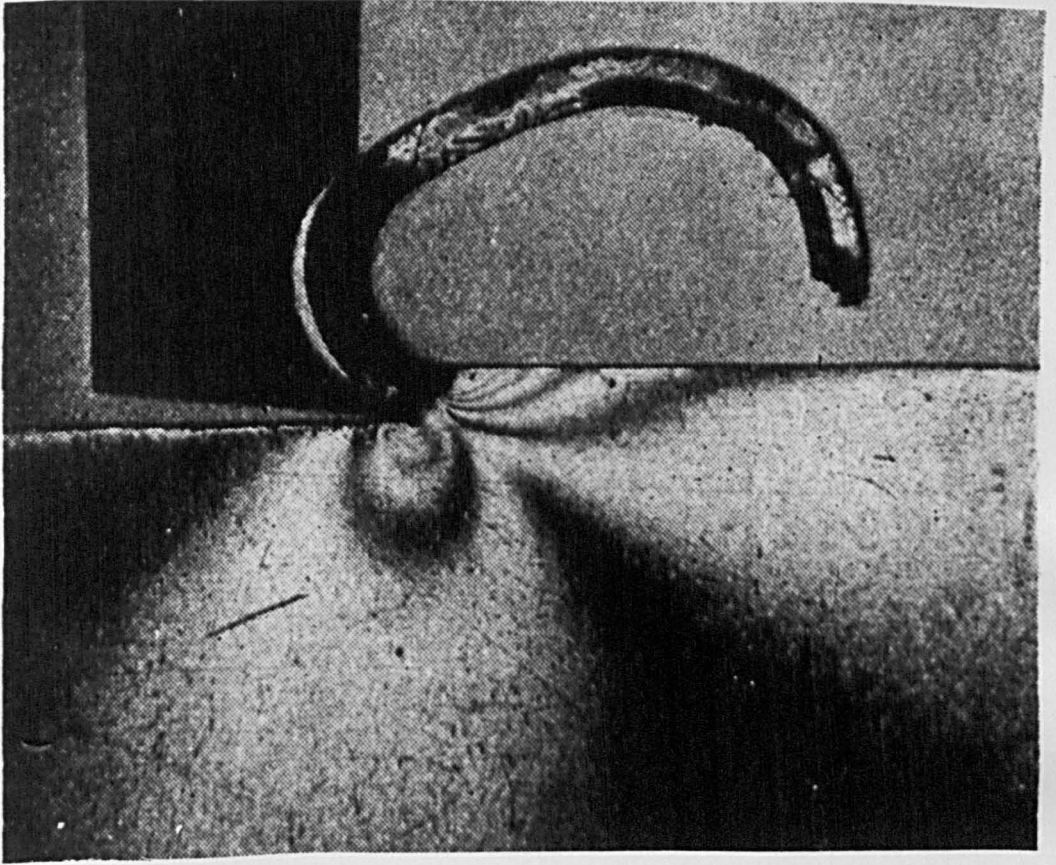


FIG.16 B. TYPICAL FRACTURES.

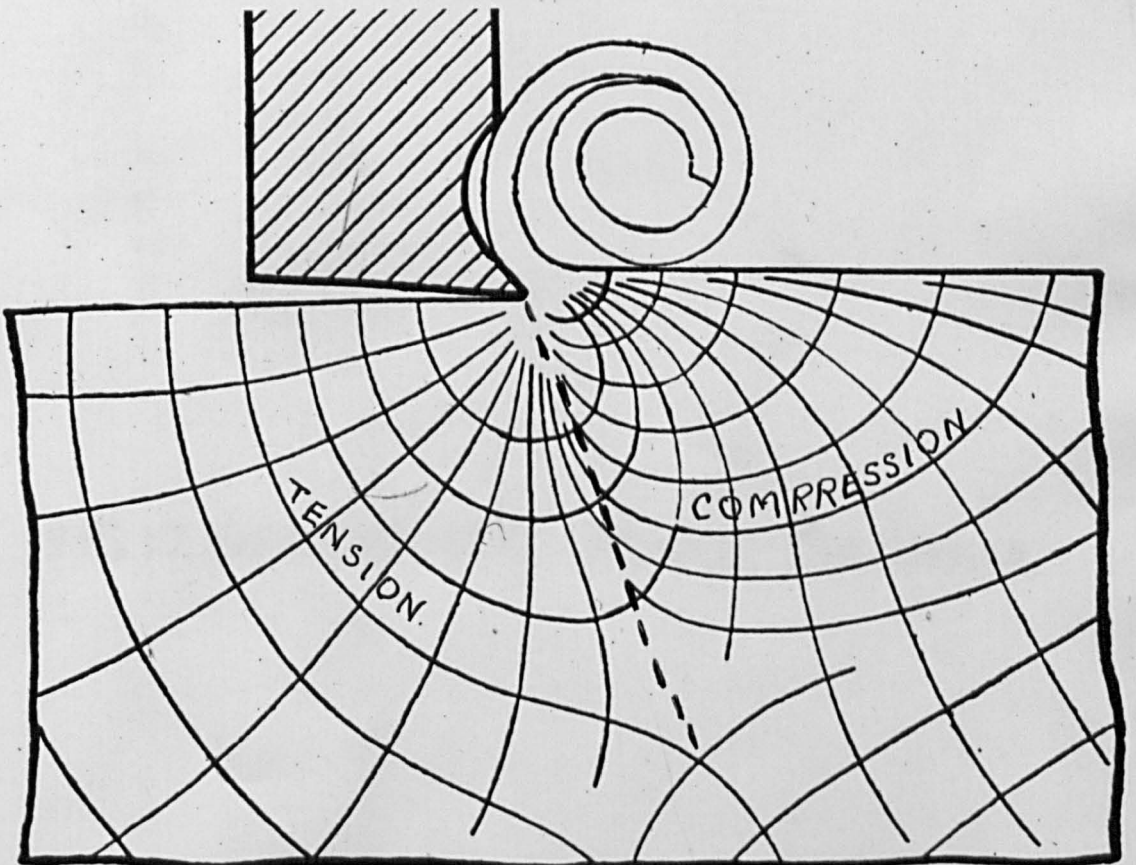
and the rake angle; although later tests to determine the effect of variation in rake angle on the cutting force show that a relationship does exist. The heterogeneous and anisotropic nature of rock is such, however, that instantaneous conditions vary widely with corresponding change in the direction of resultant force and fracture. The effect of any variable must, therefore, be calculated as a probability. Several fractures, for example Fractures 2, 3 and 4 in Test XI 3, Fractures 1 and 3 in Test XI 6, and Fractures 1 and 3 in Test XI 8, indicate that failure may be initiated in Tension swinging through an angle of approximately $40-50^\circ$ to continue in Shear. Others occur directly from the tool tip in shear.

The tool may thus periodically lose contact with the rock as a result of initial tensile fracture which causes rock to be removed below the line of cutting. It is interesting to consider the mechanism of such fractures since their occurrence would appear at first examination to invalidate the force diagram derived by Merchant (Fig.17) and also the stress field obtained by Photoelastic analysis (Fig.18). In both these derivations it will be observed that the region ahead of the tool is in a state of compression in which shear failure alone is possible. It is considered, however, that the tensile stress necessary to initiate this fracture must be supplied by the reaction to the tool face frictional force acting on the rock. This force, as shown earlier, is considerable and may occasionally be sufficient to nullify the compressive stress, replacing it by a resultant tensile stress which, when cutting across weaknesses or points of stress concentration, e.g. cracks or inhomogeneities, is adequate to initiate tensile fracture.

It is noticeable that, although the resultant force inclination at fracture may be much the same, there is a general tendency for the force components to increase with decrease in rake angle, e.g. of Components in Test XI 1 ($+20^\circ$ rake) and Test XI 5 (-20° Rake). This indicates that stresses imposed on the rock as a result of a given force acting in a certain direction are lower for a low or negative rake tool than for a positive. The inference that may be drawn is that the low rake tool has a larger

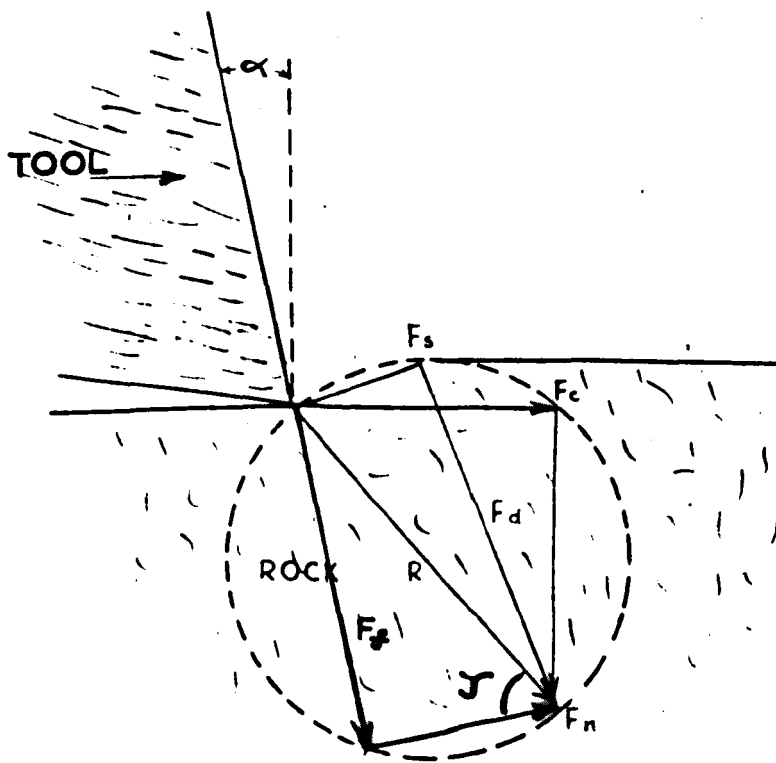


FRINGE PATTERN.



PRINCIPAL STRESSES.

FIG 18.



- | | | |
|----------|-------------|------------------------------|
| F_s | SHEAR FORCE | |
| F_c | CUTTING " | |
| F_n | THRUST " | |
| F_d | NORMAL " | (COMPRESSIVE ON SHEAR PLANE) |
| R | RESULTANT " | |
| F_f | FRICTION " | |
| α | RAKE ANGLE | |
| ϕ | FRICTION " | |

FIG 17. MERCHANT'S FORCE DIAGRAM.

contact area i.e. the degree of "rounding off" of the tip increases with reduction in rake angle.

The examination of major fractures leads, therefore, to the following general conclusions.

Conclusions.

- (1) The angle of fracture is not constant and ~~is~~ is much influenced by lines of weakness and stress concentrations in the rock immediately ahead of the tool.
- (2) Fracture may initially occur in tension from the tool tip causing rock to be removed from below the cutting path. This results in a complete drop of forces on the tip which loses contact with the rock.
- (3) Reduction in rake angle reduces stresses in the rock as a result of the "less sharp" tip. It should be noted that conversely this will produce lower stresses in the tip itself.

Basic Mechanism of Rock Cutting as deduced from the study of the Rock Planing Action.

The only force applied to the rock in planing tests is that acting in the direction of cutting. Immediately the tool starts to cut a component normal to the cutting force, and acting downwards into the rock, is induced on the tool producing a resultant force inclined at some angle below the cutting path.

On consideration it is apparent that this normal component can only be introduced as a result of friction on the front face. The force system at the tip as a result of friction is shown in Fig. 19.

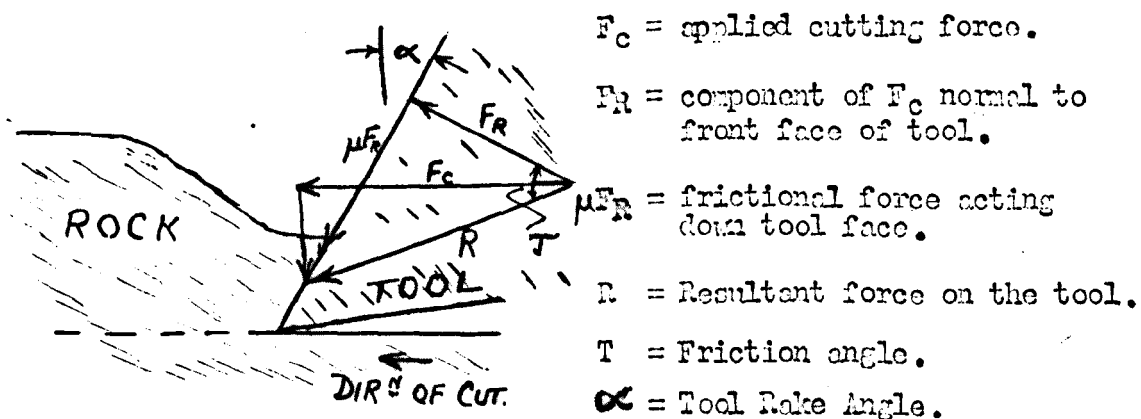


FIG. 19. FORCES ACTING AT THE POINT OF A TOOL.

The inclination, ($T - \infty$), of the resultant below the cutting path is, as has previously been seen, very variable and often attains high values. Extremely high values, i.e. those approaching 90° should be regarded with reserve since they are, for the most part, derived from high indicated values of thrust force (i.e. the vertical component of the resultant) and comparatively low values cutting force where errors in measurement assume maximum importance. The variability and magnitude of these inclinations suggest that the coefficient of friction on the front face is very variable and generally of a high value. It is interesting to note that inclinations greater than -45° are frequent with all values of rake angle used. Thus, in the case of a $+10^\circ$ rake tool, the coefficient of friction is $\tan^{-1} 55^\circ = 1.43$. Such unusually high values of friction coefficients have also been observed in metal cutting. Shaw¹⁴ and his associates suggest that the friction process at the point of a tool is not normal sliding friction and that it varies with rake angle. The explanation is given in more detail in Appendix C. Whether this is also true for rock cutting is not known.

The variable nature of the coefficient of friction is a result of the heterogeneous nature of most rocks. Microscopic examination usually reveals a considerable number of different constituent mineral particles of variable size and orientation. The particular arrangement of crystals and matrix material in contact with the tool tip at any instant is as a result likely to be very variable, and since the frictional properties of each constituent will differ, a variable overall coefficient of friction will result. A further factor which may possibly have some influence is the varying effective hardness of the rock surface in contact with the tool face as determined by the rock behind the surface. This aspect will not be dealt with further since there is no definite indication of the effect in rock cutting. It is considered in Appendix C previously referred to. This wide variation in coefficient of friction has not been observed in metal cutting research, due no doubt to the greater degree of homogeneity exhibited by most metals.

Effect of Abrasive Wear on Under Face of Tool.

Abrasion of the under face of the tool begins immediately the tool starts cutting and it is therefore important to include the effect of wear in any theory. The stress required for fracture may be assumed constant for a given direction of resultant force. Where the contact area is small, as when using a sharp tool, the stresses due to a given force will be high. These will be reduced as the area of contact increases, i.e. as the tool wears; hence the force required to produce fracture stress will be increased in direct proportion to the width of flat worn on the tool.

Effect of Rake Angle.

The force system analysis in Fig. 20 shows the resultant force to be inclined below the cutting path at an angle $(T - \alpha)$, where T = angle of friction, and α = tool rake angle. Assuming constant average coefficient of friction, decrease in the value of α will result in a steeper downward inclination of the resultant force which will then vary the stress distribution such that the maximum shear stress in the region ahead of the tool lies at a lower angle from the direction of cutting. If it is further assumed that the most probable direction of fracture is along this plane of maximum shear stress (or some other related to it, e.g. plane of most effective shear stress), then the reduced angle of fracture line will necessitate an increase in shear force proportional to the increased length of the shear plane.

This theory of rock cutting is an adaptation of basic metal cutting theory modified to incorporate factors observed in rock planing tests carried out by the writer. It may be summarised as follows:-

Summary of Rock Cutting Theory.

1. The direction of the resultant force on the tool tip during cutting is determined solely by
 - (i) the coefficient of friction between the front face of the tool and the rock;
 - (ii) the tool rake angle;
2. The magnitude of the resultant force is directly proportional to the width of flat developed by wear

of the under face.

3. The coefficient of friction varies widely during cutting as a result of the heterogeneous nature of the rock and may attain values greater than unity.
4. The resultant force inclination varies widely during cutting. This is a direct result of (1) and (3).
5. The direction of chip fracture at any time is dependent on (i) the instantaneous direction of the resultant,
(ii) the presence of local heterogeneities and similar stress raisers in the immediate vicinity of the tip.
6. Fracture may occasionally be initiated in tension due to the high frictional force on the tool-chip interface.

Practical implication of the above theory.

An important practical implication of this theory is in relation to the drilling thrust of rotary drills. The magnitude of the thrust (W) required for a given drilling rate in rotary drilling is determined by the following equation (which can be obtained simply from Fig.20) :-

$$W = K.a. \sin [T - (\alpha_a + \delta)]$$

where K is a constant involving the mean shear stress to cause fracture along the shear plane.

T is the angle of friction at the tool chip interface.

α_a = nominal rake angle of drill bit.

δ = inclination of helical path.

a = mean width of flat on under face of bit.

N.B. $(\alpha_a + \delta)$ is the effective rake angle.

Of these angles the most important is the friction angle, reduction of which could considerably reduce the thrust required for a certain drilling rate. Reduction in coefficient of friction may be obtained by

- (a) the use of hard and smooth metals at the tool tip, e.g. tungsten carbide,
- (b) the use of lubricants. The high contact pressures

between the tool and rock on the front face will probably necessitate high pressure lubricants.

Since drilling thrust is regarded by some authorities as being a probable limitation to rotary drilling the use of lubricants appears to be a possible effective means of either reducing the thrusts required to drill at a certain rate or conversely increasing drilling rates for a given thrust.

Investigation of the effect of variation in the conditions of cutting.

As already explained, the complex nature of rotary drilling does not allow the effect of individual variables to be readily determined. Elimination of rotational effects resolves most of these difficulties and a much closer control of variables is possible. The results may then be modified to incorporate rotation and will thus indicate the actual effects in full-scale drilling.

The variables investigated were:-

1. Tool Rake Angle.
2. Depth of Cut.
3. Width of Cut.
4. Number of Free Faces.
5. Angle of Obliquity of Tool.
6. Speed of Cutting.
7. State of Wear of Tool.

Rocks were selected from various localities in order to ensure that the results obtained were not to a particular rock type. Power limitations of the milling table motor prevented the testing of rocks of more than moderate hardness.

Rocks used are shown in Table ~~14~~.

The results now presented are not intended to provide accurate quantitative information. As has been shown earlier, conditions vary considerably during cutting and several tests of long duration are required before reliable quantitative data may be obtained. It was first desirable, however, to eliminate those factors which have no significant effect so that detailed and

thorough testing of those shown to have most influence may then be carried out. These tests should therefore be regarded as indicating general trends to indicate the most ~~xxx.~~ ^{important} variables.

Presentation of Results.

Test results were initially obtained as a series of dial readings recorded on cine-film. It was considered impracticable to tabulate these individually in the thesis, the total number of readings being approximately 40,000. Mean force values for each test have been determined and tabulated. Although considered most satisfactory, this method of presentation occasionally fails to reveal some important detail. Where this is so the individual values have been plotted and the graph included.

1. Effect of Variation in Rake Angle.

Five Rake Angles:- $+ 20^\circ$, $+ 10^\circ$, 0° , $- 10^\circ$, $- 20^\circ$ were used. Full test details and results are contained in Table 2. (See Section 6.) and shown graphically in Fig. 20. These confirm the result predicted by theory that, where other factors remain constant, increase in rake angle results in reduced forces due mainly to the overall reduction in downward inclination of the resultant force on the tool.

2. Effect of Variation in Depth.

Four depths of cut were tried at 0.025" intervals up to .100" beyond which stalling of the motor occurred. It was noticeable when cutting at increased depths that the tension-shear type fracture became more frequent, being especially prevalent at the highest depth when the resultant cut surface was severely pitted. This results in more severe oscillations of force, and since rock is effectively 'cut' to a somewhat greater depth than that noted the results appear erratic. These are shown in Table 3 and Figs. 21 and 22. No definite correlation is possible and longer tests are desirable. The general indication, however, is that peak loading values are somewhat more than proportionately increased with depth due to the increased probability of tension initiated fractures. It should also be noted that the rapid release of a heavy peak load on a cutting tool results in acceleration of the tip at a rate

dependent on its stored energy. Thus severity of impact will be more than proportionately increased with depth, a fact of importance in rotary drilling where impacts should be minimised.

3. Effect of Variation in Width.

When cutting in the body of a rock, i.e. with only one surface free, it is necessary to fracture rock from the sides as well as the base of the cut. Tests were conducted to ascertain whether this side fracture, which remains constant independent of the width of cut, has any significant effect of what would otherwise be expected to be a linear relationship. Results tabulated in Table 4 and plotted in Fig. 23, generally seem to indicate no significant effect however, although the results from Rock 2 at 0.075" depth of cut would appear to contradict this. This should, it is felt, be rejected in favour of the relationship shown by the other tests since Rock 2 is very heterogeneous and results are more likely to be inaccurate. These tests seem to indicate, therefore, that reduction in width of cutting tool will produce a pro rata reduction in force for a given depth of cut over the practical range of tool width. This last remark is added since it is not thought that this would be the case for very narrow tool widths.

4. Effect of Variation of the Number of Free Faces.

Where the cut is being taken in the body of the rock the applied force must be sufficient to cause fracture across the sides as well as from the base of the cut. Where two free faces exist one side only must be fractured together with the base, whilst where three free faces are present fracture takes place from the base only. The three conditions are illustrated diagrammatically in Fig. 24(a). Tests results are shown in Table 5 and graphically in Fig. 25. These demonstrate that the reduction in force possible may be considerable, the effect apparently becoming more marked with greater depths of cut. This is of considerable importance since it indicates a possible development of drill bit design which would step up drilling rates without increased impact severity. The pilot and reamer bit is a practical application of this principle. In this the gap between standard bit legs is replaced by a small bit in advance of the main cutting edges to cut out the

core and enable most of the cutting to be to two free faces. This type of bit has been recently shown to result in increased drilling rates.^{12.}

5. Effect of Variation in Angle of Obliquity.

The front face of a bit or tool is usually at 90° to the direction of cutting. If, however, it is turned to some angle other than 90° the angle through which the face has been turned is termed the Obliquity Angle. The principle of oblique cutting is illustrated in Fig. 24(b). It was decided to investigate this factor since it was felt that, as obliquity increases the effective rake angle, (See ^{Appendix 3.} ~~Appendix 3.~~ Fig. 28), reduction in the forces necessary to cause fracture would be obtained. The values of obliquity, -20° , -40° , -60° , were used in addition to the normal, or 0° obliquity tool, all taking the same width of cut, i.e. the actual cutting edge was increased proportional to the sine of the obliquity angle. All cuts were taken with one free face only. Test results are tabulated in Table 6 and plotted graphically in Fig. 26. from which it can be seen that in fact the forces, after an initial slight fall, tend to increase with obliquity. It was observed whilst cutting that fracture of that side of the cut towards which the tool was turned became increasingly marked with obliquity, and it is thought that the additional force required to cause this exceeded any reduction due to increased rake angle, this latter probably being the cause of the initial reduction. The oblique tool thus directs stress in the direction normal to the cutting face. If one considers the small vertical cutting edges (i.e. those edges that form the wall and core of a borehole) at each end of the cutting leg, (A and B in Fig. 24(b)) it will be seen that the normal tool has a zero rake angle at each end, whereas the oblique tool has effectively positive rake at the outer edge B and a negative rake at the inner (A). Thus the stress required to cut edge B will be reduced and that to cut A increased. From these results it would appear that the negative increase outweighs the positive decrease with high obliquity. This, contrary to initial indications from the graph, may prove a useful principle in rotary drilling for the following reasons:-

1. The stress is directed to give more effective breaking of the core associated with U-bits and it should therefore be possible to design bits with a somewhat larger core diameter, hence reducing the actual width cut. The reduced width would, in turn, increase the axial stress component for a given thrust.
2. Oblique cutting in rotary drilling is obtained by effectively "stepping back" the cutting edges from the position they occupy in normal orthogonal cutting. (See ~~Fig 32~~ ^{Fig 32} ~~Fig 32~~). This will allow more efficient clearance of cuttings.
3. Due to rotation the effective obliquity increases as the centre of rotation is approached. The relationship is expressed by the following equation (derived in Appendix 3).

$$\sin \lambda_1 = \frac{r_1}{r_2} \sin \lambda_2$$

where λ_1 is the angle of obliquity at radius r_1
 λ_2 " " general angle of obliquity at radius r_2
 r_2 is the radius to the centre of the bit leg

Thus the "stress directing effect" increases towards the core.

4. Where cutting with two free faces it would appear that the forces will be reduced with obliquity, since there is no side restraint to increase the fracture forces. It would also seem probable that the effect observed by Stabler, referred to in Section I, Page 20, and in Appendix 3, would take place.

Effect of Wear.

The manner in which wear modified the cutting operation was determined in the following manner. A $\frac{1}{8}$ " wide tool of high speed steel, having zero leg rake angle and 7° clearance angle, was set up in the dynamometer to take a cut of 0.050" deep across a sample of Darley Dale Sandstone, a moderately homogeneous but abrasive rock (Rock 5). Starting with a sharp tool, the mean width of flat (average of 12 readings across the cutting edge)

worn on it at the end of the run was measured by means of a travelling microscope (accuracy of measurement ± 0.0005 in.) (See Fig. 27). A second cut was then taken with the same bit and the wear again measured. This was repeated until there was little further measurable increase in width of flat. Cine-camera records of the dynamometer readings were made for several of the runs to indicate how the forces were affected by wear.

Results are shown in Table 6 and plotted graphically in Fig. 28(a). These demonstrate that, as predicted by cutting theory, the forces vary directly as the width of flat developed. The rate of wear does not appear to obey any simple law but rather to involve an exponential or logarithmic function, since the points when plotted on logarithmic scales still form a curve as shown in Fig. 28(b). The graph demonstrates the rapid rate of initial wear of sharp tools emphasizing the importance of hard alloy cutting tips.

Variation in Speed of Cutting.

Results (shown in Table 7) indicate no significant variation over the low speed range of the milling table, apart from the somewhat more rapid rise in forces up to peak values. The table speeds are much lower than those in rotary drilling, and strain gauge apparatus (described later) was designed to ascertain whether the above results obtained from the milling table were valid at the higher speeds. These later experiments show that the characteristic force distance curves are basically unchanged.

General Conclusions.

Tests indicate:-

1. Increase in Rake Angle reduces the mean forces required for a given depth of cut.
2. The forces required for fracture under a given set of conditions vary directly as the state of wear of the under face of the cutting tool.

The above two facts confirm the theoretical predictions made earlier.

3. Within the range of tool widths tested (which is also the practical range) the forces required for fracture at a

given depth of cut vary directly with the width of the tool.

4. Deep cuts result in a somewhat more than proportionate increase in peak forces, this being considered to be due to increased probability of fractures initiated in Tension. Impacts of the tool on release of load are consequently also more severe.

5. Considerable reductions in force required for drilling at a given rate may be obtained by

(i) employing the principle of two-free face cutting where possible. (e.g. by the use of pilot and reamer bits).

(ii) by the use of oblique bits.

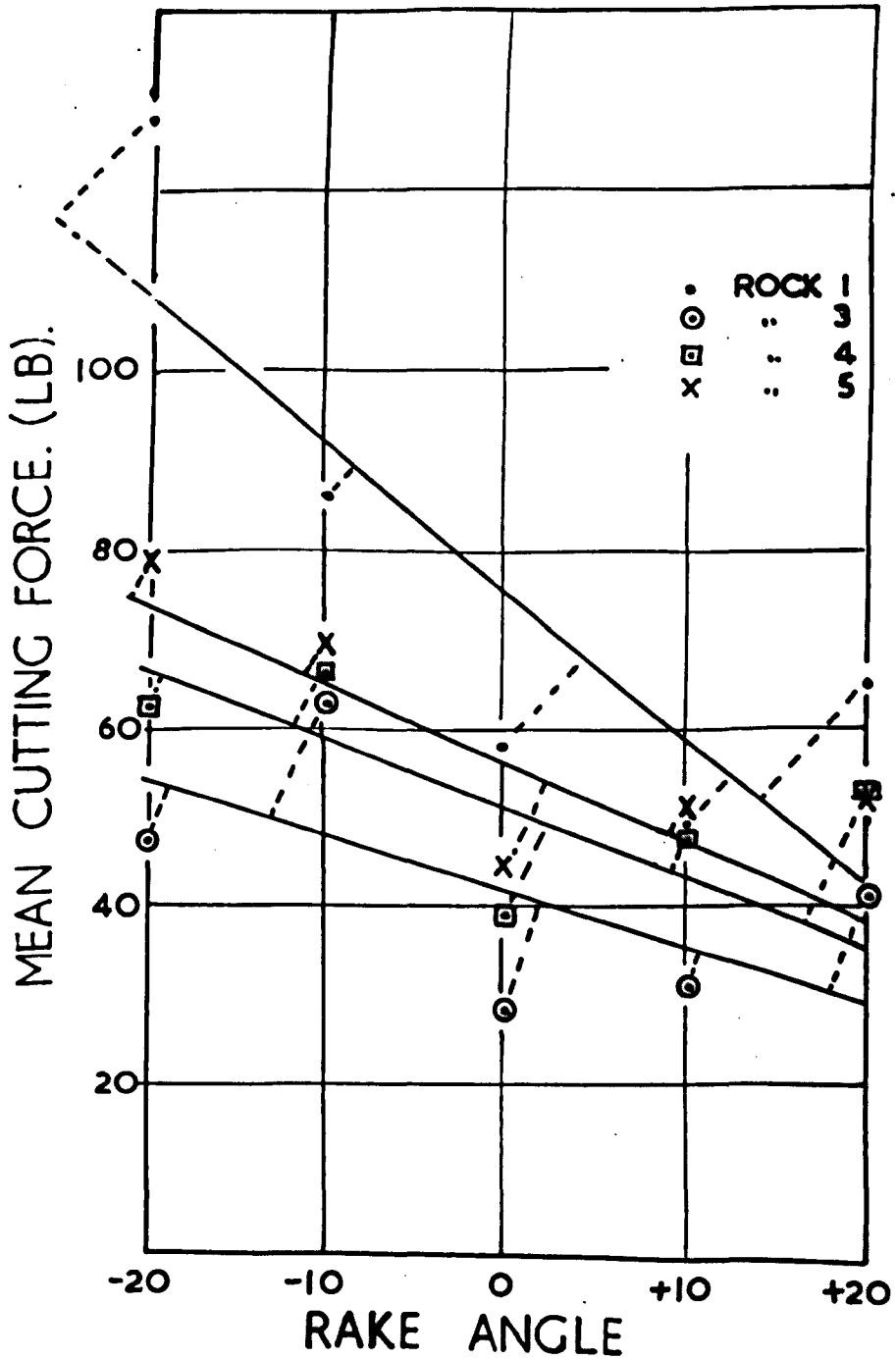


FIG 20. EFFECT OF VARIATION OF RAKE ANGLE

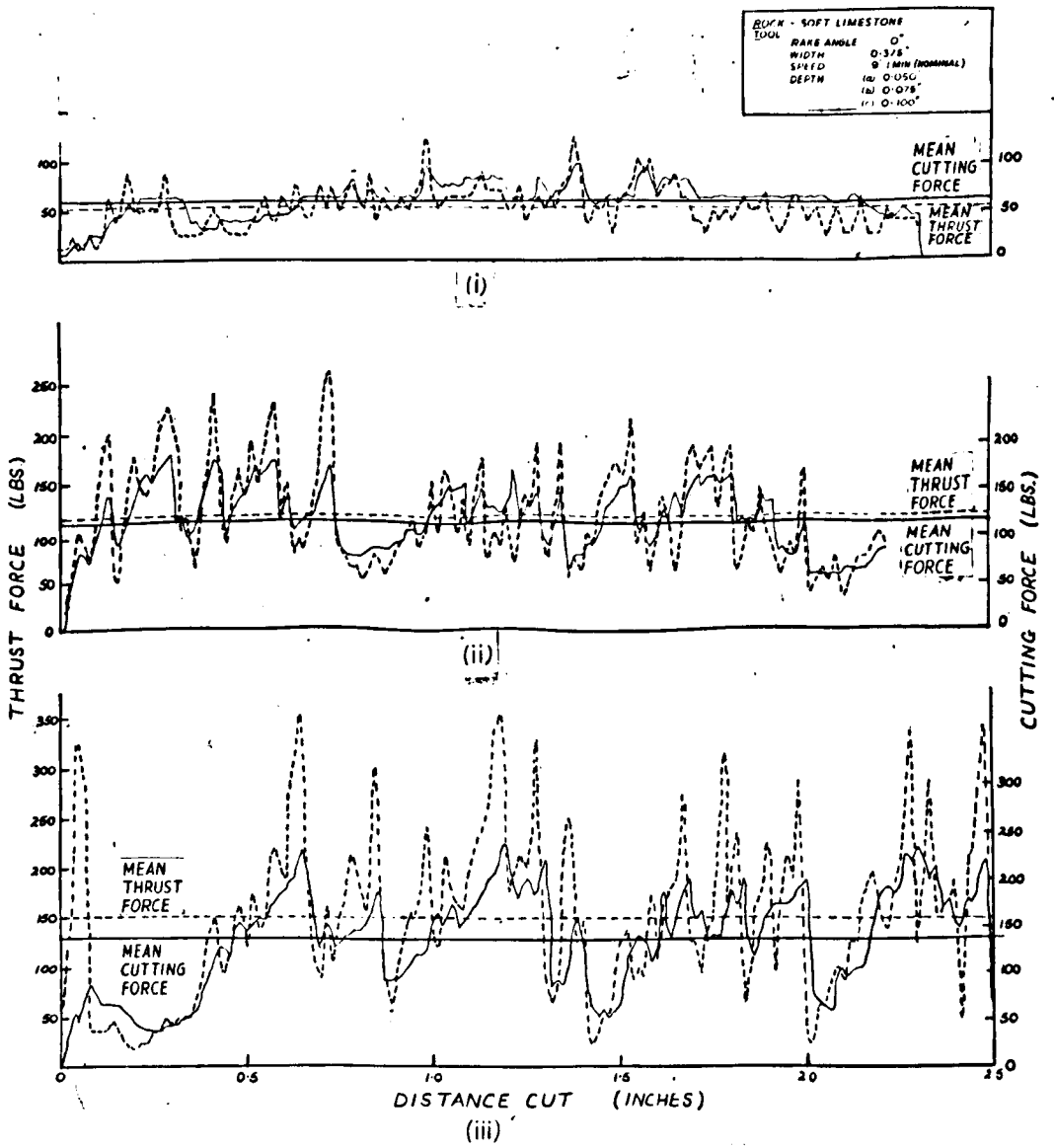


FIG 21. EFFECT OF VARIATION OF DEPTH.

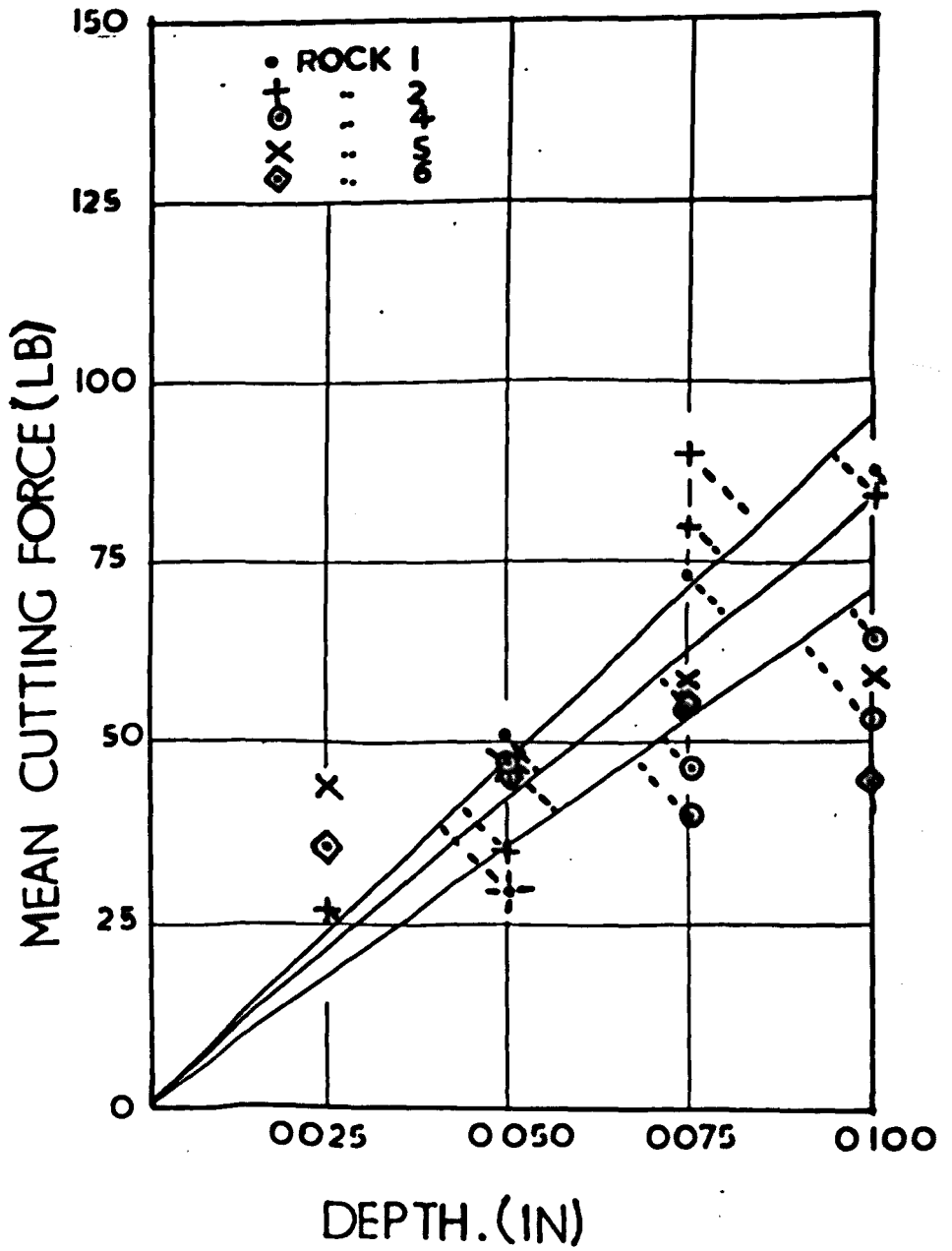


FIG. 22. EFFECT OF VARIATION OF DEPTH

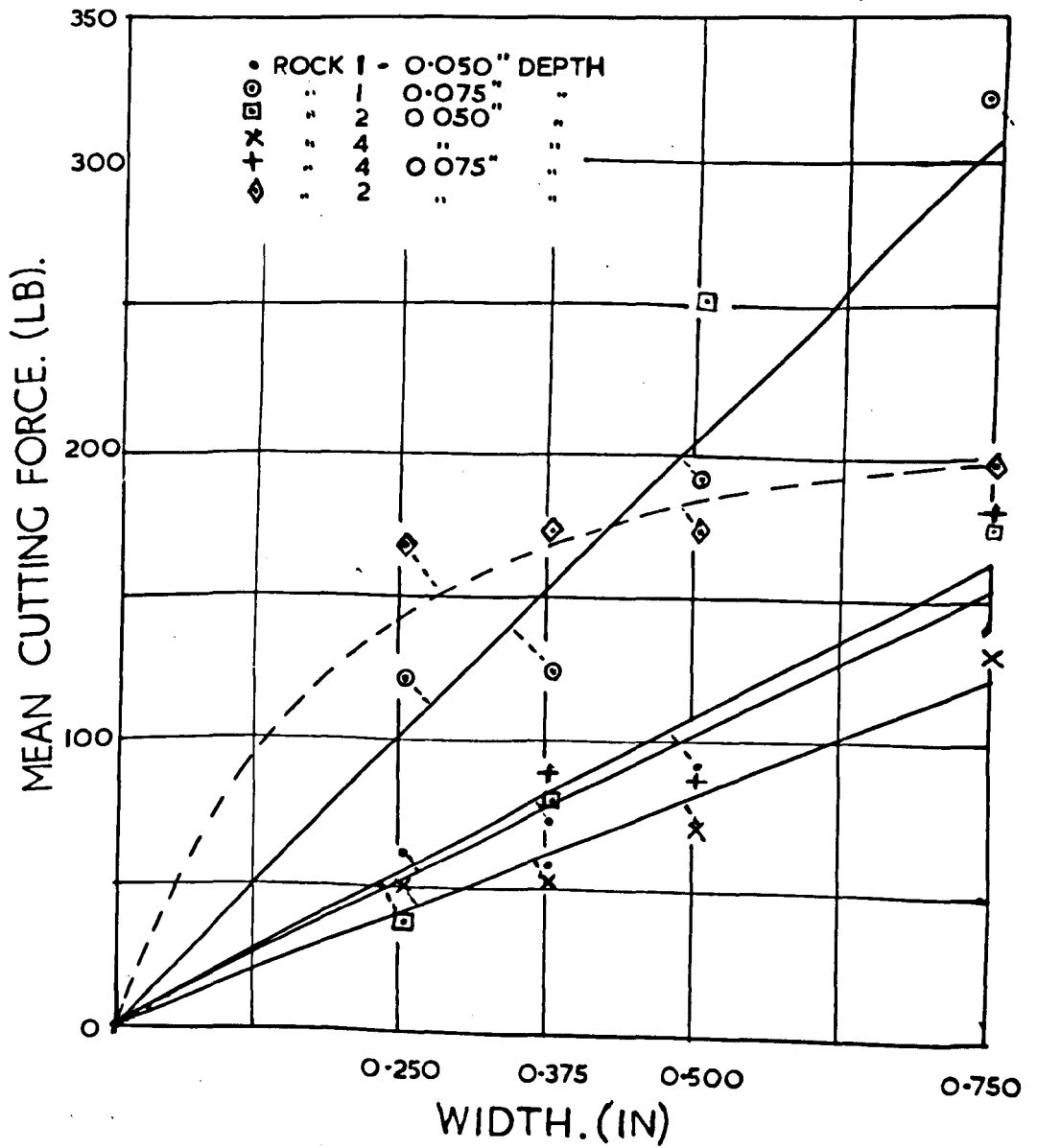


FIG 23. EFFECT OF VARIATION OF WIDTH OF CUT

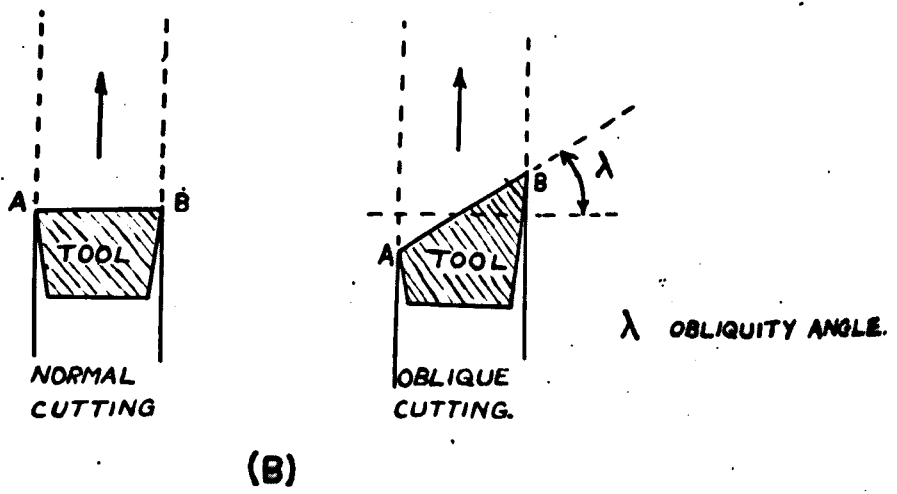
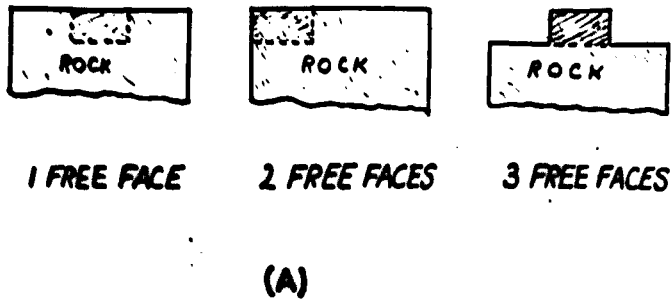


FIG 24. TO ILLUSTRATE (A) VARIATION OF FREE FACES.
(B) OBLIQUE CUTTING.

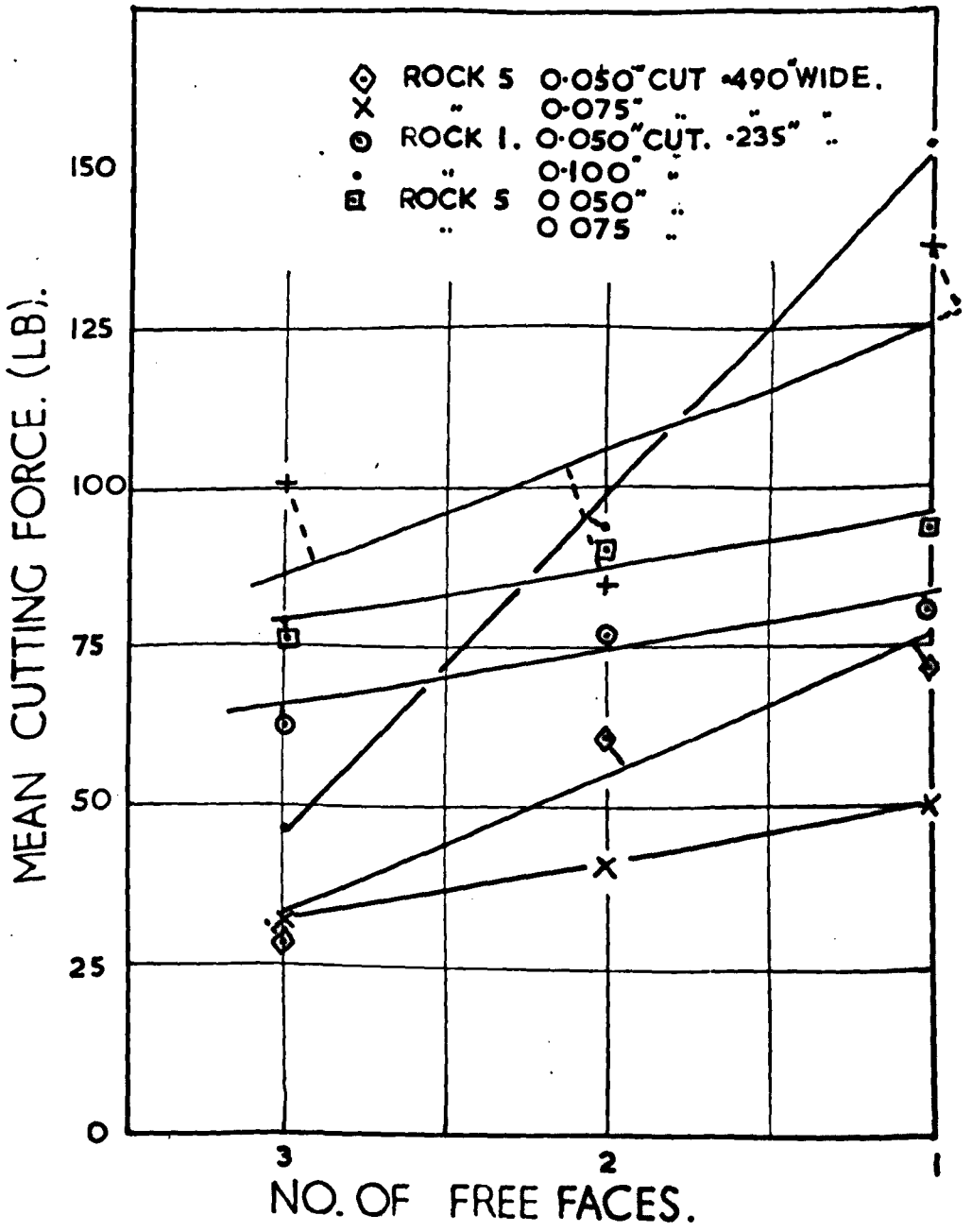
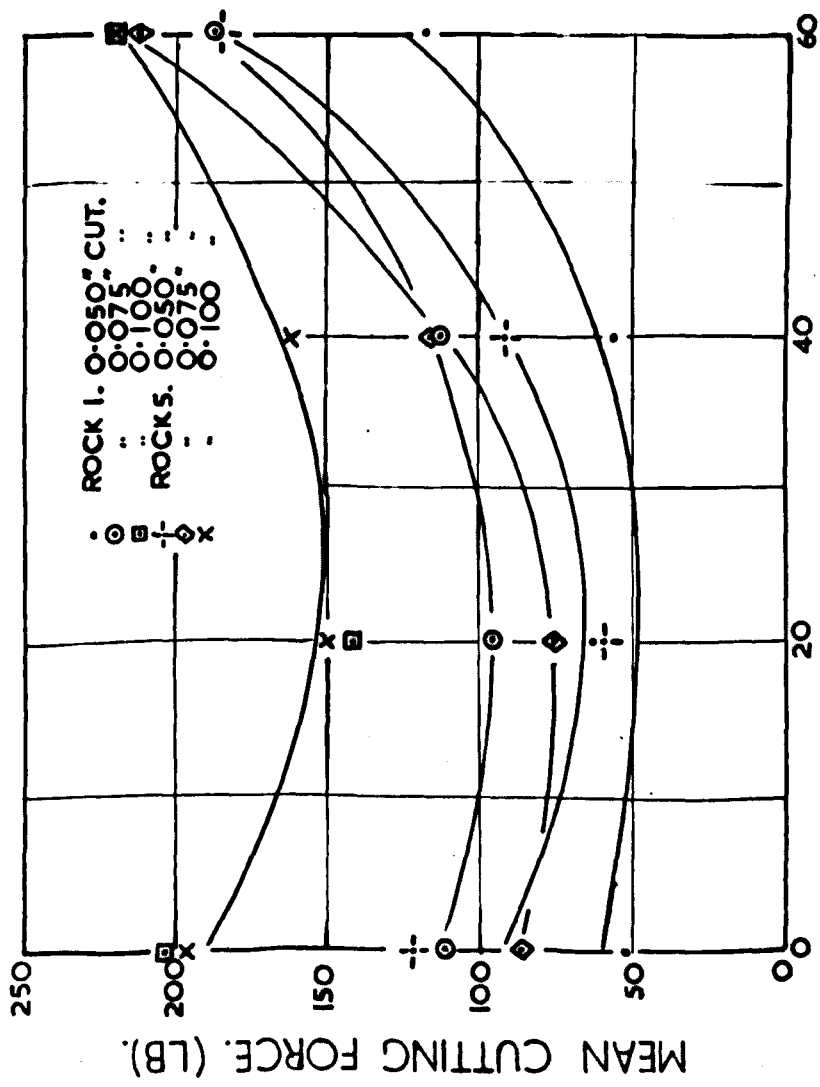


FIG. 25 EFFECT OF VARIATION OF NO. OF FREE FACES



ANGLE OF OBLIVITY

FIG. 26 EFFECT OF VARIATION OF ANGLE OF OBLIVITY

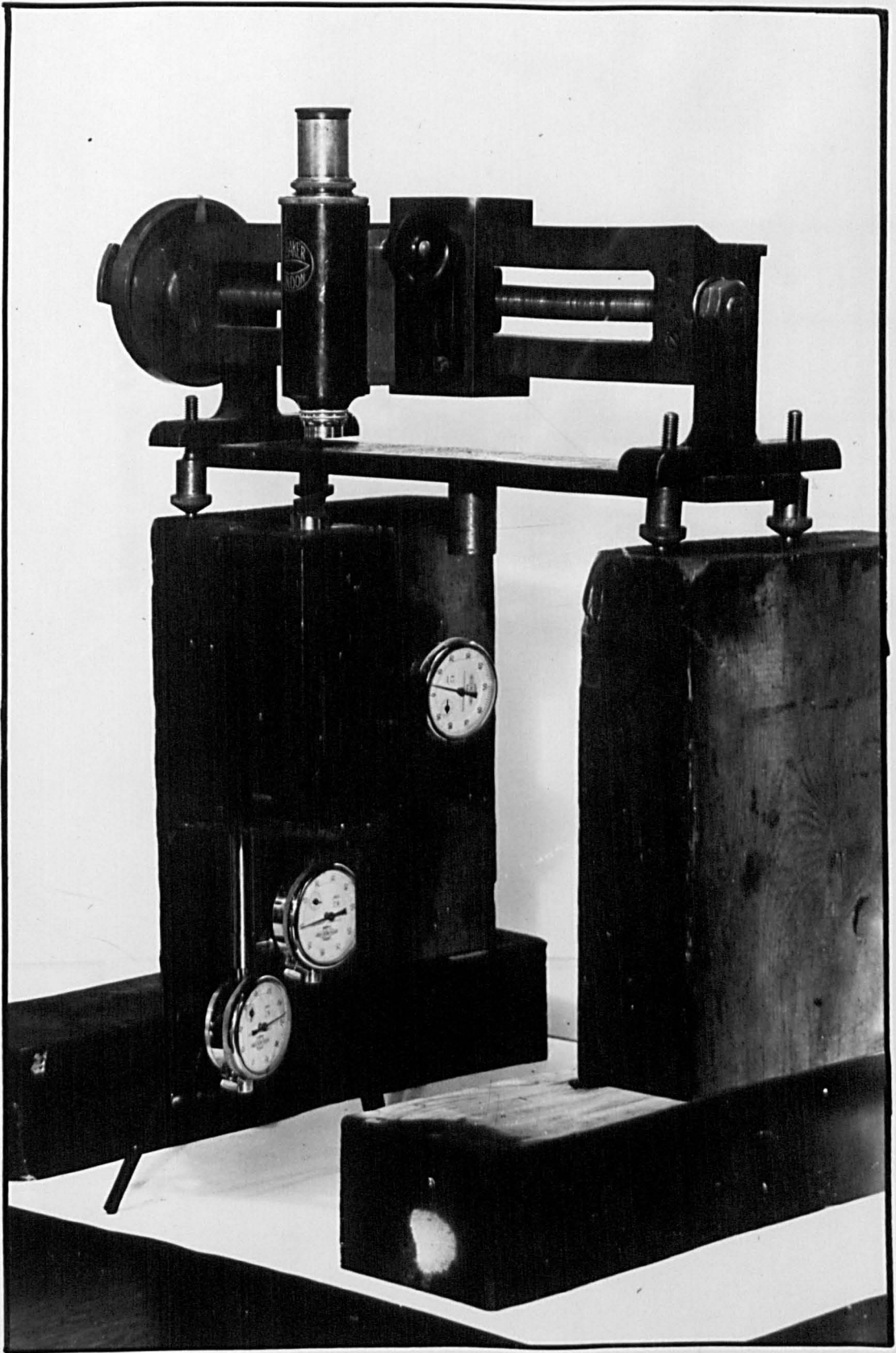


FIG.27. WEAR MEASUREMENT APPARATUS

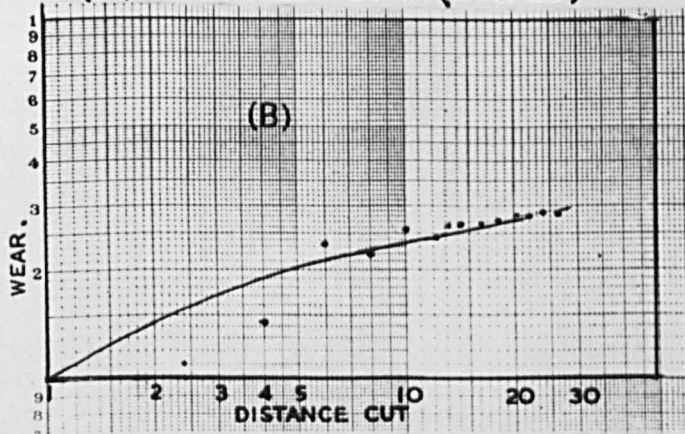
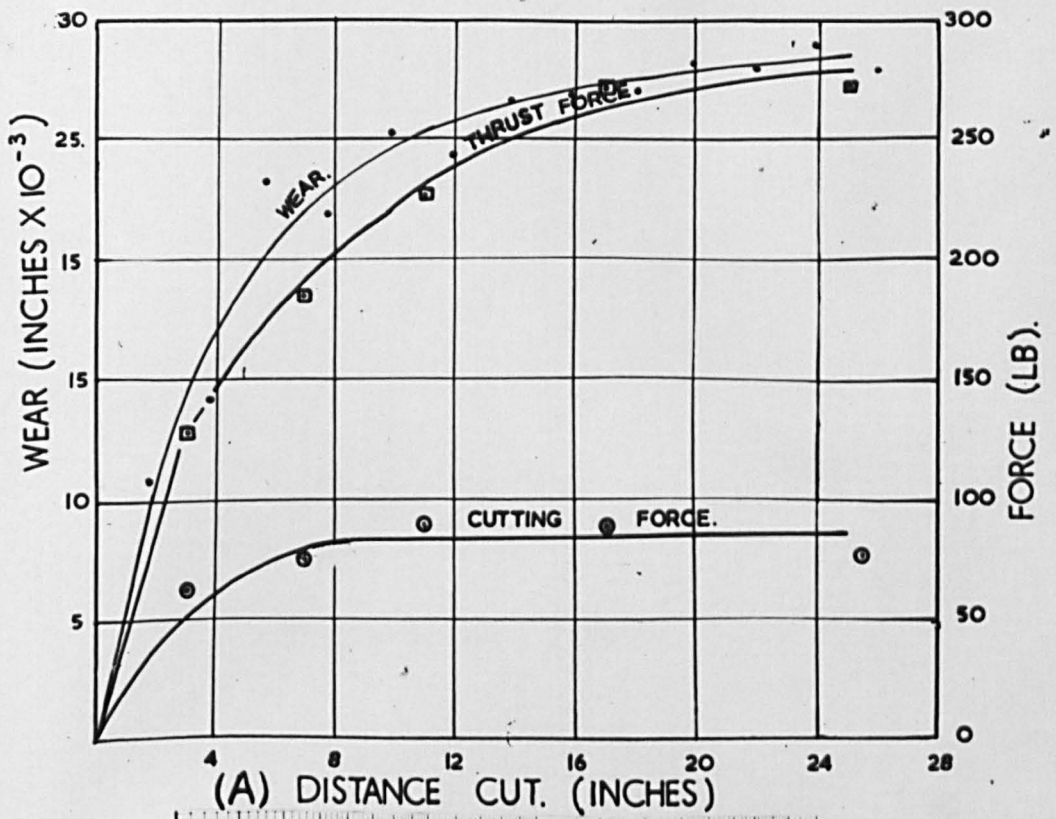


FIG 28. EFFECT OF WEAR.

SECTION III.

ROCK DRILLING TESTS.

ROCK DRILLING TESTS

Apparatus.

Existing rock drilling apparatus, used for earlier research in the Mining Department, was in the process of conversion to enable it to be used for drilling tests at thrusts beyond the range of 600 lb. when the writer commenced investigation. This consisted of a $1\frac{1}{4}$ H.P., 125 v. Siemens-Schuckert rotary drill with nominal rotary speeds of 320, 430, 500, 600 R.P.M. mounted between two horizontal round steel guides, $1\frac{1}{2}$ " diameter in an angle steel framework. The thrust, previously from a 3" diameter air-leg cylinder was now supplied by a 9" diameter cylinder with a 4' long ram attached behind the drill motor. A penetrometer (Fig. 29) designed by Dr. Shepherd had been installed to record instantaneous drilling rates. It consisted of a 3" diameter drum approximately 2'0" long which rotated at a constant speed of 1 R.P.M., driven by a fractional H.P. single phase A.C. motor, and a stylus (B) (a ball-point pen mounted in a holder) which traversed the length of the drum, driven by a feed-screw (C). A wire (E) attached to the drill motor was lapped around the pulley (F) and held taut by a dead-weight suspended from the wire behind the apparatus. The pulley (F) was connected through gears to the feed screw which thus rotated as the drill machine advanced, drawing the stylus over graph paper wound around the drum. In this way a continuous record of the drilling rate during a test was obtained. Constants for the penetrometer graph were:-

1" horizontally on graph = 2.375" hole depth.

1" vertically " " = 6.32 secs. drilling time.

Further modifications were found necessary as a result of introducing the larger ram, viz.

1. Replacement of air-leg control valve by one of higher capacity due to excessive pressure drops across it. (V in Fig. 29).
2. Provision of a pressure gauge attached to the forward inflow end of the ram cylinder and set in the control table. (G in Fig. 29).

Torque and Rotary Speed Determinations.

It was considered essential, for the correct interpretation of drilling test results, to devise some means of measuring instantaneous fluctuations in drilling torque and rotary speed. Previous workers had employed the principle of suspending the drill motor in bearings and measuring the torsional forces on the motor by means of spring balances fixed to prevent rotation of the motor casing. This method was not adopted, however, since it was considered that vibration of the drill frame would make reading of the spring balances extremely difficult. Further it would require additional and cumbersome apparatus. It was therefore decided to determine the brake characteristics of the motor before commencing drilling tests, calibrating them against input electrical power. By this means it would then be necessary only to note the three-phase power input in order to ascertain the rotary speed and drilling torque.

Brake Characteristics of the 1¹/₂ H.P. Drill Motor.

The Brake Test apparatus consisted of a Cast Iron Pulley 1'0" diameter, 3" wide fitted with a 1" diameter shaft that engaged in the driving chuck of the drill motor. Two wood brake-shoes, lined with Ferodo brake lining were designed to fit around the drum, braking pressure being applied by tightening the shoes together through bolts. A lever arm 4'0" long attached to the lower shoe and resting on a beam balance enabled the braking torque to be measured. Measurements of rotary speed were taken by tachometer from the brake drum spindle. By this means the torque and speed characteristics, using power input as the base, were obtained for the working range of the motor. Results are shown tabulated in Table 9 and graphically in Fig. 30.

From the results it is obvious that the fall in speed is considerable over the working range, demonstrating the necessity of having some indication of instantaneous torque and speeds. It was also apparent from work of earlier investigators that the motor torques would be inadequate for drilling hard rock and a higher H.P. motor was purchased as a replacement. Unfortunately no variable speed drill motor was available and it was necessary to use a 5 H.P.

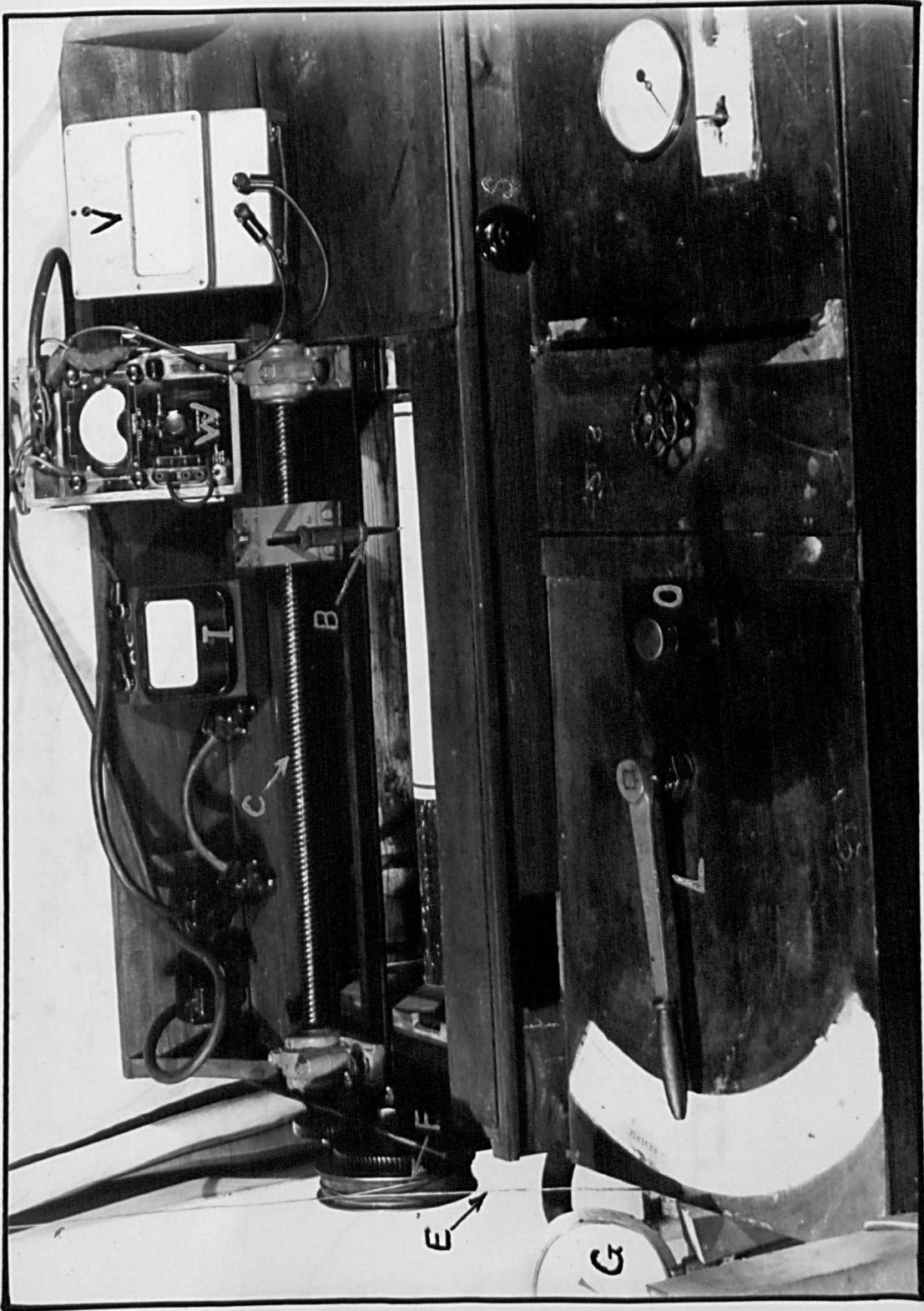


FIG 29 DRILL CONTROL PANEL.

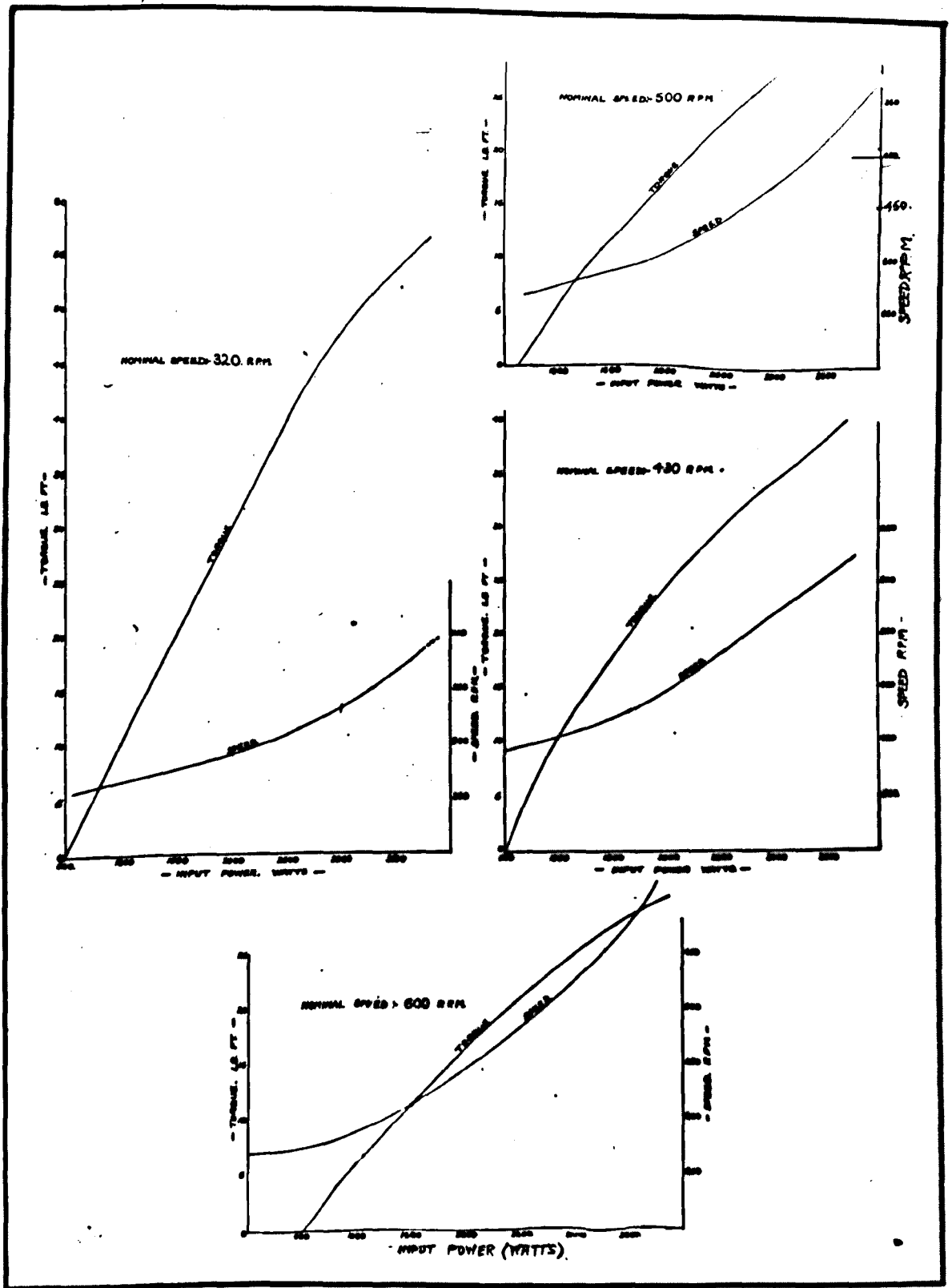


FIG.30.CHARACTERISTICS OF 1/4 HP DRILL MOTOR

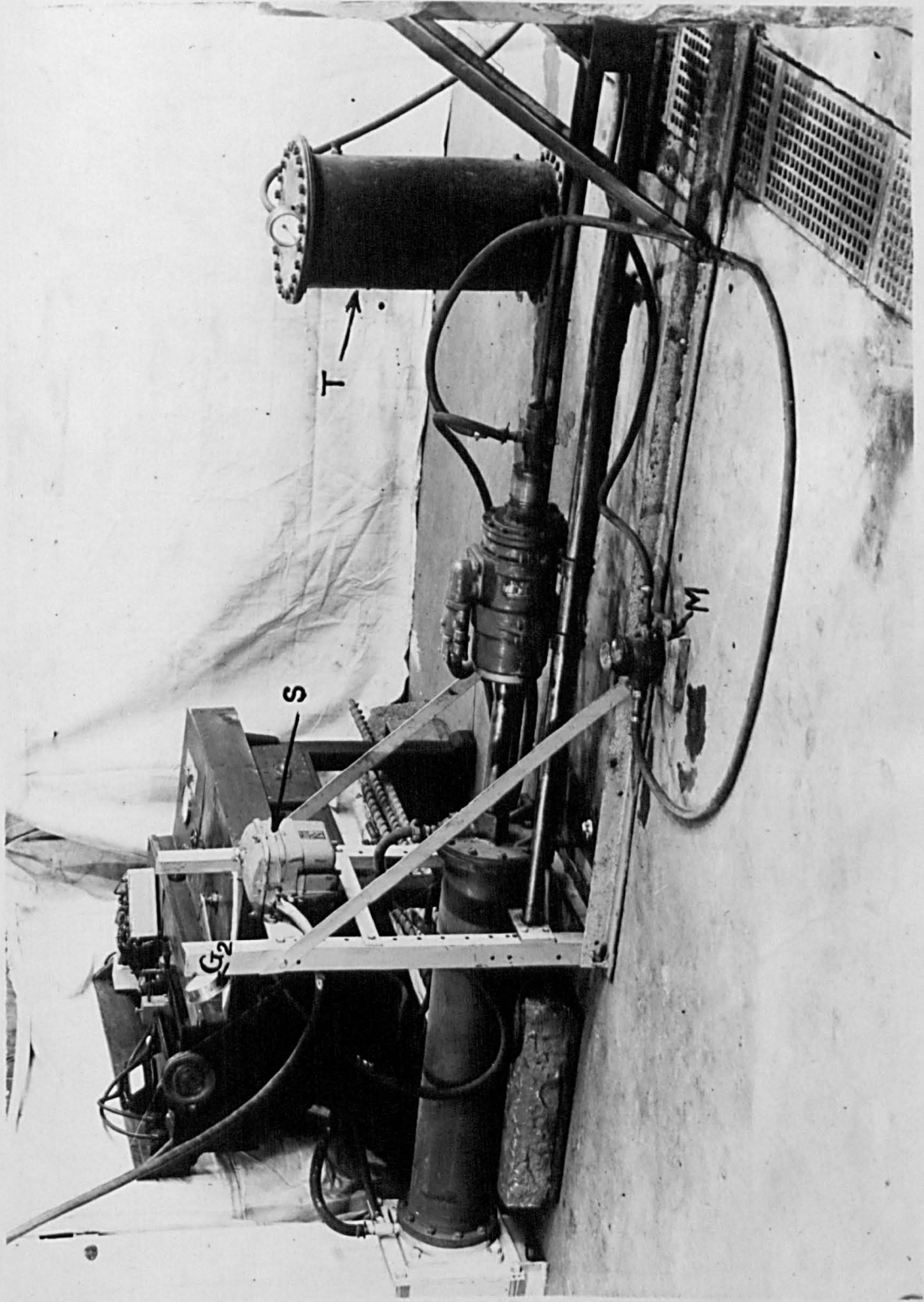


FIG 31. FULL SCALE DRILLING RIG.

Hardypick track motor (as used for driving the tracks on the Hardypick drifter) adapted for drilling by fitting a standard wet drilling chuck to the final drive shaft. Rotary speeds available by gear changing were 62.5 and 125 R.P.M.

Since the motor was to be used under heavy axial thrusts, tests were carried out at the Hardypick works to determine the effect, if any, of these thrusts on the bearings. It was found that there was no perceptible increase in power input to the motor when loaded with a direct hydraulic thrust of 1,500 lb., thus effectively demonstrating the efficiency of the thrust bearings used in the adapted drive head.

Introduction of the Hardypick motor necessitated several modifications to the drilling test apparatus, viz:

1. Replacement of the $1\frac{1}{2}$ " diameter guides by similar rods $2\frac{1}{2}$ " diameter to support the increased weight.
2. Mounting of the motor on top of slides on the guides to facilitate gear changing.
3. Changing to 400 volts supply incorporating an Ellison starter (S in Fig. 31) with overload trip coils and no-volt release.

The ram was attached behind the motor such that the thrust was transmitted to the drill-head through the casing with no direct load on the rotor shaft.

The final drill test apparatus is shown in Fig. 31. In addition to parts already described it includes:-

1. Water tank (T) of 15 gallons capacity in which water was stored under compressed air of 90 lb/sq.in. for wet drilling; together with a control tap to regulate outflowing water pressure.
2. Water flow meter (M) to measure the rate of flow of flush water.
3. Bourdon pressure gauge (G2) to measure the water pressure at inlet to the wet attachment. The gauge was fitted to the control table so that any blockage of water flow could be immediately

detected by a rise in water pressure at the inlet.

4. Electrical instruments

- (i) 3 phase wattmeter to measure input electrical power (W).
- (ii) 0 -600 V Voltmeter (V) to note any voltage fluctuations which may affect motor characteristics as determined.
- (iii) A.C. Ammeter (I).

Also visible on the control desk (Fig. 29) is the forward-reverse lever to the ram (L), the ram oil feed (O) and the switch to the penetrometer drum motor (S).

Determination of Brake Characteristics of 5 H.P. Hardypick Drill Motor.

In view of the high drill chuck torques developed by the 5 H.P. motor it was impracticable to obtain the brake characteristics in the manner used for the $1\frac{1}{4}$ H.P. motor. Similar apparatus was therefore constructed at the Hardypick works which enabled them to be determined direct from the rotor shaft.

The drill chuck speed (i.e. speed through reduction gears) on no load was observed by tachometer and the corresponding rotor speed noted. This gave a direct conversion factor by which the drilling torques for given inputs were calculated, viz.

$$\frac{\text{Drill Chuck Speed}}{\text{Rotor Speed}} = \frac{63.5}{1490}$$

$$\therefore \text{Drilling Torque} = \text{Rotor Torque} \times \frac{1490}{63.5}$$

Results are shown in Table 10 and the characteristics plotted in Fig. 34 A

Test Procedure.

1. The rock to be drilled was set in position in front of the drill frame and rigidly staked against the wall to prevent any movement during drilling.
2. The hole was drilled to a depth of approximately 1", using an old bit to avoid damaging the bit to be used for the test. Each hole was started or "collared", using

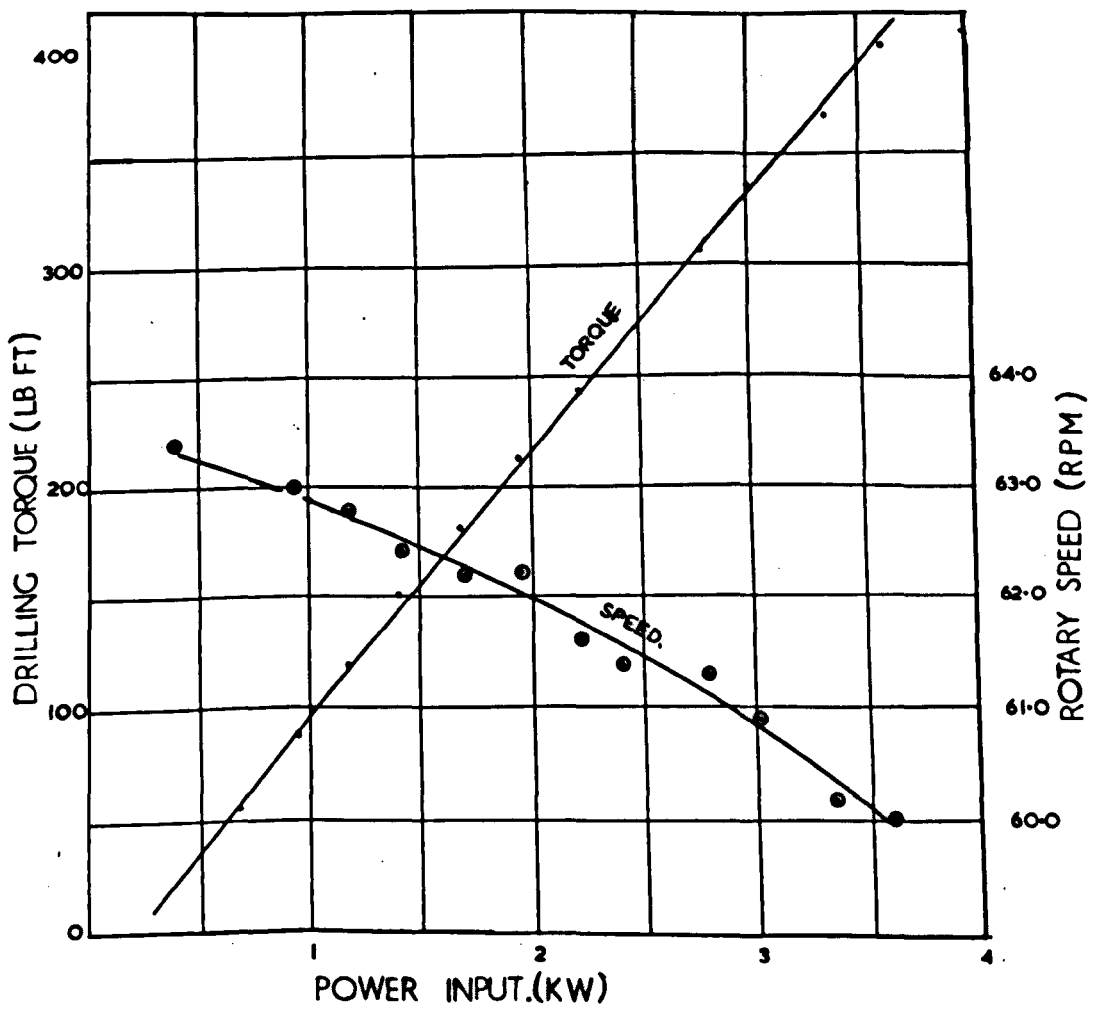


FIG 31A CHARACTERISTICS OF 5. H. P.
HARDYPICK DRILL MOTOR

guides to ensure correct centralisation.

3. Full details of the bit, rod, etc. were noted on a data sheet.
4. The drill rod with the test bit was then set up in the drill machine and advanced to the hole ready for drilling.
5. When wet drilling, the inlet water pressure was adjusted.
6. The Penetrometer drum was loaded, the pen set on the paper and the drum motor switched on.
7. The drill motor was switched on.
8. Observations were made of voltage, current and power readings.
9. Thrust was built up to required value by rapidly opening the control valve.
10. The instant the required thrust was reached the penetrometer was marked and a stop-watch started to enable power readings to be taken at 10 second intervals during drilling.
11. The hole was drilled to the requisite depth.
12. The thrust was cut off, the motor withdrawn from the hole, the water supply then switched off and the motor stopped.
13. The bit was examined and its condition noted.

Early tests indicated that rotary bits of standard design were unsuitable in many ways for use in hard rocks when heavy loads are required, and consequently the major part of drilling investigations was confined to an analysis of the factors causing failure and the development and testing of improved designs.

Results.

Details of drilling tests are shown in Table 11 from which it will be observed that several bit types have been tested, including standard and modified designs. All bits were carbide tipped, this being essential for economic drilling rates in most rock.

Comparison of performance of Standard Concentric and Eccentric Bits.

The two most widely used types of drill bit are the two-legged Standard Concentric and Eccentric which differ, as shown in Fig. 32. by the fact that the cutting tip points are symmetrical about the axis of rotation on the concentric type, and non-symmetrical on the eccentric type. It was observed that Eccentric type bits were unable to withstand thrusts beyond approximately 900 lbs. when failure occurred by bending from the base of the leg inwards towards the core-gap. Concentric bits failed in a similar manner at thrusts in the region of 1700 lbs., i.e. almost double that of the eccentric type. (N.B. These values are valid only for the bits tested). The reason for failure in this manner may be appreciated by considering the cutting action of the two types, shown diagrammatically in Fig. 33.

Eccentric.

- Fig. 33 (a). The initial profile at the back of the hole caused by one leg of the bit.
- Fig. 33 (b). Profile one-half revolution later when the second leg has cut across the initial profile.
- Fig. 33 (c). General profile of the hole developed after one half revolution. Repeated rotation removes rock as shown. It is also interesting to note that part of the rock is cutting with two free faces.

Concentric.

Figs. 33 (d),(e),(f) similarly show the development of the profile of a concentric bit.

This demonstrates that generally the eccentric bit is in contact with rock on part only of the total cutting edge, leg A (known as the leading leg) cutting on the outer part in the vicinity of the tip, whilst leg B (known as the core-breaker leg) cutting on the inner part, again in the vicinity of the tips.

The drilling rate at which the full edges come into contact is given by the simple formula

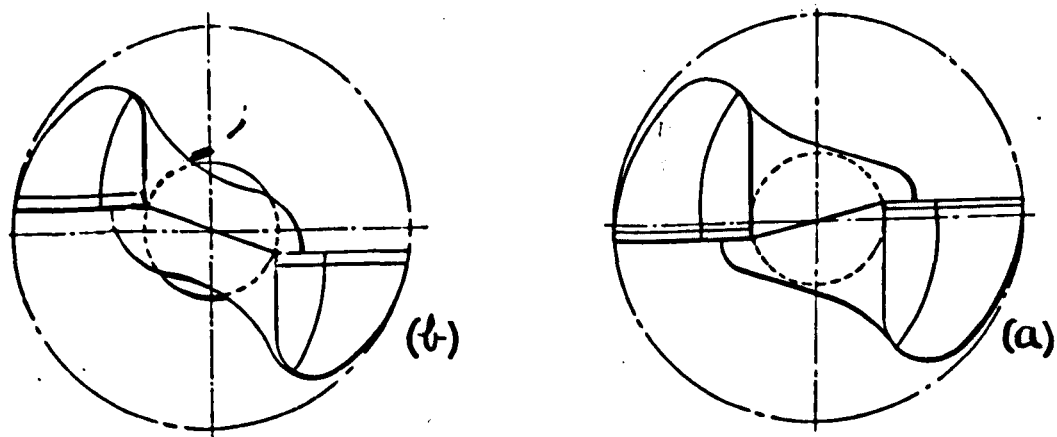
$$P = 2(W - 2a) \cot \phi$$

where P = Penetration per revolution

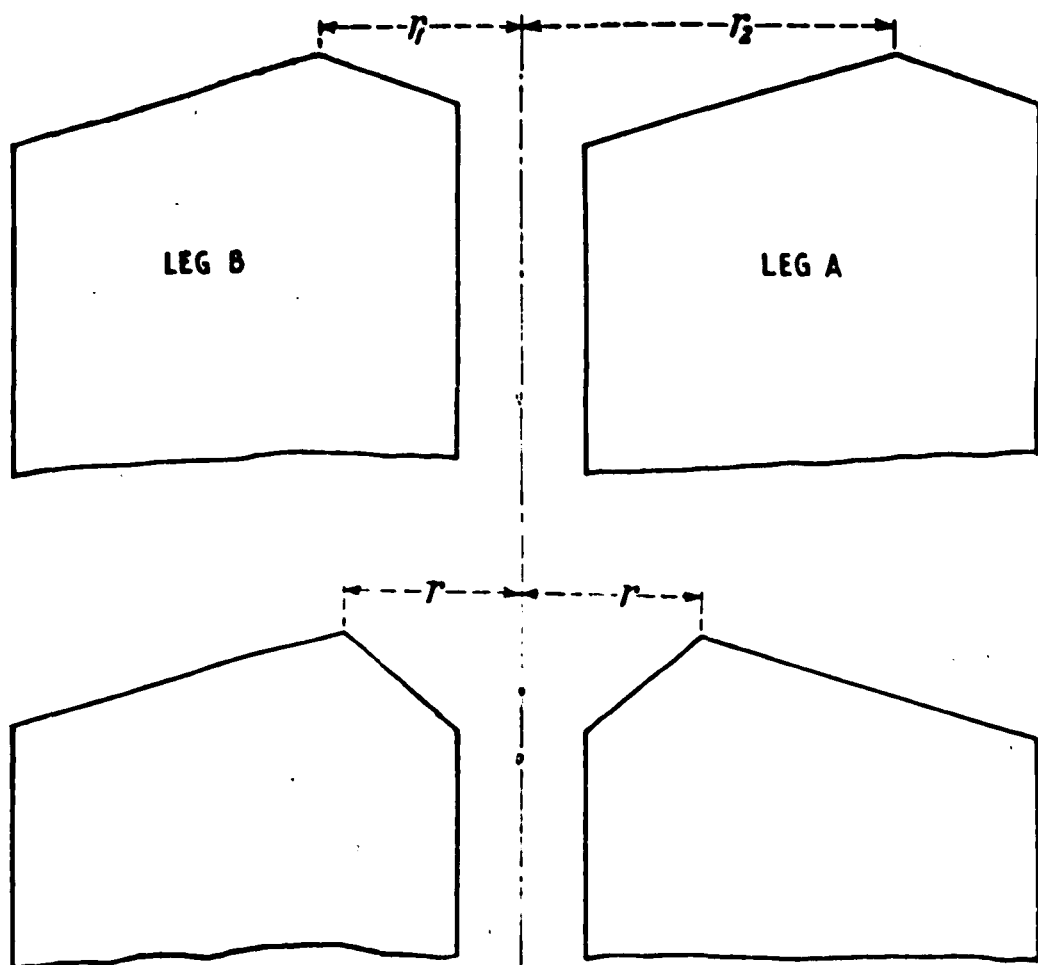
W = Width of legs

a = radius from axis of rotation to tip point on the core-breaking leg.

2ϕ = point angle.

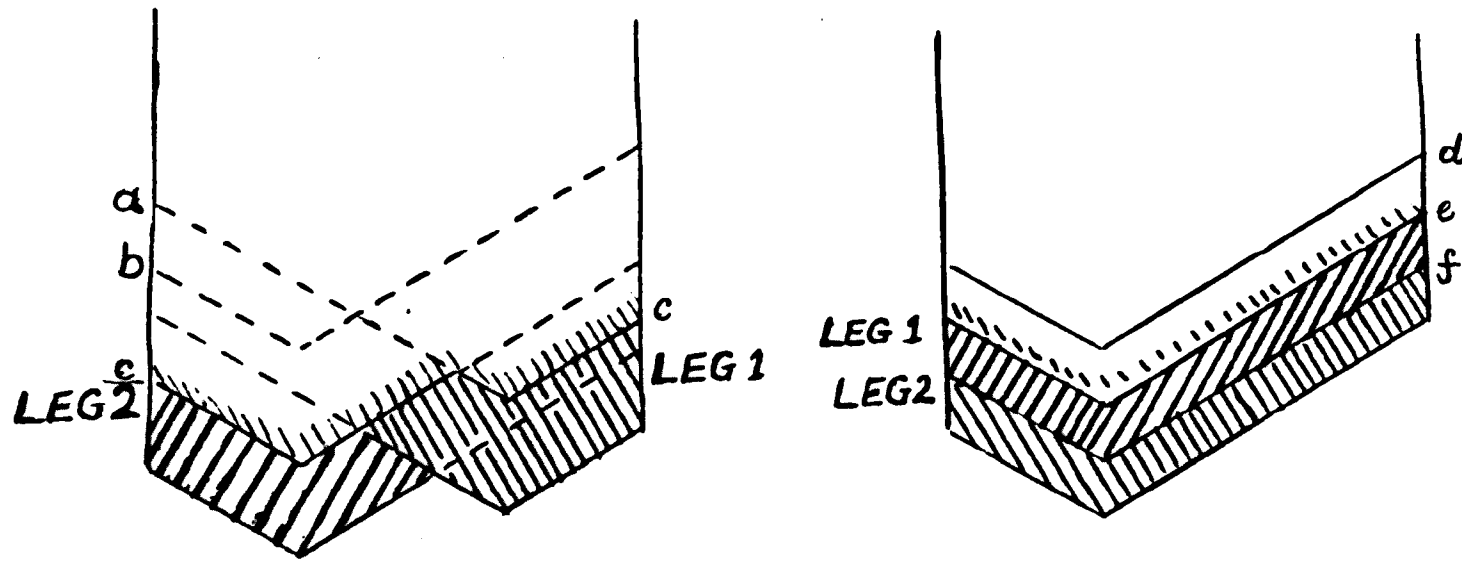


“ Oblique ” rotary drilling bits



Concentric and eccentric bits

FIG. 32.



ECCENTRIC.

CONCENTRIC.

FIG. 33 CUTTING IMPRINTS OF ECCENTRIC AND CONCENTRIC BITS

The derivation of this formula is shown in Appendix 2.

Typical drilling rates given by this formula for a bit where $2\phi = 120^\circ$, $W = 1\frac{1}{8}"$, $a = \frac{3}{8}"$ are

R.P.M.	Drilling Rate for contact across full cutting edge.
180	78.0"/min.
320	138.5"/min.
500	216.0"/min.

or 0.433"/revolution, which is considerably higher than usual. It should also be noted that even when this occurs the contact pressure is still non-uniform across the cutting edge.

Thus under usual drilling conditions the total width of cutting edge of an eccentric bit in contact with the rock is approximately half the total width of the bit legs, i.e. the contact pressure between bit and rock for a given thrust is approximately twice as great as that resulting from the same thrust on a concentric bit. This accounts for the well-proven fact that eccentric bits will drill approximately twice as fast as concentric bits when using the same thrust. Due, however, to the increased flake thickness the eccentric bit suffers more severe impacts during cutting and consequently chipping will occur at lower thrust values.

Examination of cuttings suggests that, although fracture across the whole of the cutting edge in one flake does occasionally occur, it is infrequent. More often the tip point appears to cause sufficient stress concentration to result in separate and distinct chips on each side of the tip. When the fracture occurs on the inner tips the load on the outer edges is unbalanced resulting in a considerable bending moment tending to bend the legs inwards against the core together with the usual bending moment due to the torsional cutting force. Where the core has fractured with the inner flake, as often occurs, or where it is weak, the leg will bend inwards, failing generally across its base.

Since loading conditions as described are much more severe for the eccentric bit it is not surprising that it fails at thrusts approximately one half of those possible with concentric bits. As neither type was suitable for heavy thrusts in its existing form, further tests were carried out using alternative types.

Spearhead Type.

This differs from the two previously described in that the carbide insert is in one piece set into the bit with no gap at the centre. (See Fig. 34) iii)

Tests revealed that the bit is able to withstand much higher loading without fracture although drilling rates are much reduced. This reduced rate is due to the fact that grinding instead of cutting is taking place in the vicinity of the axis of rotation, as can be seen from the following example.

Example.

Spearhead bit (Drilling Rate 10^3 /min. at 60 R.P.M. i.e. $\frac{1}{6}$ "/revn.
Leg Clearance Angle 20°

$$\text{Inclination of cutting path } \delta_p = \tan^{-1} \frac{p}{2\pi r}$$

Grinding will occur where the full under face of the bit is in contact with the rock. i.e.

$$\delta_p = 20^\circ$$
$$\therefore \frac{1}{6} \tan 20^\circ = \frac{1}{2\pi r}$$

$$r = 0.073"$$

Thus crushing must occur in a region slightly more than $\frac{1}{8}$ " diameter around the axis of rotation. This is a very inefficient process and will absorb a considerable proportion of the total drilling thrust resulting in overall low drilling rates.

The higher loading limit is due mainly to three features:-

1. The bit is solid across the centre, therefore there can be no inward bending moment.
2. The insert is in one piece, therefore deflections due to impacts on one face are resisted by impacts in the opposite direction on the other face. Stresses due to tip deflection are reduced, hence also the impact velocity due to acceleration of the deflected bit tip upon release of load.
3. There are fewer regions where stress concentrations will occur, i.e. pointed tips.

Spearhead bits cannot be considered as a solution to the problem of designing bits for hard rocks but nevertheless indicate ways in which failures may be reduced.

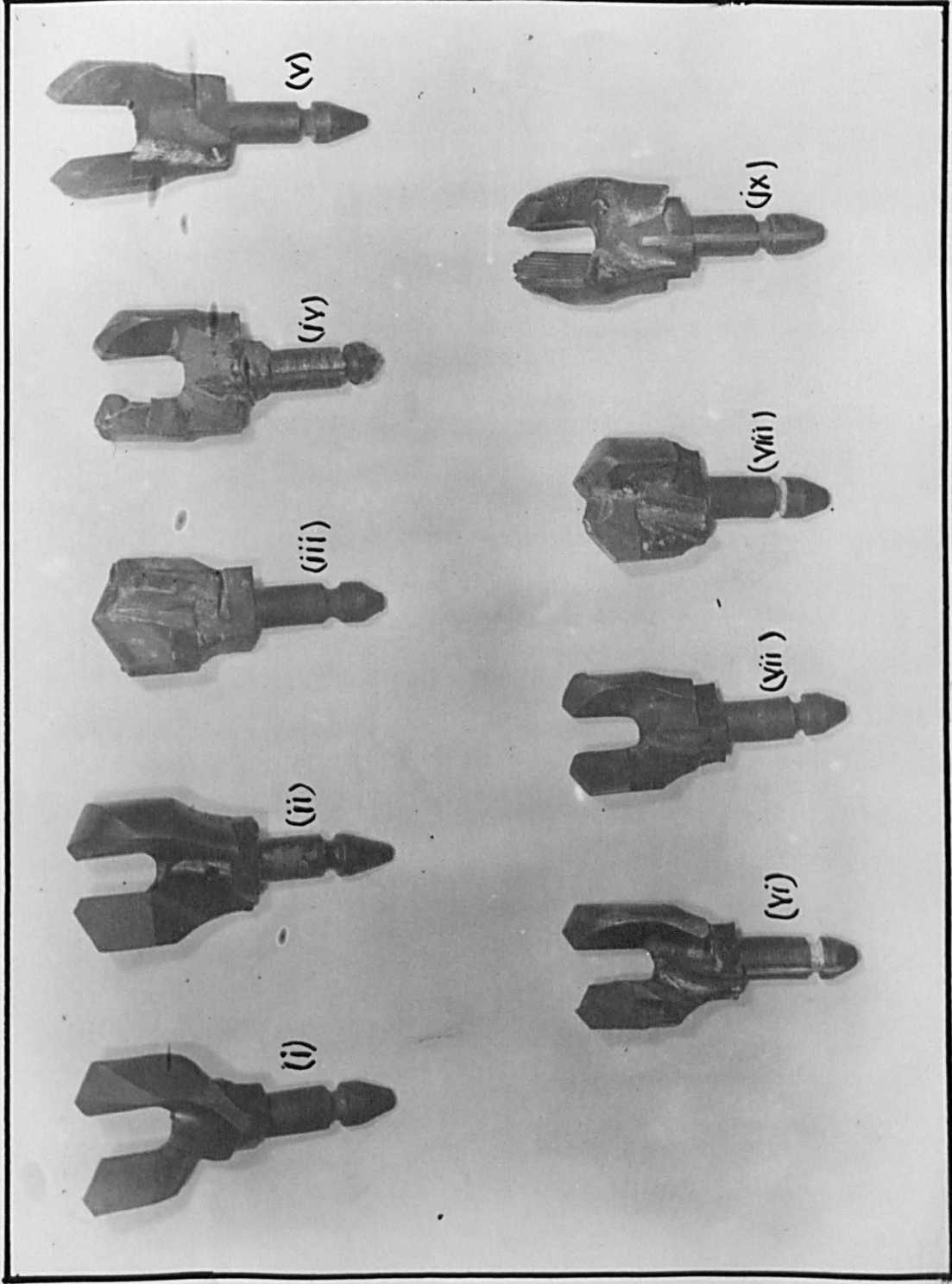


FIG.34 BITS USED IN DRILLING TESTS

Alloy body bits (Concentric type).

These bits were recommended as a possible solution to bit failure. They were of the scroll body design (Fig. 34)⁽ⁱ⁾ of the National Coal Board Specifications and were somewhat larger in cross-section at the base of the legs.

Tests demonstrated that the bits were able to withstand much higher thrusts than the standard types, although failure of the carbide tips now became the limiting factor.

This may be explained as follows:-

Although the alloy may have a higher elastic limit than the plain carbon and consequently sustain greater deflections before failing, the Youngs Modulus of Elasticity remains virtually unchanged with the result that deflections of the tip under load are of the same order and hence the risk of carbide failure is unaltered.

Oblique bits.

Oblique cutting has been described briefly in the introductory section. The idea was first conceived in attempts to utilise positive rake cutting without, at the same time, reducing the backing material supporting the carbide tips. Whereas other types are designed with the front faces of the legs along a diameter of the bit cutting circle the oblique bit, as its name implies, is inclined at an angle (termed the Obliquity Angle) to the diameter through the centre of the cutting edge. In this way the rake angle presented to the instantaneous direction of cutting is increased. The effective rake angle being given by the expression

$$\tan \alpha_e = \tan \alpha_a \sec \lambda$$

where α_e is the effective rake angle

α_a is the nominal rake angle

λ is the angle of obliquity

Oblique bits may be of two types (See Fig. 39)

- (a) Those in which the legs are effectively stepped forward in the direction of cutting,
- (b) Those in which the legs are effectively stepped back from the direction of cut.

Type (a), initially considered to be a means of allowing more backing material behind the cutting edge, was not tested since

planing tests indicated that the cutting forces would be increased. Stress would be directed towards the solid wall of the borehole and serve no purpose.

Several bits of Type (b)^{Fig 34(v)} were designed and tested. The leg cross-section at the base had been reduced in stepping back the legs and failure soon occurred in the manner of the standard types under thrusts below 1000 lb. Although not further tested this type is of interest in view of the stress-directing effects observed in the planing tests. It has been demonstrated (Appendix 3) that the obliquity increases towards the inner radius, i.e. as the core is approached. Consequently the stress will be directed across the core, resulting, it is thought, in more efficient core destruction. Thus, whilst oblique cutting with one free face results in higher cutting forces, it may be possible in practice to increase the permissible core diameter (i.e. that which can be effectively broken) and hence the actual width over which cutting takes place. In this way it may be possible to increase drilling rates for a given thrust. Whilst the writer himself has been unable to test this theory it is now being investigated by a firm of drill-bit manufacturers on the basis of the above reasoning.

Having investigated the modes of bit failure it was then necessary to design a bit in the light of information obtained. Failure of the legs could be overcome by increasing the cross-sectional area at the base. The probability of carbide failure, however, can be reduced by several means as the following analysis shows.

Carbide failure in rotary drilling.

It is now well-established that the magnitude of impact stress waves is directly related to the velocity of impact. The velocity of impact of a bit tip on the rock surface after fracture may conveniently be considered to be affected by two components.

1. Velocity due to acceleration of the rod upon release of stored energy.
2. Velocity due to acceleration of the drill bit upon release of energy stored in deflection of the tip.

Of these the higher velocity will be that resulting from

deflection of the tip. Tip deflection also induces tensile bending stresses in the front face and consequently reduction of tip deflection will have a two-fold beneficial affect.

The calculation of tip deflection (y) under load has been made for a somewhat idealised bit form and is shown in Appendix 5 to this thesis. This shows that the principal factors affecting deflection are:

- (a) Loading (W) $y \propto W$
- (b) Wedge angle (η) ... $y \propto \cot^3 \eta$
- (c) Length of leg (L) . $y \propto L^3$
- (d) Point angle (2ϕ) .. $y \propto \cot \phi$
- (e) Youngs Modulus of Elasticity of Bit leg (E) $y \propto 1/E$

Reduction in deflection may therefore best be obtained in the following ways:

- (i) Increase the wedge angle, i.e. reducing clearance angle, and use of negative rake angle bits.
- (ii) Reduce length of legs.
- (iii) Increase point angle.
- (iv) Increase effective Youngs Modulus, i.e. increase carbide thickness.
- (v) Reduce load on tip, e.g. increase number of cutting edges, or use pilot and reamer bits.

Method of attachment of bit to rod.

Most manufacturers have employed the slot and pin attachment between bit and rod, which, whilst useful for rapid attachment and removal of the bit, is unsatisfactory in that considerable play may often occur in the slot. This allows the bit to be turned through several degrees relative to the rod and may be considered not connected to it from the rotational aspect. Thus on sudden release of load whilst drilling the bit acceleration is determined by the low inertia of the bit alone, with a consequently high impact velocity. Where the bit is rigidly connected to the rod, the acceleration of the bit body is governed by the acceleration of the rod and is much lower than in the previous case due to the increased inertia. It is thus

desirable that the connection between rod and bit should be rigid as may be obtained, for example, by the use of a screw attachment.

Of the design features so far noted, increase of wedge, reduction in length of legs, increase in point angle, and screw attachment, are relatively easy to introduce. Increase of carbide thickness is not recommended unless essential since it is a very expensive means of increasing rigidity. Multi-leg bits are of maximum advantage when core drilling, or drilling large diameter holes where more space is available for clearance of cuttings.

Modified bit designs.

Having considered the factors affecting bit performance, drill-bits incorporating some of the above features were designed and tested. These are shown in Fig. 36(II)

Modifications are:-

- (i) Increased cross-section at base of legs.
- (ii) Reduced clearance angles 15° .
- (iii) Increased point angle (150°).
- (iv) Shorter legs.
- (v) Increased carbide thickness ($3/16''$ - usually approx. $1/8''$)
- (vi) Screwed attachment. ($8''$ B.S.W.)

N.B. One feature in the above bits which is not recommended, but was incorporated by mistake, ^{concerns} ~~is~~ the position of the tip points. These should preferably be situated closer to the axis of rotation in order to reduce the peripheral velocity and minimise impact stresses on this vulnerable region.

Tests with modified bits.

The rocks used were:

- (i) Parkgate sandstone, an abrasive and moderately hard carboniferous rock, and
- (ii) Derbyshire Limestone, a non-abrasive but hard and brittle rock much more resistant to penetration than those previously used.

Early tests in the sandstone indicated that the maximum thrust of 4800 lb. could be used without damaging the carbide, but it was soon apparent that the screw attachment used had certain defects.

1. The male thread on the bit was initially too narrow ($\frac{1}{8}$ " B.S.W. thread) and sheared off under heavy torques.
2. Increase of thread diameter (to $\frac{3}{8}$ " B.S.W.) necessitated removal of too much material from the 1" diameter round rod for the female thread, with the result that the material around the thread on the rod flowed plastically under heavy thrust.

The design was therefore modified and a $\frac{3}{8}$ " diameter B.S.W. floating stud of 2% Ni-Cr-Vo alloy of high torsional strength used to connect female threads on the bit and rod. This proved satisfactory and no further trouble was experienced, even at torques in the region of 270 lb.ft (Bit seen in Fig 36(iii))

A further alternative which may be used, but which was not adopted when the stud proved satisfactory, is to have the female thread on the bit. Since the bit is overall larger in diameter than the rod the internal thread could be made larger and the male thread on the rod could be correspondingly increased with no ill-effects.

Although considerably strengthened, the carbide inserts still showed a tendency, at high thrusts, to flake and chip at the inner and outer points, although not at the rounded tip where previously it had also been prevalent. Points are regions of stress concentration and are generally to be avoided wherever possible; thus rounding off of all tips is necessary when drilling hard rocks. The writer is of the opinion, however, that the pointed imprint caused by a bit with pointed tips will also result in stress concentrations in the rock, which may aid rock fractures to develop, and it would be interesting to carry out tests to determine whether drilling rates are significantly affected by the use of bits with rounded profiles.

Multi-leg bit.

A further bit type designed by the writer and not yet tested is shown in Fig. 36(iv) It is similar in most respects to the previous types but,

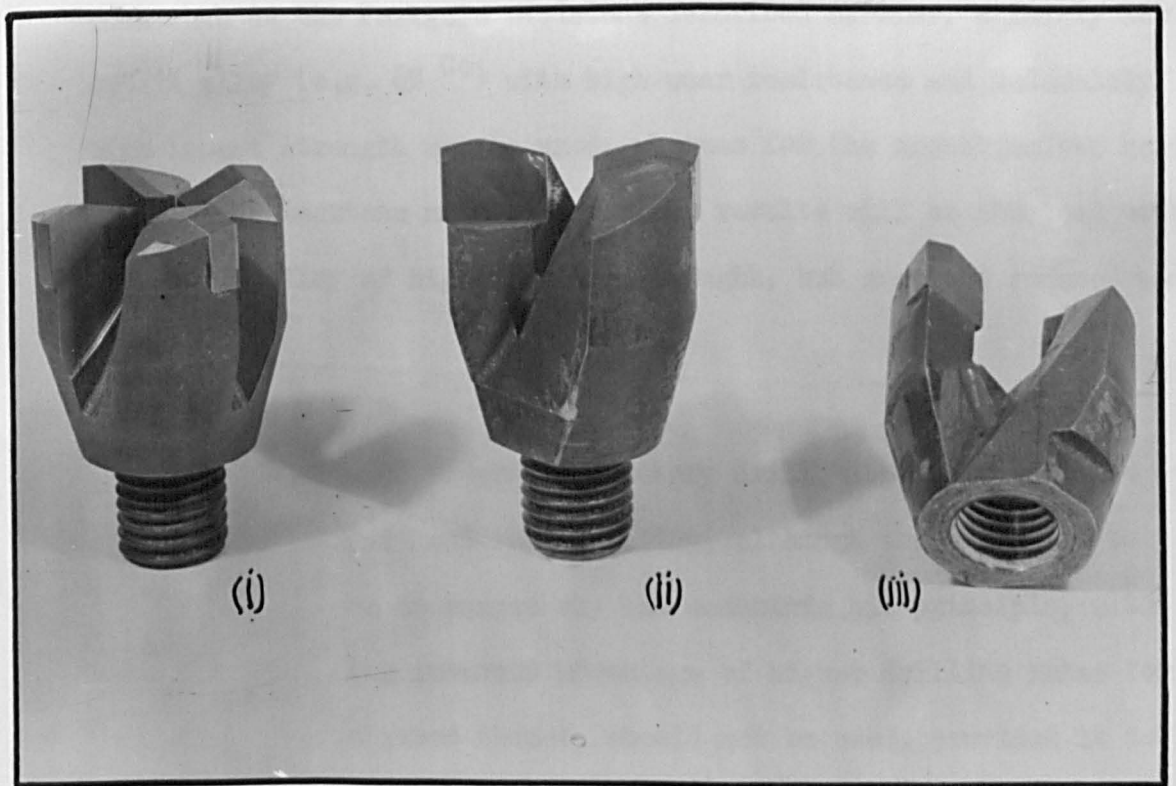


FIG 36. MODIFIED DRILL BITS.

1. has four legs instead of the usual two.
the legs are shorter to counter
2. the loss in rigidity which arises as a result of reducing the backing material to allow adequate clearance.

Choice of carbide grade.

Tungsten carbide is manufactured in several grades of varying grain size and cobalt content, these two factors combining to produce carbide alloys of different wear and impact resistance properties. Unfortunately increased wear resistance appears to be possible only at the cost of reduced impact strength, although research is being carried out to increase these values. Care must be taken to select a carbide having adequate impact resistance, together with wear resistance. Thus, in a medium hard, abrasive rock such as the Parkgate sandstone described earlier, a fairly low cobalt alloy (e.g. 6% Co) with high wear resistance and moderately high impact strength may be used, whereas for the non-abrasive, hard Derbyshire Limestone more satisfactory results will be obtained with a 9% - 10% alloy of higher impact strength, but somewhat reduced wear resistance.

Conclusions.

1. Standard type rotary drill bits are unsuitable for hard rock drilling, although there appears to be no reason why the eccentric bit principle, with its inherent advantage of higher drilling rates for a given thrust, should not be used, provided it is made sufficiently rigid.
2. Spearhead bits are very inefficient but are much stronger than the U-types. The principle of having the two cutting legs solidly connected across the centre strengthens them considerably and helps to reduce failure. This principle may well be used to advantage in pilot and reamer bits where the central core is destroyed ahead of the main bit.
3. The principle of oblique cutting may be advantageous where it is necessary to destroy a rock core, e.g. when drilling with hollow or tubular rods,

or when using U-type bits.

4. The slot attachment used with standard type rotary bits and rods is unsatisfactory for drilling hard rocks. A more rigid connection, e.g. screw attachment, is necessary.
5. All points on the cutting edge profile should be radiused off to avoid excessive stress concentrations.
6. Maximum rigidity is essential for hard rock drilling bits. The most marked improvements may be obtained by (i) Reduction in clearance angles, with maximum thickness of backing material,
(ii) Reduction in length of legs.
7. Multi-leg bits may be advantageous where the additional legs may be introduced without reducing rigidity or impairing the efficiency of flow of cuttings from the tips.

Notes on Tests II.

The effect of reduced rigidity may be appreciated from the results of Test Series II. Drilling tests were carried out using a bit with alloy stud connection. Tests appeared successful until II(f), when vibration and noise considerably increased, and the wattmeter readings became more variable than usual. Cuttings were also noticeably smaller than in the earlier tests. It will be observed that although the torque and thrust were considerably increased the drilling rate was practically unchanged. Examination of the bit later showed the carbide to be undamaged. The bit had been internally threaded too close to the base of the legs and examination revealed that a crack had developed from the core base to the base of the internal thread, the nett effect being to increase the length of the legs and hence reduce rigidity. This appears to indicate that increased impact results in less efficient rock breakdown, as shown by the higher power consumption and reduced size of cuttings.

Analysis and Examination of Rock Cuttings.

Later drilling tests were carried out using plain round, 1" diameter drill rods, with water flush. It was considered that the cuttings would thereby suffer almost no comminution as they passed along the bore-hole, and that an examination of them may indicate some details of the rotary cutting action. Samples were accordingly collected from a series of holes drilled in Derbyshire Limestone at varying thrusts. These were then dried and sieved.

Results of the sieve analysis are shown in Table 12. Photographs of a typical sample, together with a selection of large size cuttings, are shown in Figs. 37 and 38.

The analysis leads to the following observations:

1. Cuttings are larger in size than those obtained in percussive drilling.
2. Most sizes of cutting chips are characteristically wedge shaped.
3. The original "upper surface" of the chip may easily be distinguished from the fractured surface since the former is always lighter in colour (and occasionally shows the bit profile) - See Fig. 38. - than the latter. Rock crystals are clearly visible on the fractured surface whereas the other has a "powdery" appearance and is lined with numerous radial striations. (These are visible on several of the chips in Fig. 38. especially.
4. Two fracture surfaces, characterised by the darker colour, may be seen on each chip. The first starts at high inclination to the upper surface, the other at a lower inclination, forming the under surface of the chip.

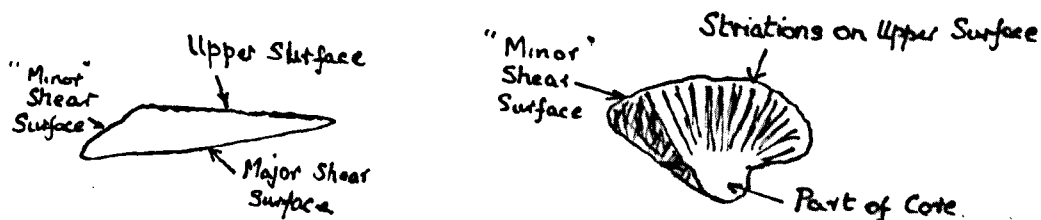


Fig. 38A TYPICAL SHAPE OF ROCK CHIPS.

The difference in coloration may be seen on the lower parts of the chips in Fig. 38, the darker part being the high inclination fracture line. It is also apparent in Fig. 37.

5. The core often forms part of the chip and is usually broken off as it develops. See Fig. 38.
6. Fracture occasionally occurs across the full width of cutting edge at one time, even though the strain rate varies with the radius of rotation of each element of cutting edge.
7. The sieve analyses show that the average weight of chips of a given sieve size increases with thrust. This indicates that the thickness is increased with penetration/revolution as would be expected.

Two important inferences which may be drawn from these observations are:

1. The rock fractures in a manner similar to that observed in planing tests. This is deduced from the shape of the chips and the steeply inclined fracture line before major fracture.
2. The striations and powdered appearance are due to heavy impact of the bit tip on the rock after fracture. A similar appearance has been noted on the surface of rock after percussive impact by Proctor¹⁹. The "powder" is considered to be due to pulverisation of surface particles.

The above corroborates views held by the writer that the rotary cutting action is essentially planing, and that cutting tips undergo frequent severe impacts during the drilling of hard rock.

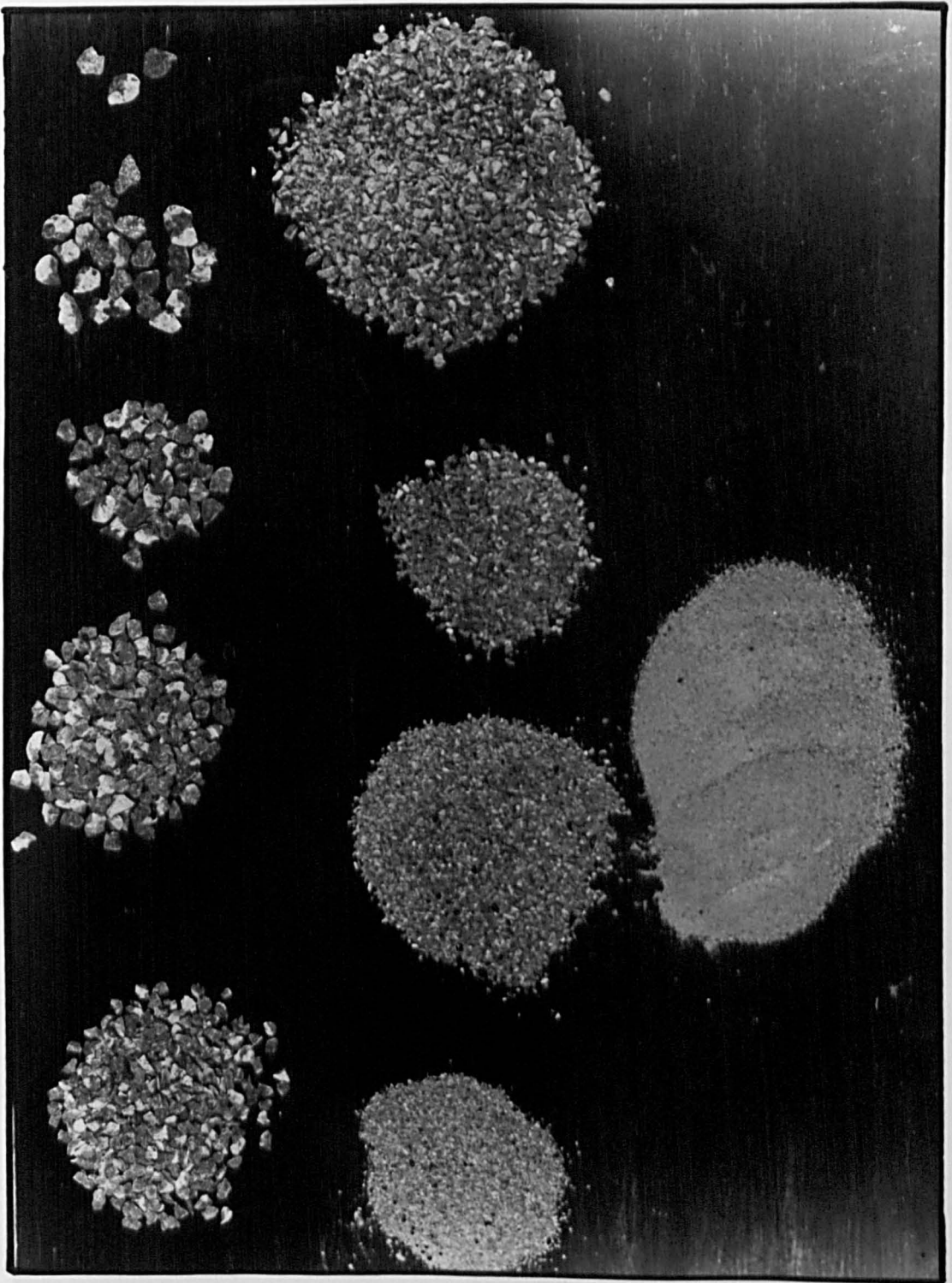


FIG.37 TYPICAL SAMPLE OF CUTTINGS



FIG. 38. $\frac{7}{8}$ " B.S.S. ROCK CUTTINGS

Determination of Instantaneous Torsional Fluctuations during Rock Drilling.

In view of the low cutting speeds of the milling machine used for planing tests, it was considered advisable that further tests be carried out with full scale drilling apparatus to obtain corroborative evidence that the cutting action in drilling was fundamentally similar to that observed in planing, and hence justify the application of planing test results to rotary drilling at comparatively high speeds. The apparatus required would have to be capable of measuring very rapid fluctuations, accurately recording events occurring over periods of the order of milliseconds. This consideration led to the adoption of electrical resistance strain gauge apparatus in conjunction with a cathode-ray oscillograph.

Apparatus.

1. Arrangement of Strain Gauges.

A 1" diameter round drill rod 3' long was machined smooth to a finished size of $\frac{15}{16}$ " and threaded internally at one end to fit a screw-type drill bit. The rod surface was then cleaned and prepared to take the resistance strain gauges, arranged as shown in Fig. 39. The gauges, supplied by British Thermostat Co. in matched pairs, each 2000 Ω resistance, were mounted in pairs symmetrically placed at 45° to the axis of the rod, one pair diametrically opposite to the other. The gauges were cemented to the rod, lightly clamped using a felt lined wooden clamp, and allowed to set in warm air for 48 hours. The technique of fixing the gauges was that recommended by Dobie and Isaac. (P.10).

The four gauges were connected to form a closed Wheatstone bridge network. Strain effects due to bending and axial compression of the rod by the drilling thrust are eliminated, the effect of tensile bending strains in gauges A and B for example being cancelled by compressive bending strains of C and D; and all gauges ^{are} being uniformly strained by direct compression, thus having no nett effect on the signal output from the bridge circuit. The bridge was energised from a 60 volt dry cell battery and the output fed to a Southern Instrument strain gauge bridge panel via copper slip rings rotating in mercury. The slip ring assembly is shown in Fig.40.

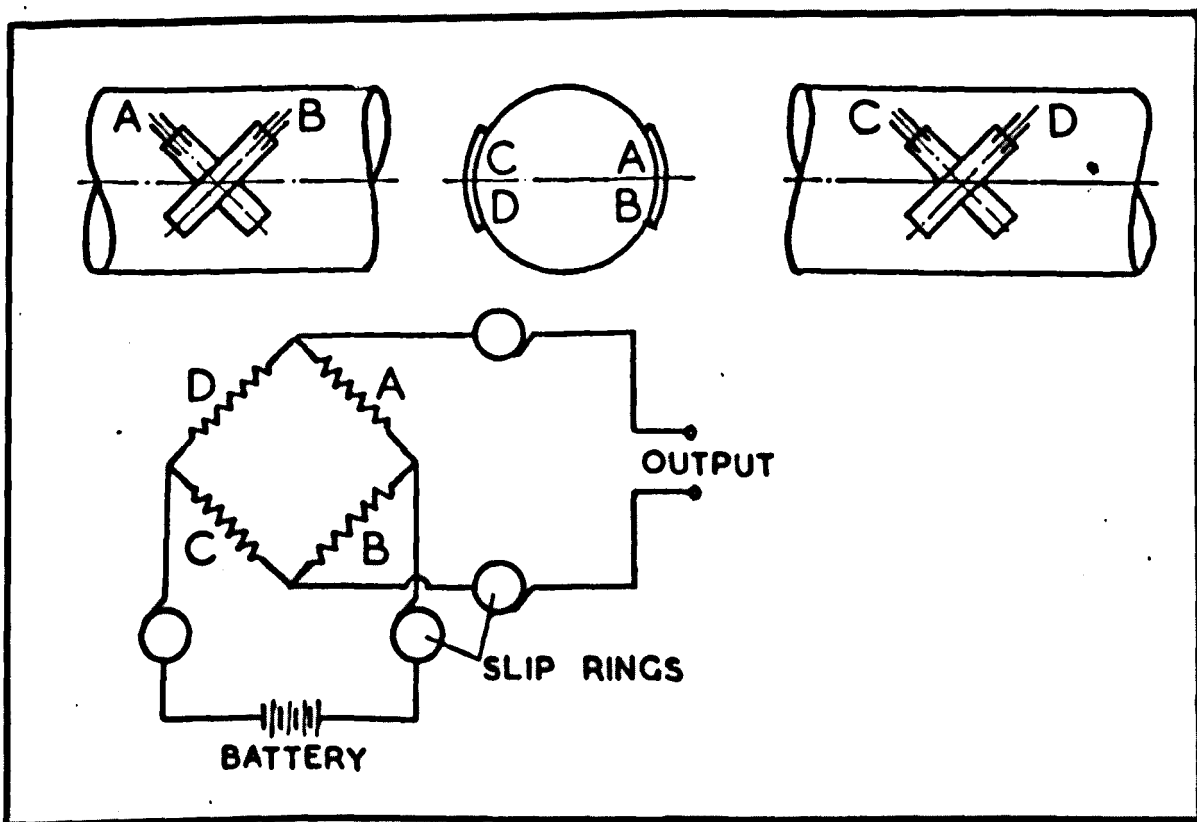


FIG 39. STRAIN GAUGE LAYOUT.

This consisted of four copper discs, $\frac{1}{8}$ " thick, $4\frac{3}{4}$ " diameter, mounted on circular "Perspex" seatings on a 1" bore aluminium shaft and separated by "Perspex" spacer rings, thus being insulated from the shaft and each other. At each end of the disc-spacer ring assembly was fitted a ball-bearing to support the outer "Perspex" casing. Two nuts, tightened against the inner race of each bearing ~~thus~~ firmly clamping each disc between the seating and spacer. The base of the casing was divided (as shown) into four compartments, again by Perspex, ensuring that each was electrically insulated from the others. Stainless steel rivets set in the base of each compartment connected with terminals on the underside of the casing. Signal wires were connected to the discs via holes drilled in the wall of the aluminium shaft and connecting holes through the Perspex spacers. The compartments were filled with mercury to provide electrical contact between the discs and the steel rivets. When in use the assembly was electrically screened (to prevent pick-up of stray electrical charges) by a sheet steel casing, part of which can be seen in Fig. 40. The assembly was then mounted on the drill rod, being held in position by grub screws through the aluminium shaft. The output signal and input E.M.F. were fed by screened "Co-axial" cable to and from the Southern Instruments Strain Gauge Bridge unit, as can be seen in Figs. 41 and 42.

The bridge was balanced using a variable high resistance on the bridge panel in parallel with one arm of the bridge.

The output signal from the bridge was then amplified through the Southern Instrument D.C. Pre-Amplifier from whence it was applied to the Y plates of a Southern Instruments M.950 Universal Cathode Ray Oscillograph, Fig. 42

Records were obtained photographically using the I.M731 Universal Variable high speed drum camera, shown attached to the oscilloscope in Fig. 43. Sensitive photographic paper was placed around the periphery of the drum which was then set rotating. When running at full speed a switch on the camera was depressed which, through a cam arrangement in the camera triggered the beam, (oscillating under the action of the variable signal from the strain gauge circuit), onto the oscilloscope screen for one revolution of the

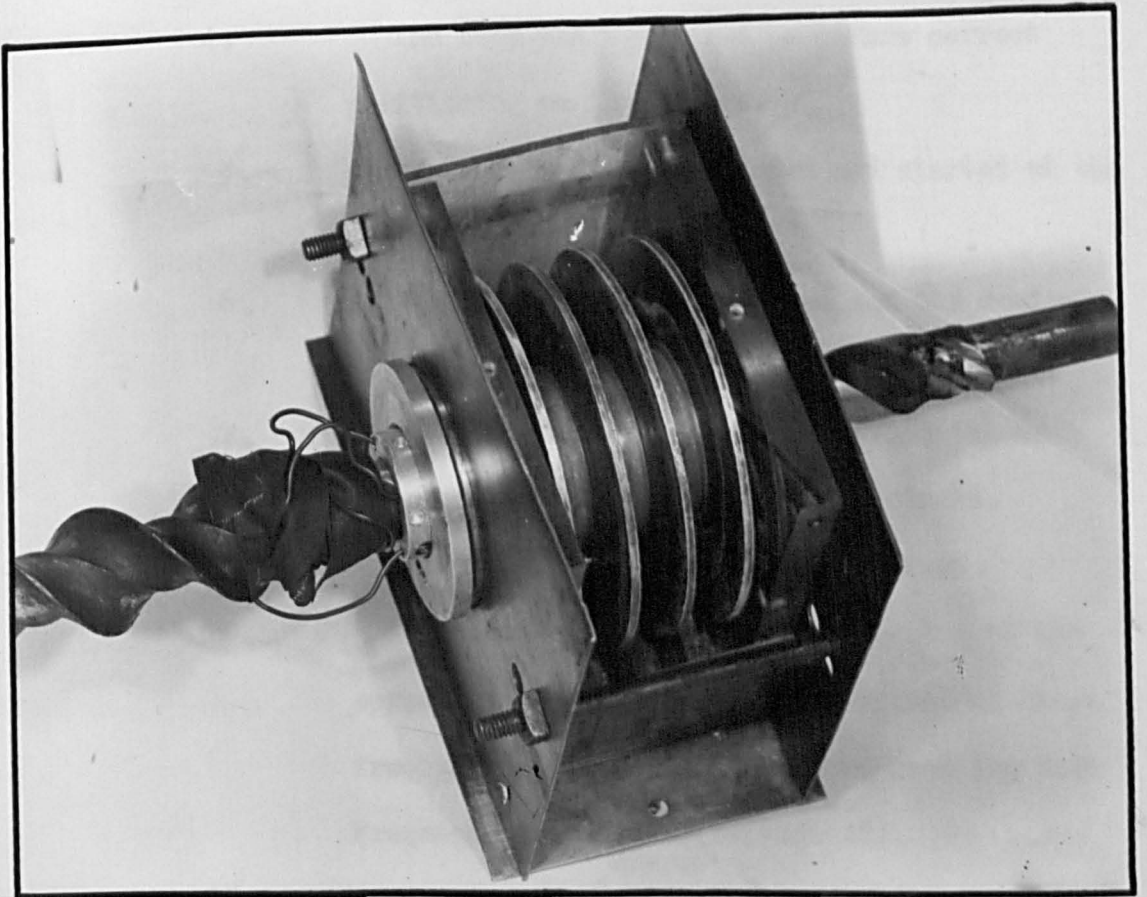
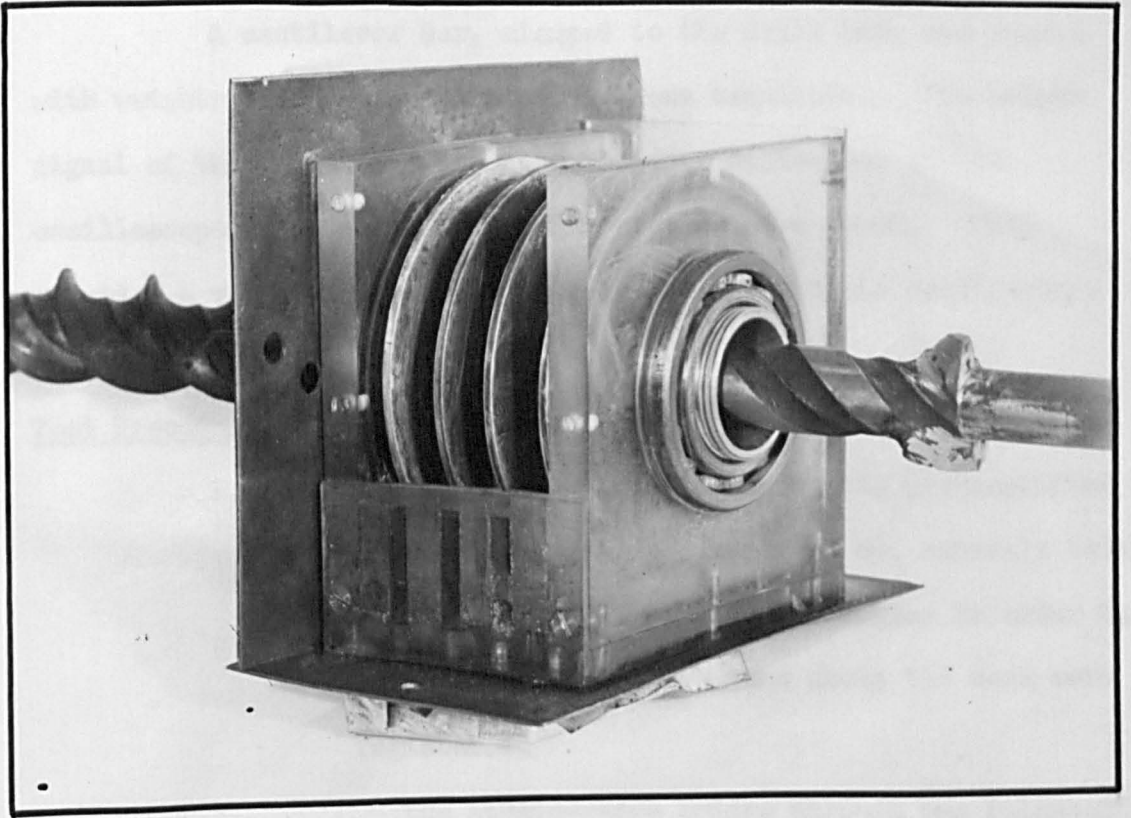


FIG 40. SLIP RING ASSEMBLY.

drum, thus avoiding repetition of the trace over the photographic paper.

Static Calibration of Gauges.

A cantilever bar, clamped to the drill bit, was loaded with weights to impose a torsion of known magnitude. The output signal of the gauges and the corresponding deflection of the oscilloscope trace at various gain settings were noted. This provided a vertical calibration scale for the dynamic oscillations during drilling.

Test Procedure.

1. The Pre-Amplifier heater unit, pre-amplifier and oscilloscope were switched on, controls being set to Resistance Capacitor Coupling in order that only oscillations of torque about the mean were registered.
2. The strain-gauge bridge circuit was balanced using a micro-ammeter to indicate zero output signal from the strain gauge bridge.
3. The pre-amplifier was checked for drift and the hum-correctors adjusted.
4. The beam was triggered to ensure correct positioning on the screen.
5. The camera drum was loaded and started at the required speed.
6. The drill motor was started and the desired thrust applied.
7. The camera shutter was opened and the beam triggered - The shutter was then closed.
8. The drill was stopped and withdrawn.
9. The beam was adjusted to the bottom of the screen and a small oscillating signal of known frequency applied to the Y input from the Beat Frequency Oscillator (B)(Fig. 42).
10. The camera shutter was opened and the oscillation triggered onto the photographic paper to provide a time-base for the record.

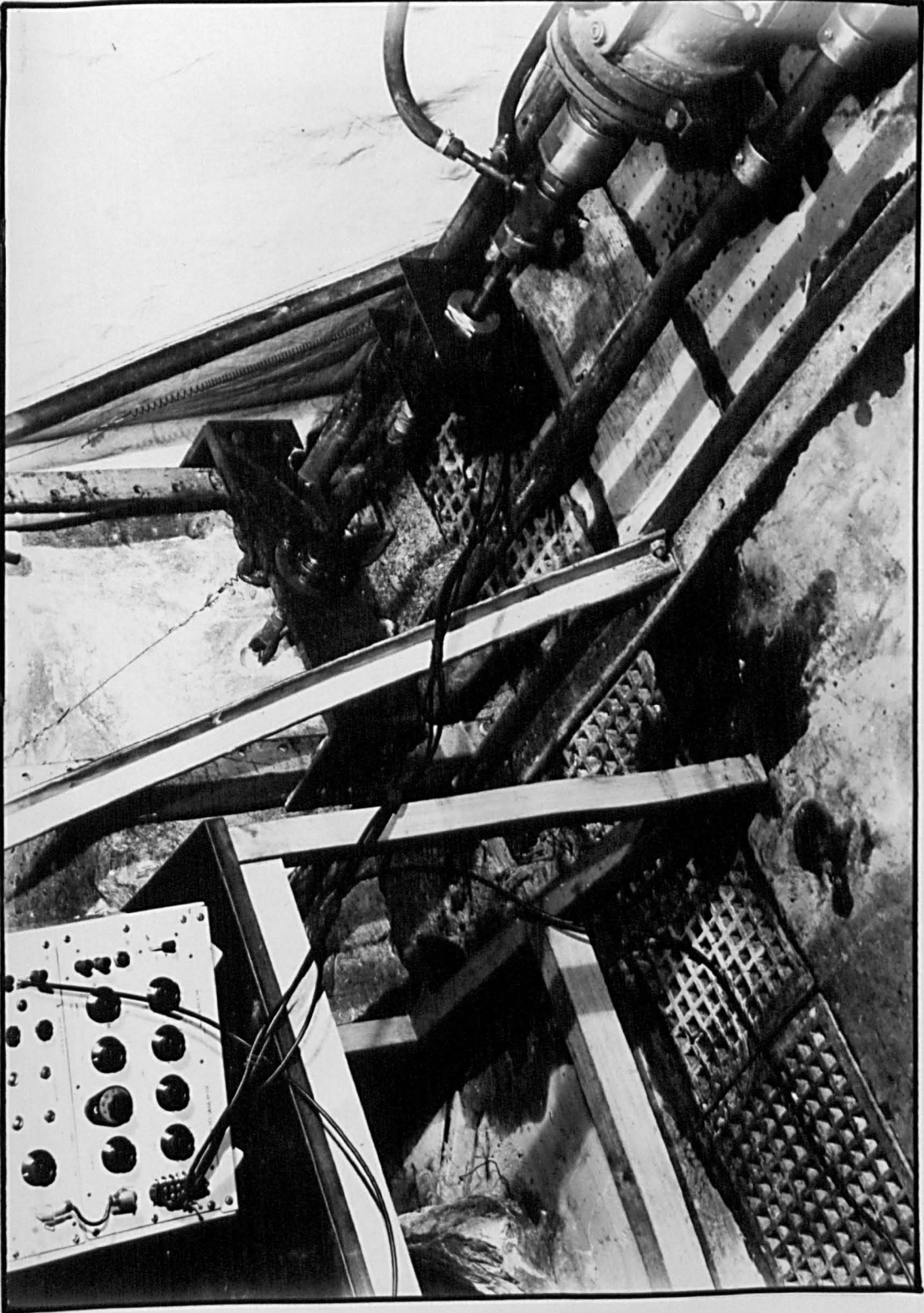


FIG.41. VIEW OF STRAIN GAUGE DRILLING APPARATUS

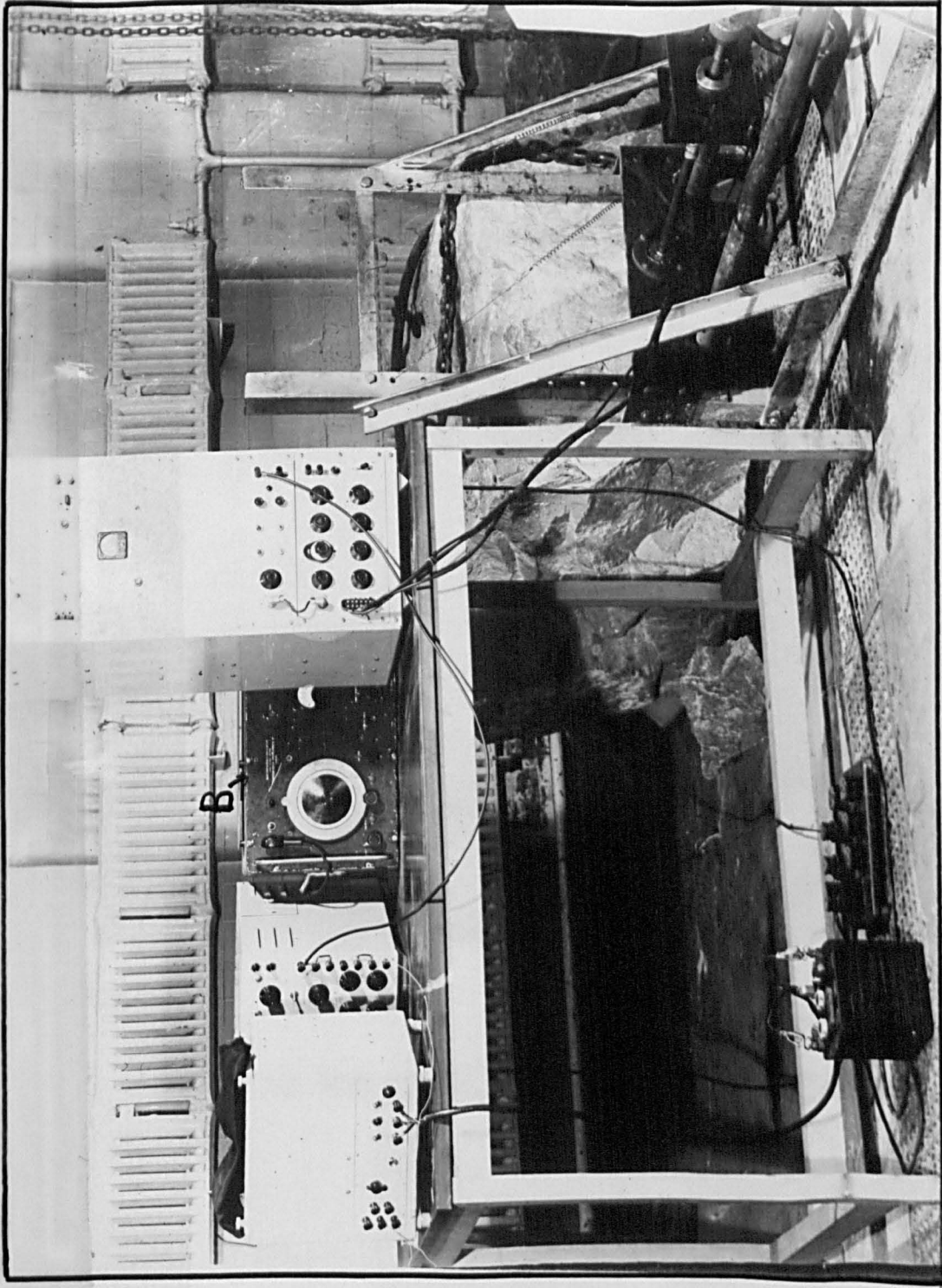


FIG 42. VIEW OF STRAIN GAUGE DRILLING APPARATUS.

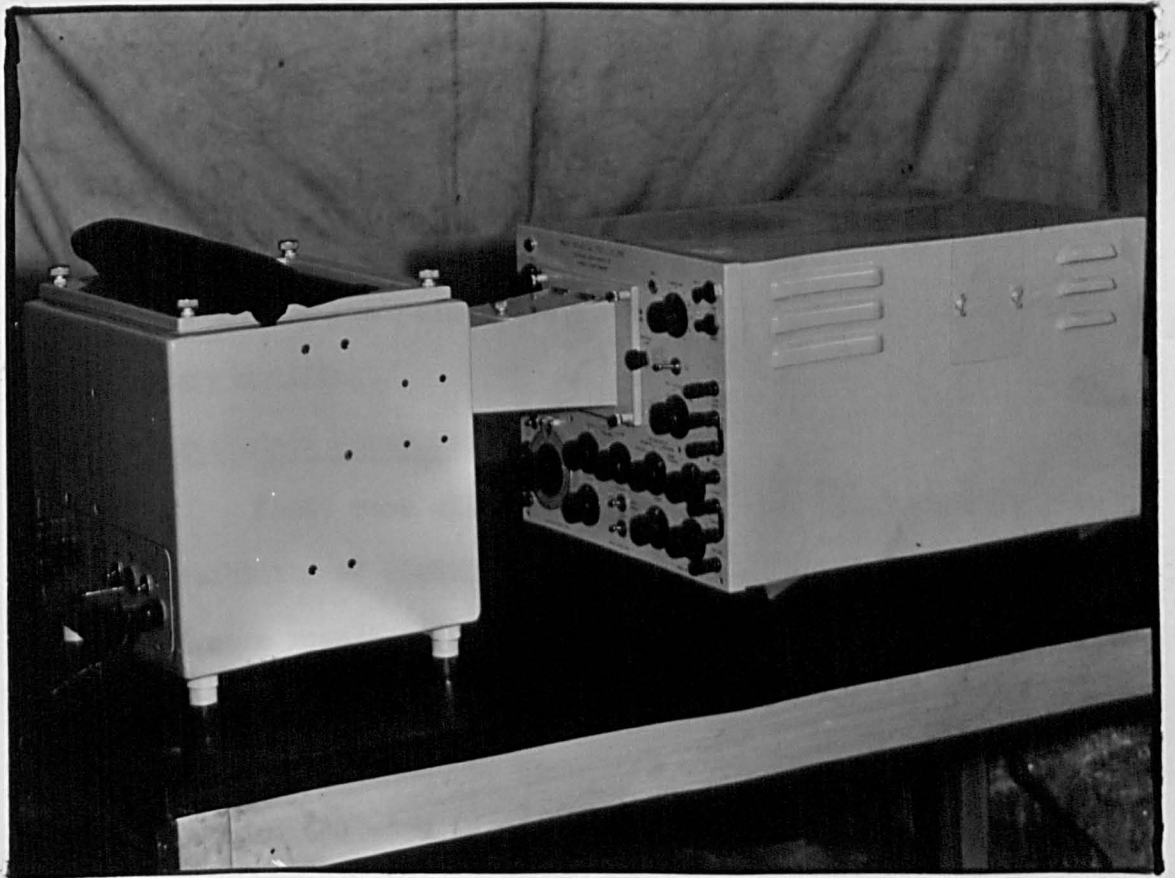


FIG 43. OSCILLOSCOPE-CAMERA
ASSEMBLY.

11. The shutter was closed, the drum stopped, and the photographic trace removed for developing.

Results.

Tests were carried out using Derbyshire Limestone, a hard, non abrasive, very brittle rock.

Typical oscillograph traces are shown in Fig. 44 (a) (b).

The traces immediately reveal the highly oscillatory nature of the drilling torque. Fig. 44 (c) shows in more detail the characteristic form of the torsional force/distance cut which is of exactly the same type as that observed in planing. The force builds up with slight drops when minor fractures occur, until the peak value is reached. Fracture then occurs with a rapid fall in force. This rapid fall represents the period during which the bit and, to a lesser extent, the rod is accelerating due to energy stored in deflection. The bit hits the rock and the force then builds up again to another peak value.

This analysis reveals several important details relating to rotary drilling.

1. Magnitude of Force Oscillation.

Tests were all carried out at 1200 lb. thrust in view of the possibility of shearing of the bit thread which had to be reduced as a result of the reduced rod diameter. The mean torque in Derbyshire Limestone at this thrust was approximately 60 lb. ft. The fluctuations about the mean, as measured by the gauges, is also of this order (50 - 60 lb. ft.) When it is considered that this result is measured approximately 12" from the actual bit tip, i.e. after damping of the stresses due to internal friction, it will be appreciated that the oscillations are extremely high, probably of the order of $\pm 75\%$ $\pm 100\%$ even at this comparatively low thrust. These fluctuations will undoubtedly increase with thrust, as is shown by planing tests on depth of cut variation.

This may be regarded as conclusive evidence of the necessity to design bits able to withstand very severe impact shocks.

2. Frequency of Impact.

If it is accepted that impact occurs after each major fracture then it is possible to form some idea of the frequency of

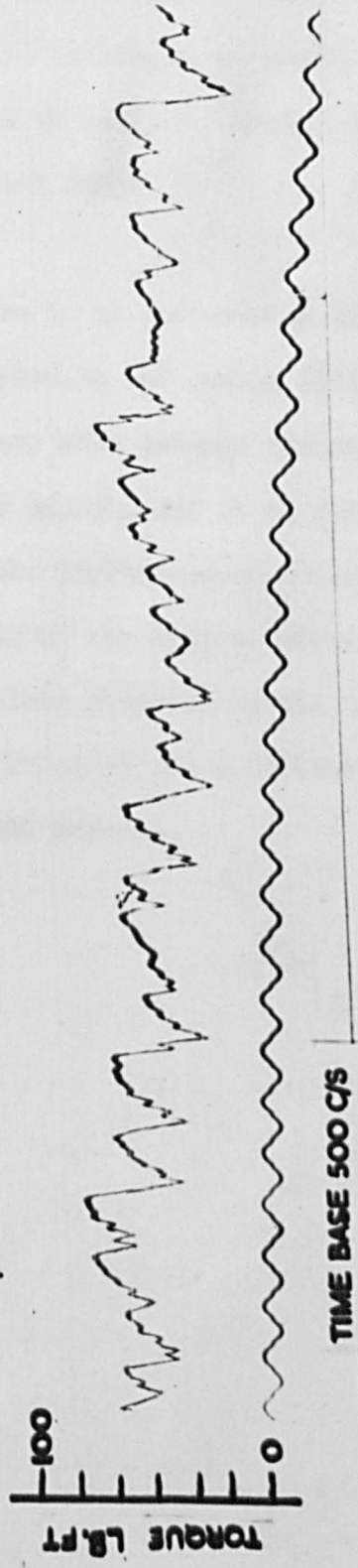
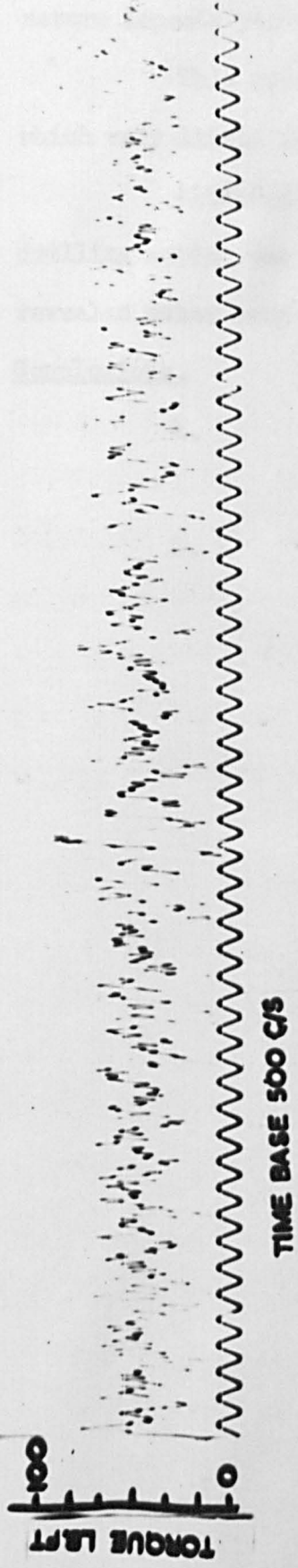


FIG. 44 OSCILLOGRAPH TRACES

impact. In Fig. 44 (b) one fracture occurs approximately every $\frac{3}{500}$ sec. = 0.006 secs. The drill rotational speed was 125 R.P.M. i.e. 2 R.P. sec. (approx.). The number of major fractures here is thus of the order of 80 - 90/revolution.

Taking this a step further, a bit will endure 10,000 severe impacts per minute, drilling time.

This reveals the possibility of impact fatigue about which very little is known in relation to tungsten carbide alloys.

Although designed initially to establish that the rotary drilling action was similar to planing, these tests have thus revealed other very important data.

Conclusions.

1. There is no fundamental difference between rock planing and rotary drilling.
2. Rotary bits undergo frequent and very severe impacts and it is felt that the ultimate limitation of rotary drilling is the ability of the bits to withstand them. The striations observed on the surface of fractured rock chippings are a further indication of the frequent impacts.

Tests to determine principal sources of pressure loss in the flush water supply circuit.

Adequate water supply to the bit tips is essential in rotary drilling to facilitate evacuation of the cuttings and prevent over heating of the bit tips. Experiments originally designed solely to calibrate the water flow rates against water pressure at entry to the wet drilling attachment revealed certain points of high pressure drop in the supply circuit and tests were consequently extended to locate the principal sources.

Test Procedure.

Water under pressure from a supply tank (See. Fig.31) was passed via a water flow-meter and control tap through a standard wet drilling attachment and along the central $\frac{1}{4}$ " diameter bore of 4'6" long drill rod to the bit. Two $\frac{1}{8}$ " diameter holes were drilled 3'6" apart on the rod to connect with the central bore, and Bourdon gauges fitted to measure the water pressure at these points. A further gauge (Fig.45) was also fitted at entry to the wet attachment.

Readings of the three pressure gauges were noted for various flow rates under various conditions, viz.

1. Using a slot in type bit with two $\frac{1}{8}$ " diameter side water-holes fed from a central $\frac{1}{4}$ " diameter hole connected to a normal plain round drill rod, having a $\frac{1}{4}$ " central water bore and a standard wet drilling attachment.
2. Similar to (1) but replacing the slot-in bit with a screw in type having similarly placed holes $\frac{1}{8}$ " diameter.
3. Similar to (1) with modifications to the standard wet attachment. The standard attachment is as shown in Fig. 45. water entering at A, passing around the annular space between the rubber sealing rings (B) via the diametral hole (C) connecting with D, and thence along the drill rod water bore. Modifications to this design were
 - (a) enlargement of the space between the rubber

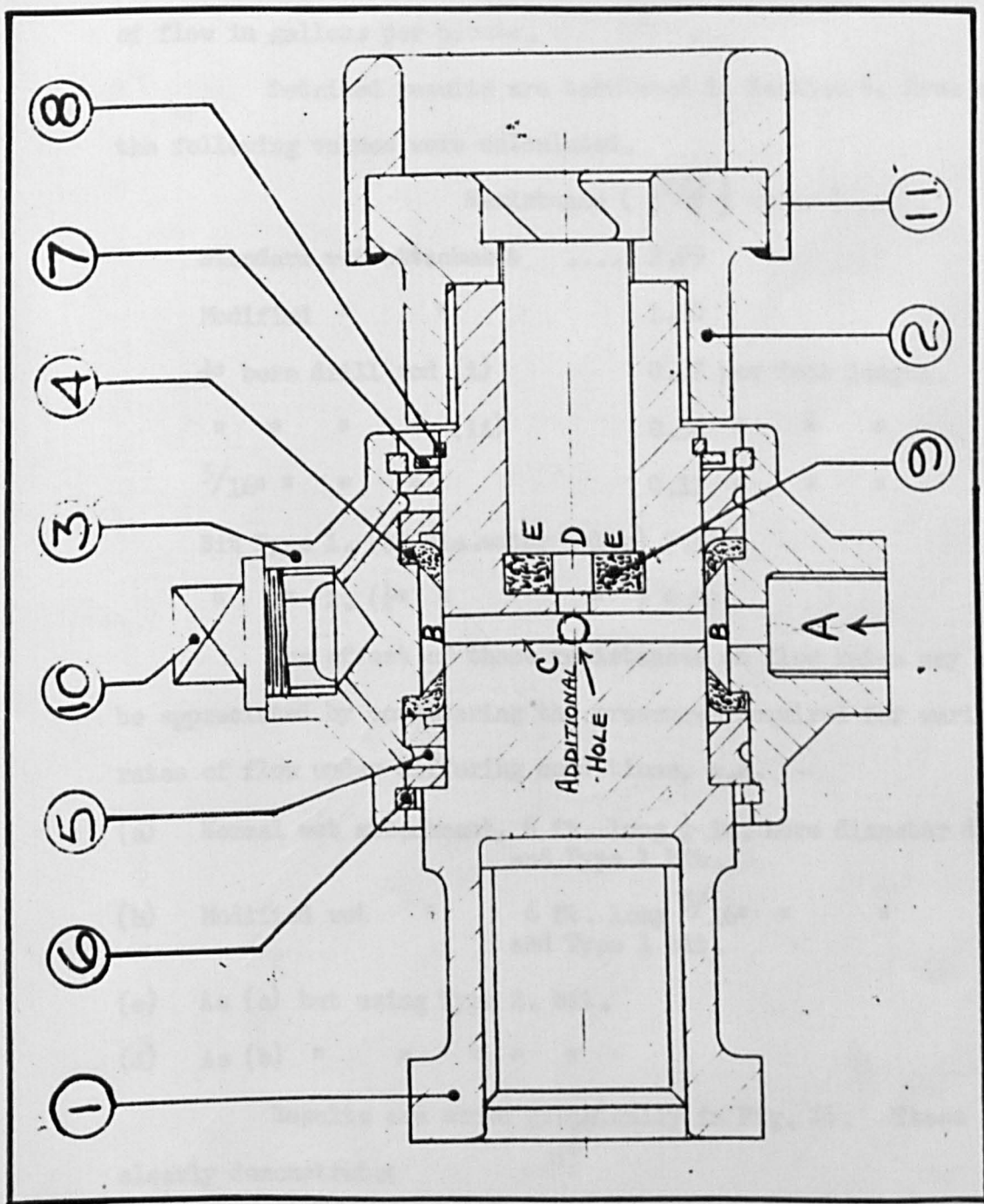


FIG.45 WET DRILLING ATTACHMENT

sealing rings, by $\frac{1}{4}$ " in diameter.

(b) A second hole was drilled at right angles to the existing one (C) to connect with the water exit (D).

Pressure drops were noted for various rates of flow and the resistance of each part of the system determined. Values for resistance were obtained by plotting values of P against values of Q^2 , where P is the pressure drop in lb. per sq.in. and Q is the rate of flow in gallons per minute.

Detailed results are tabulated in Section 6, from which the following values were calculated.

	Resistance ($\left\{ \frac{P}{Q} \right\}$ units)
Standard wet attachment 2.95
Modified " "	1.20
$\frac{1}{4}$ " bore drill rod (i)	0.37 per foot length.
" " " " (ii)	0.54 " " "
$\frac{5}{16}$ " " " "	0.12 " " "
Bit Type 1. ($\frac{1}{8}$ " dia. water holes)	7.50
" " 2. ($\frac{1}{4}$ " " " ")	0.70

The effect of these resistances on flow rates may best be appreciated by considering the pressures required for various rates of flow under differing conditions, e.g.

- (a) Normal wet attachment, 6 ft. long $\frac{1}{4}$ in. bore diameter drill rod and Type 1 bit.
- (b) Modified wet " 6 ft. long $\frac{5}{16}$ " " " " " and Type 1 bit.
- (c) As (a) but using Type 2. bit.
- (d) As (b) " " " " "

Results are shown graphically in Fig. 46. These clearly demonstrate:

1. That as much as 80% of the total pressure drop may occur in the bit water holes and that modification of these is the most effective way of increasing water supply.
2. That the required water pressure for a given rate of flow may be reduced by the order of 25% by modifying the wet attachment and increasing

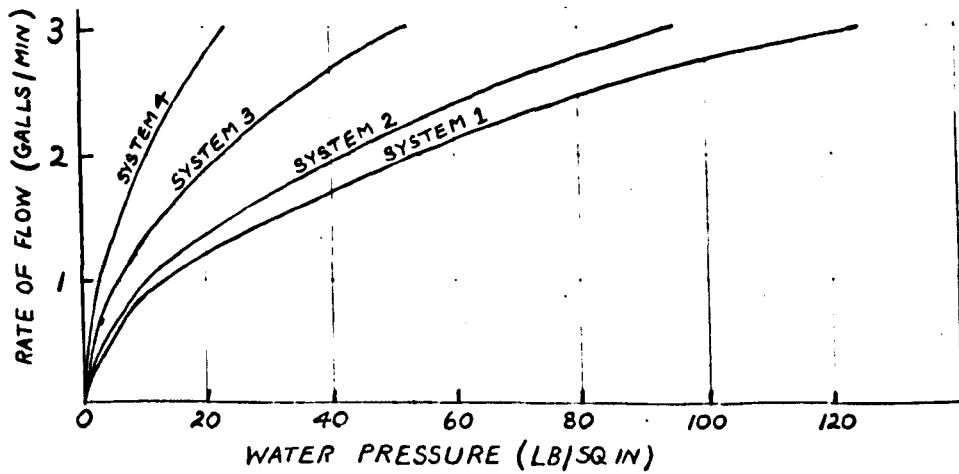
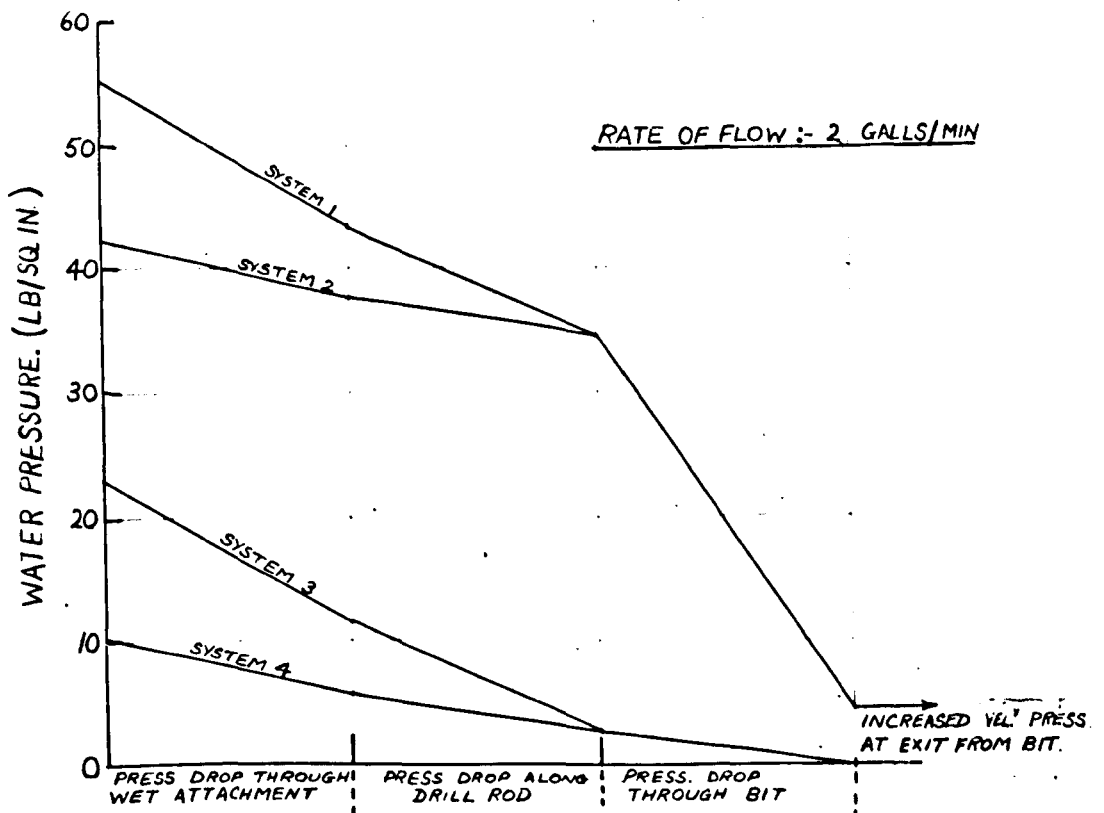


FIG. 46 PRESSURE LOSSES IN WATER FLOW SYSTEMS

the rod water bore from $\frac{1}{4}$ " to $\frac{5}{16}$ ".

3. That water pressures for high rates of flow may become excessive with standard equipment and bits having $\frac{1}{8}$ " water holes. It should be noted that the water jet at exit from bits having the larger diameter water holes will be reduced, which would be disadvantageous under low rates of flow. Where the higher rates are required for transportation of cuttings, e.g. in fast drilling, the jet velocity would, it is thought, be adequate.

Trouble was experienced early in tests as a result of using drill rods with shanks slightly longer than the wet attachment was designed to take. Although water flowed normally whilst the machine was running idle it stopped immediately as soon as any load was put on the drill rod. It was discovered that the drill rod shank, approximately $\frac{1}{16}$ " too long, engaged in the chuck drive as soon as drilling started and compressed the rubber sealing washer E until the hole in it was completely closed, thus preventing water flow. Removal of the washer causes water leakage at the chuck so that it is essential to ensure that the rod shank is exactly of the required length.

Conclusions.

Alpan and others have stated that failure to remove cuttings as they are formed during drilling may be a serious limit to the drilling rates attainable in practice. Tests indicate that this may be largely overcome by the modification of the component parts of the flush water circuit.

SECTION IV.

SUMMARY OF MAIN CONCLUSIONS.

BRIEF SUGGESTIONS FOR FURTHER RESEARCH.

ACKNOWLEDGEMENTS.

SUMMARY OF MAIN CONCLUSIONS.

Rock Planing Tests.

1. The rock cutting action in rotary drilling is characterised by brittle fracture of the rock, resulting in rapid drop of force and consequent rapid release of energy stored in the tool.
2. Local inhomogeneities influence the direction of fracture. Fracture usually occurs by shear failure but may be initiated in tension.
3. The direction of the resultant force on a tool is determined mainly by the coefficient of friction on the front face which also varies widely and may attain high values.
4. Since the frictional process has such influence on the resultant force direction, which in turn determines the thrust required for a given drilling rate in rock, it should be simulated in Drillability tests. The mechanism of this frictional process requires further research.
5. The magnitude of the resultant force in rock cutting is directly proportional to the width of flat on the under face.
6. Increase in Tool Rake Angle reduces the mean forces required for cutting.
7. Increased Depth of Cutting results in high instantaneous force fluctuations and tensile initiated fractures become more frequent.
8. The mean forces are directly proportional to the width of cut over the usual practical range.
9. Considerable reduction in forces is obtained by increasing the number of free faces in cutting.
10. The use of the Oblique Cutting principle should be advantageous in Rotary drilling, especially when in conjunction with "two free face" cutting as in pilot and reamer bits.

Rock Drilling Tests.

1. Standard bit designs are unsuitable for hard rock.
2. Improved designs must be as rigid as possible.

This may be obtained in several ways, viz.

- (a) reduction in clearance angles.
- (b) heavier backing to the insert.
- (c) use of shorter bit legs.
- (d) rigid attachment to drill rod.
- (e) use of multi-leg bits with as many legs as possible commensurate with adequate clearance for cuttings.

3. Pointed edges must be avoided since it is here that failure first occurs.
4. Rock cuttings obtained from drilling tests indicate that the cutting action is basically the same as that in rock planing.

Strain Gauge Tests.

1. The characteristic force oscillation in rotary drilling is exactly similar to that in planing.
2. Rotary drill bits undergo very severe and frequent oscillatory loads.

Water Flow Tests.

1. By far the greatest pressure loss in the water flow circuit of a rotary drill usually occurs in the drill bit.
2. Modifications in the circuit may reduce pressure requirements by the order of 400%.

The above thesis represents the results of three years research into the very complex problem of rotary drilling. Practically no previous research had been published on the application of the method to hard rocks. As will have been observed from reading this thesis the problem is complicated by the large number of interacting variables and it has been necessary to determine to some degree the nature and effect of the more important of them.

The writer considers the information contained herein to reveal several factors, previously not considered to be of major importance in determining drilling performance e.g. the frictional

process on the front face of the bit, the frequency and severity of impacts on the brittle carbide tips.

The developed theory of rock cutting will lead to a clearer understanding of the fundamental principles involved and, it is hoped, form a basis for more detailed research into this aspect. Rock cutting has been shown to have basic similarities ^{to} ~~with~~ metal cutting and, provided the stated limitations are considered, much benefit may be obtained by the application of metal cutting theory to rock.

Equipped with this knowledge it is possible to invent and design so that the range of application of rotary drilling may be extended and present performances considerably improved.

BRIEF SUGGESTIONS FOR FURTHER WORK.

The research has revealed several aspects of the problem which the writer considers of importance and upon which information is at present lacking. These are detailed below in the hope that future workers may perhaps be spurred to attempt their solution.

1. Practical full scale testing of the effects observed in the planing tests.

Whilst the effects observed in planing will also be present in rotary drilling practical difficulties not envisaged by the writer may make the application of suggested improvements impracticable.

2. A detailed study of the frictional processes in rock cutting of the planing or rotary drilling type.

The importance of this work cannot be over emphasised since friction has been shown to be the main factor determining the drilling thrust which is a limiting factor in application of the method. The use of lubricants may possibly result in improved performance.

3. A study of the temperatures attained by rotary drill bits under various conditions.

- (i) to indicate the risk of igniting methane oil in oil bearing strata, etc.
- (ii) As a manner of determining the overall efficiency of the drill bit, i.e. by obtaining an "energy - balance for the process". Since most of the energy will be liberated as heat this would appear the most suitable method. The maximum temperature may be calculated from thermo-couples set in the bit or, since the temperature gradient will be high, and errors probably large, it may be possible to use "artificial rocks", i.e. concrete blocks (with added abrasives) through which are preset small diameter metal rods. These rods would be so placed that contact-between the bit tip and rod - was made every revolution. The two dissimilar metals (i.e. tungsten carbide and the metal rod) would form a thermo-couple and the maximum temperature would

be obtained. Alternatively this may be used in conjunction with inset thermo-couples as a temperature calibrating device (i.e. to determine tip temperatures for known inset thermocouple signals).

4. Correlation of Drilling Speeds with basic physical quantities such as the Modulus of Rigidity and Youngs Modulus, together with rock abrasiveness and friction characteristics. These tests are suggested in view of the demonstrated dependence of cutting forces on the shear strength of the rock and its friction characteristics. This research may well be carried out in conjunction with suggestion 2.
5. Photoelastic determination of stress concentrations due to various point angles and rounded tips, etc.
6. Investigation of the upper rotary speed and depth of cut limits using the rigid bits suggested.

ACKNOWLEDGEMENTS.

The writer wishes to express his thanks to Professor I.C.F. Statham for his constant encouragement, and, more recently, to Professor F.S. Atkinson; to Dr. R. Shepherd for his advice and help, to Mr. H.J. Bunt whose assistance and interest, especially with the cine-camera tests, and, later, checking of the mathematical formulae, etc. has been invaluable, to colleagues in research, especially Mr. E.J. Browning for his assistance with the photographs, to the typist for her patience and painstaking effort at short notice; to Mr. H. Barker and the Technical Staff of the Department for their friendly co-operation; to Professor J.V. Connolly of the College of Aeronautics, for his helpful advice regarding the use of the dynamometer, to Messrs. Coventry Grinders Ltd. for loan of the dynamometer; to Messrs. Padley and Venables Ltd., especially Mr. Morrison, and Firth Brown Tools Ltd., especially Messrs. Burden and Robinson for their advice and supply of drill rods and bits; to Messrs. Hardypick Ltd. for their assistance with drill motor tests and modifications, and to many others.

SECTION VI.

APPENDICES.

APPENDIX I.

TERMS USED IN ROTARY DRILLING.

Leg Rake Angle.

- (i) Apparent Leg Rake Angle. Angle between front face of bit leg and plane through cutting tip parallel to axis of rotation.
- (ii) Effective Leg Rake Angle. Angle between front face of bit leg and plane through cutting tip normal to direction of cutting.

Point Angle.

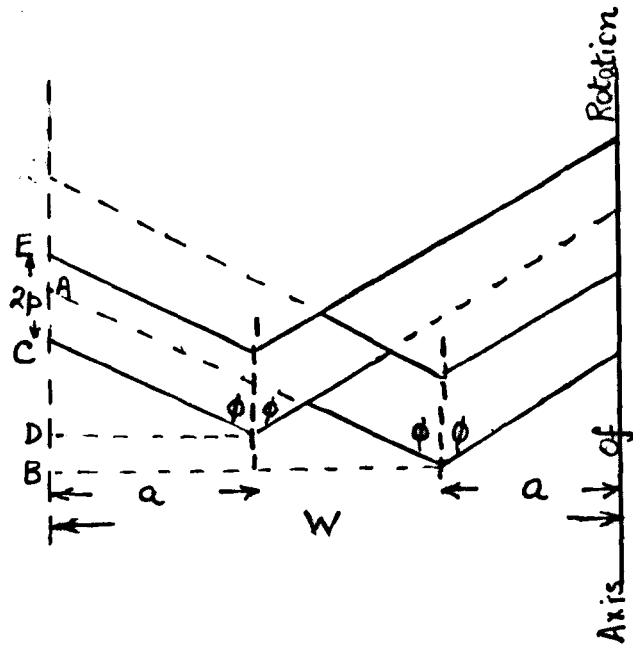
Included angle between cutting edges on front face of bit leg.

Clearance Angle.

- (i) Apparent Clearance Angle. Angle between under face of bit leg and plane through cutting tip normal to axis of rotation.
- (ii) Effective Clearance Angle. Angle between under face of bit leg and plane through cutting tip parallel to direction of cutting.

Other terms have been defined as used in the text.

Cutting Action of Eccentric Bit



$$AB = (W-a) \cot \phi$$

$$CD = a \cot \phi$$

$$BD = p$$

$$CE = 2p$$

$$AC = AB - CD - DB$$

$$= (W-a) \cot \phi - a \cot \phi - p$$

$$= (W-2a) \cot \phi - p$$

W = width of inserts

a = distance to tips from outer and inner periphery (respect.)

2p = Penetration/revolution

2φ = Point Angle

$$\text{Overlap} = (W - 2a) \cot \phi - p$$

∴ For full cutting edge to be operative

$$p \geq (W - 2a) \cot \phi$$

Also thickness of flake on this portion when cutting on full edge

$$t = p - (W - 2a) \cot \phi$$

e.g. if $W = 1\frac{1}{8}"$

$$a = \frac{3}{8}"$$

$$\phi = 60^\circ$$

$$\text{Total penetration } (2p) \text{ for "full cutting"} = \frac{3}{4} \frac{1.732}{3} = .433"/\text{rw.}$$

R.P.M.	Drilling Rate
180	78.0" / min.
320	138.5" / min.
500	216" / min.
700	303" / min.

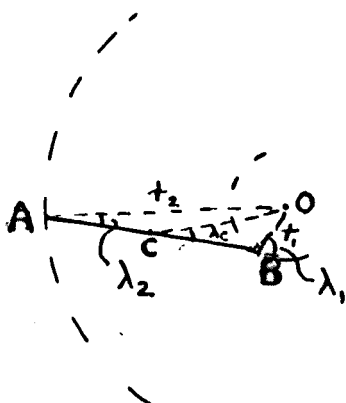
APPENDIX 3

Oblique Cutting in Rotary Drilling

Consider general case where bit edge is inclined at λ to the radius passing through its centre. (Most general way of expressing obliquity)

Definition The angle of obliquity at any point is the angle that the element of cutting edge at that point makes with the radius to the same point.

Variation of obliquity angle across bit edge



Let $\lambda_1, \lambda_2, \dots, \lambda_n$ be the angle of obliquity at any required position along AC.

λ_c is the angle of obliquity at centre of insert.

From ΔOCB

$$\frac{r_2}{\sin(180^\circ - \lambda_c)} = \frac{r_c}{\sin \lambda_1}$$

$$\therefore \sin \lambda_1 = \frac{r_c}{r_2} \sin \lambda_c$$

where r_c and r_2 are radius to centre and bit diameter respectively.

Calculation of obliquity at centre given bit radius, core radius and perpendicular distance 'D' between legs

$$r_c = \frac{\sqrt{(2r_2^2 + 2r_1^2 - b^2)}}{2}$$

$$\text{Hence } \sin \lambda_c = \frac{D/2}{\frac{\sqrt{(2r_2^2 + 2r_1^2 - b^2)}}{2}}$$

$$= \frac{D}{\sqrt{2r_2^2 + 2r_1^2 - b^2}}$$

APPENDIX 1

Effect of Variation of Point Angle on Effective Wedge Angle
(and hence Effective Rake and Effective Clearance angles)

See accompanying diagram (Fig. (i))

Let plane BCK be $px + pq + rz + d = 0$ (i)

p, q, r are direction cosines

C is $(0, 0, c)$ and is on plane BCK $\therefore rc + d = 0$ (ii)

K is $(a, b, 0)$ and is on plane BCK $\therefore pa + qb + d = 0$ (iii)

Directions - cosines of normal to plane ACK (i.e. of ON altitude of $\triangle AOC$) = $\sin \alpha, 0, \cos \alpha$.

Direction - cosines of BCK - p, q, r

But BCK and ACK are \perp $\therefore lp + mr = 0$ (iv)

\therefore Eliminate p, q, r, d from (i) and (iv)

(to find equation of BCK)

$$\begin{vmatrix} x & y & z & 1 \\ 0 & 0 & c & 1 \\ a & b & 0 & 1 \\ 1 & 0 & m & 0 \end{vmatrix} = 0$$

$$x \begin{vmatrix} 0 & c & 1 \\ b & 0 & 1 \\ 0 & m & 0 \end{vmatrix} - y \begin{vmatrix} 0 & c & 1 \\ a & 0 & 1 \\ 1 & m & 0 \end{vmatrix} + z \begin{vmatrix} 0 & 0 & 1 \\ a & b & 1 \\ 1 & 0 & 0 \end{vmatrix} - 1 \begin{vmatrix} 0 & 0 & c \\ a & b & 0 \\ 1 & 0 & m \end{vmatrix} = 0$$

$$x (bm) - y (cl + am) + z (-bl) - 1 (-bc) = 0$$

$$(bm)x - (cl + am)y - (bl)z + blc = 0 \quad \dots \text{I}$$

To determine angle BKC

Direction cosines KC

KC joins $(a, b, 0)$ to $(0, 0, c)$

Direction ratios $a, b, -c$ (see diagram)

Direction cosines $\frac{a}{\mu}, \frac{b}{\mu}, \frac{-c}{\mu}$

where $\mu^2 = a^2 + b^2 + c^2$

But BK joins B to K

Co-ords of B

Substituting $x = 0$, $y = 0$ in I

$$OB = \frac{blc}{cl + am} = \lambda \text{ (say)}$$

K is $(a, b, 0)$

B is $(0, \lambda, 0)$

Direction ratios of BK are $a, (b - \lambda), 0$.

Direction cosines of BK are $\frac{a}{w}, \frac{b - \lambda}{w}, 0$.

$$\text{Where } w^2 = a^2 + (b - \lambda)^2$$

$$\text{D-Cs for KC} = \frac{a}{\mu}, \frac{b}{\mu}, \frac{-c}{\mu}$$

$$\text{D-Cs for BK} = \frac{a}{w}, \frac{b - \lambda}{w}, 0.$$

$$\cos \angle BKC = \cos \theta = \frac{a^2}{\mu w} + \frac{b(b - \lambda)}{\mu w} \quad \dots \text{ II}$$

From geometry of diagram

$$\tan \eta = \frac{a}{b} \sec \alpha \quad \dots \text{ (v)}$$

$$\tan \alpha = \frac{c}{a} \quad \dots \text{ (vi)}$$

$$\lambda = \frac{blc}{lc + am} = b \cdot \frac{1}{1 + \frac{am}{lc}} = \frac{b \cdot 1}{1 + \cot^2 \alpha} \quad \begin{array}{l} l = \sin \alpha \\ m = \cos \alpha \end{array}$$

$$\lambda = b \sin^2 \alpha \quad \dots \text{ (vii)}$$

$$b = a \frac{\sec \alpha}{\tan \eta} \quad \dots \text{ (viii)}$$

$$c = a \tan \eta \quad \dots \text{ (ix)}$$

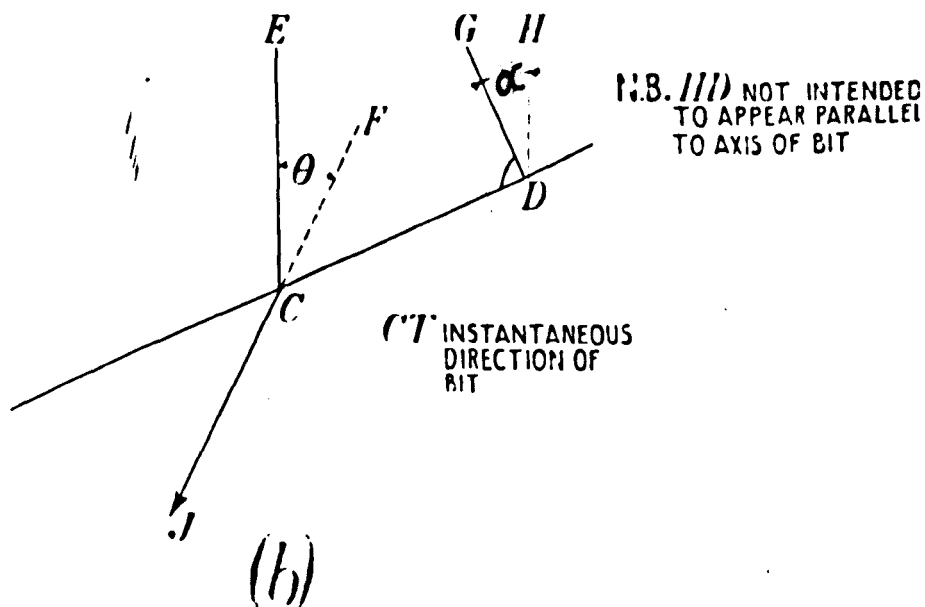
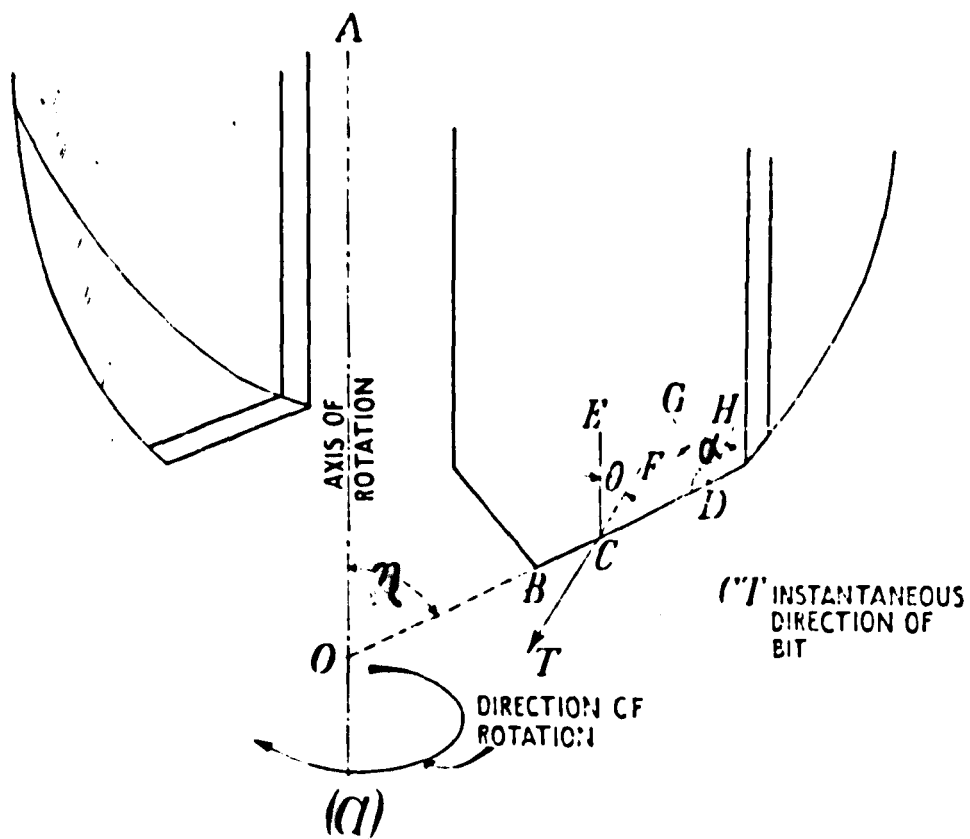
Substituting in II

$$\begin{aligned} \cos \theta &= \frac{1}{\mu w} \left(a^2 + b^2 \cos^2 \alpha \right) = \frac{a^2}{\mu w} \left\{ 1 + \frac{\sec^2 \alpha}{\tan^2 \eta} \cdot \cos^2 \alpha \right\} \\ &= \frac{a^2}{\mu w} \operatorname{cosec}^2 \eta \end{aligned}$$

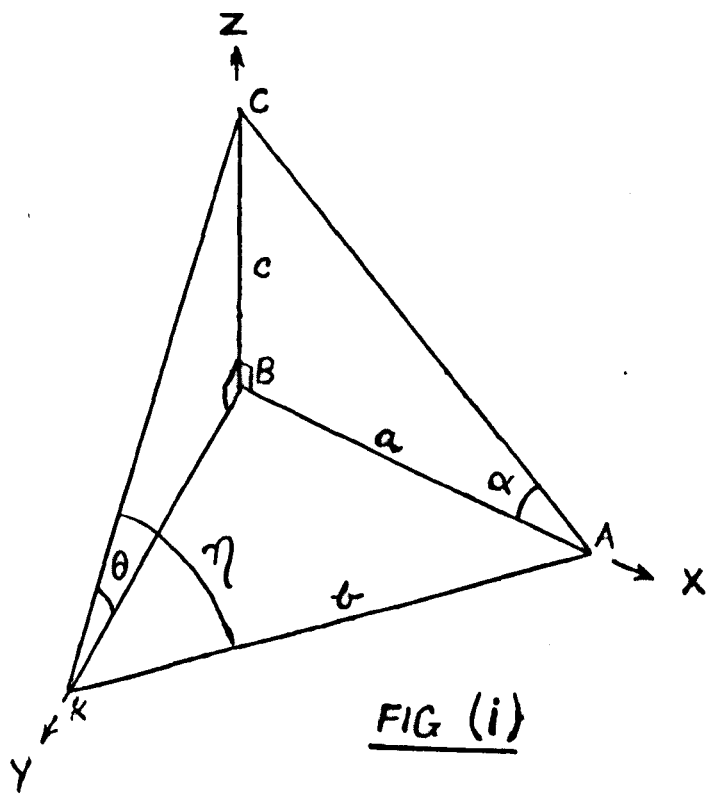
$$\mu^2 w^2 = (a^2 + b^2 + c^2)(a^2 + (b - \lambda)^2)$$

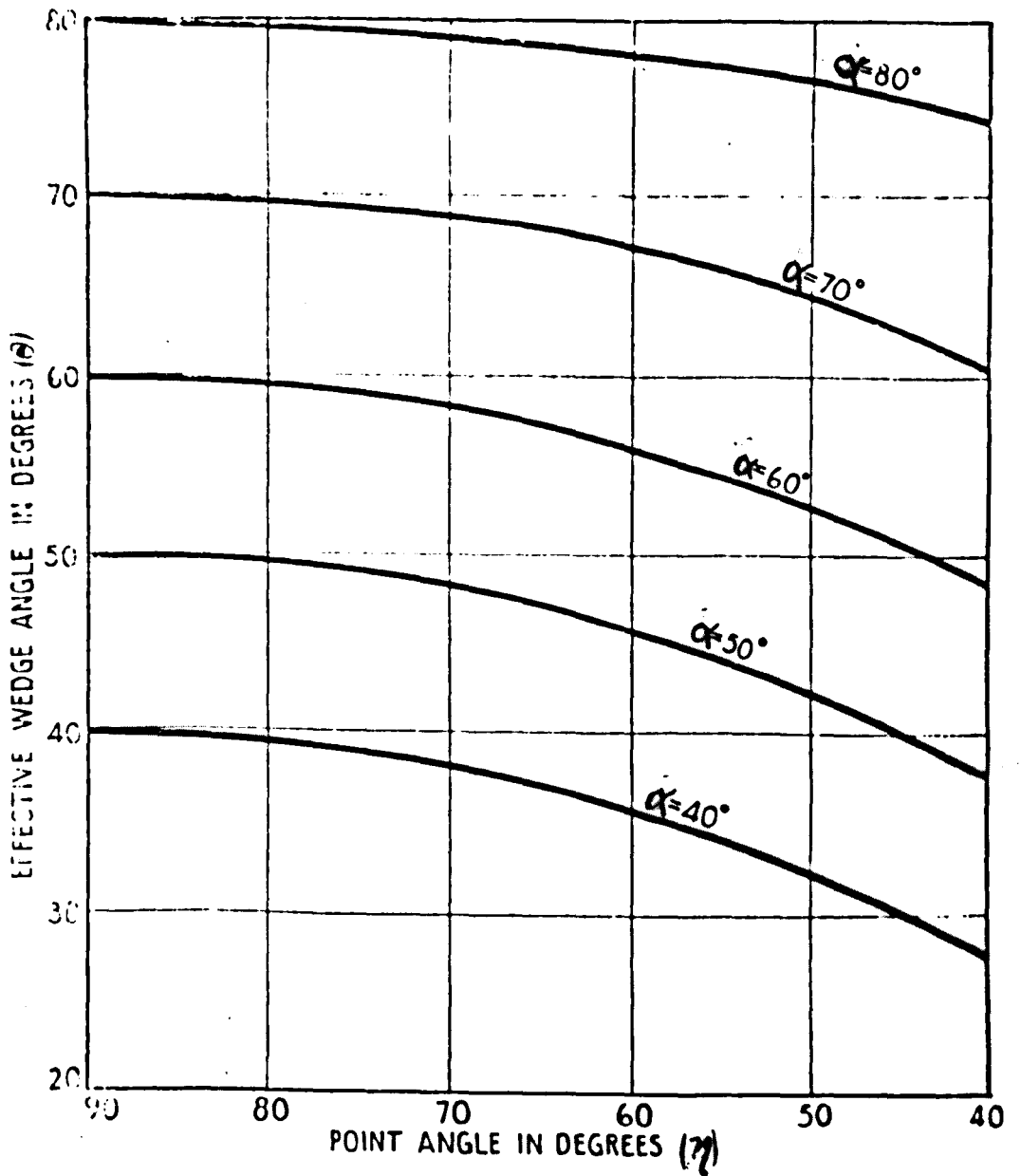
$$a^2 + b^2 + c^2 = a^2 \left(1 + \frac{\sec^2 \alpha}{\tan^2 \eta} + \tan^2 \alpha \right)$$

(ii)



To show the relationship between Point Angle, Wedge Angle, and Effective Wedge Angle





The effect of Variation of Point Angle on the Effective Wedge Angle

$$a^2 + (b - \lambda)^2 = a^2 \left(1 + \frac{\sec^2 \alpha}{\tan^2 \eta} \cos^4 \alpha \right)$$

$$= a^2 \left(1 + \frac{\cos^2 \alpha}{\tan^2 \eta} \right)$$

$$\mu_w^2 = a^4 \sec^2 \alpha \operatorname{cosec}^2 \eta \left(1 + \frac{\cos^2 \alpha}{\tan^2 \eta} \right)$$

$$= a^4 \operatorname{cosec}^2 \eta (\sec^2 \alpha + \cot^2 \eta)$$

$$\mu_w = a^2 \operatorname{cosec} \eta \sqrt{\sec^2 \alpha + \cot^2 \eta}$$

$$\cos \theta = \frac{a^2 \operatorname{cosec}^2 \eta}{a^2 \operatorname{cosec} \eta \sqrt{\sec^2 \alpha + \cot^2 \eta}}$$

$$= \frac{\operatorname{cosec} \eta}{\sqrt{\sec^2 \alpha + \cot^2 \eta}}$$

$$\cos = \frac{\cos \alpha}{\cos \eta \sqrt{\tan^2 \eta + \cos^2 \alpha}}$$

$\eta \searrow \alpha \rightarrow$	70°	60°	50°	40°	30°	80°
70°	68.9°	58.3°	48.4°	38.3°	28.8°	79.4°
60°	67.3°	56.4°	46.0°	36.0°	26.5°	
50°	64.6°	53.0°	42.4°	32.9°	23.5°	76.8°
40°	60.9°	48.5°	37.9°	29.0°	21.1°	74.5°

Above table shows values of θ (effect. wedge angle) for given values of η (2η = point angle) and α (actual wedge angle) in ~~the~~ plane \perp to face of bit and normal to cutting edge.

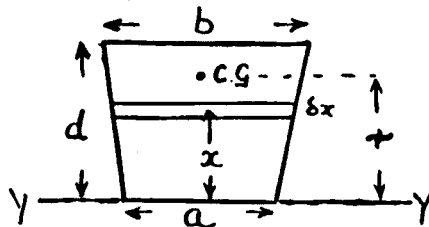
N.B. The leg rake angle of a bit is always measured in the plane of the "effective wedge angle" and consequently this value of rake should be used in conjunction with the effective wedge angle. Thus the effect of decreasing the point angle is to reduce the effective wedge angle and increase the clearance angle.

Deflection and Stresses of Bit Leg under Load

N.B. Calculations are all based on a static load. The effect of impact loading is considered later.

In order to simplify calculations the bit is considered to be of the form shown in the accompanying diagram.

1. Moment of Inertia of trapezoidal section (through centre of gravity)



Area of strip of width δx , at distance 'x' from YY is

$$\begin{aligned}
 &= \left\{ a + \frac{(b-a)}{d} x \right\} \cdot \delta x \\
 I_{YY} &= \sum_0^d \left\{ a + \frac{(b-a)}{d} x \right\} \delta x \cdot x^2 \\
 &= \int_0^d ax^2 dx + \int_0^d \left(\frac{b-a}{d} \right) \cdot x^3 dx \\
 &= \frac{ax^3}{3} \left[1 + \frac{(b-a)}{d} \frac{x^4}{4} \right]_0^d \\
 I_{YY} &= \frac{d^3}{12} (a + 3b)
 \end{aligned}$$

By theorem of parallel axes:

$$I_{C.G.} = I_{YY} - mr^2$$

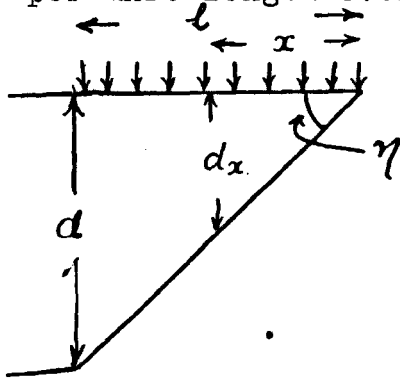
But $m = \frac{(a+b)d}{2}$ and $r = \frac{d}{3} \left(\frac{a+2b}{a+b} \right)$

$$\begin{aligned}
 \therefore I_{C.G.} &= \frac{d^3}{12} (a + 3b) - \frac{d^3}{18} (a+b) \left(\frac{a+2b}{a+b} \right)^2 \\
 &= \frac{d^3}{36} \left\{ \frac{3a^2 + 9b^2 + 12ab - 2a^2 - 8ab - 8b^2}{(a+b)} \right\} \\
 &= \frac{d^3}{36} \left(\frac{a^2 + 4ab + b^2}{(a+b)} \right)
 \end{aligned}$$

$$I_{C.G.} = \frac{\mu d^3}{36} \quad \text{where} \quad \mu = \left(\frac{a^2 + 4ab + b^2}{(a+b)} \right)$$

Cutting edge of bit = (R)(S)(T)

Consider bit as cantilever with uniformly distributed cutting force 'w' per unit length over length l.



Take origin at free end, bit considered rigid beyond l.

At any point \$x\$ from tip the bending moment

$$EI \frac{d^2 y}{dx^2} = wx \cdot \frac{x}{2}$$

and $I = \frac{\mu d_x^3}{36}$ where $d_x = x \tan \eta$

$$\therefore \frac{d^2 y}{dx^2} = \frac{wx^2 \cdot 36}{2 E \mu x^3 \tan^3 \eta}$$

$$\frac{d^2 y}{dx^2} = \frac{18w \cot^3 \eta x^{-1}}{E \mu}$$

$$\frac{dy}{dx} = \frac{18w \cot^3 \eta}{E \mu} (\log_e x + A)$$

Now $\frac{dy}{dx} = 0$, when $x = l \therefore A = -\log_e l$.

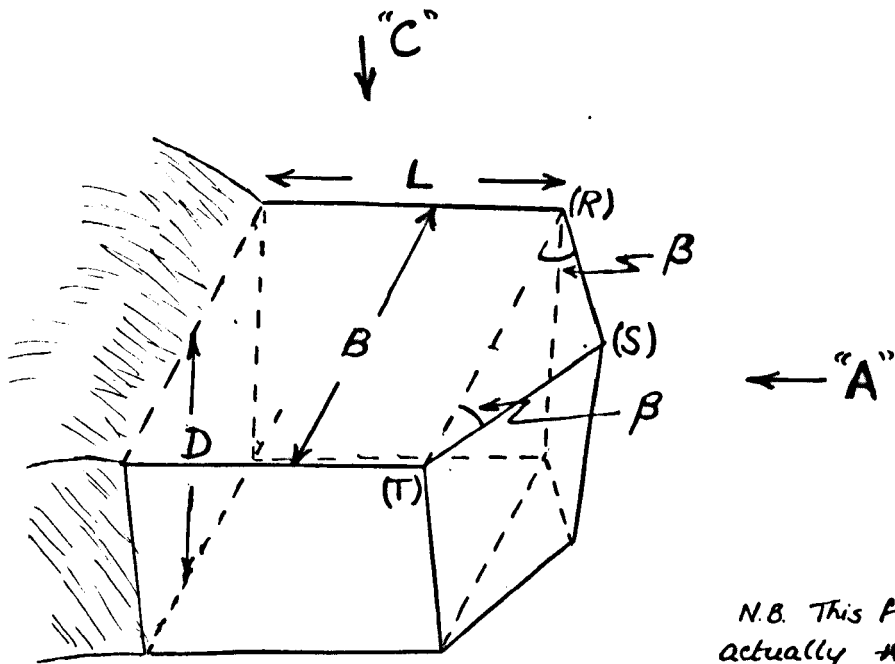
$$\frac{dy}{dx} = \frac{18w \cot^3 \eta}{E \mu} (\log_e x - \log_e l)$$

$$y = \frac{18w \cot^3 \eta}{E \mu} (x \log_e x - x - x \log_e l + B)$$

Now $y = 0$, when $x = l \therefore B = -\{1(\log_e l - 1 - \log_e l)\} = 1$

$$y = \frac{18w \cot^3 \eta}{E \mu} \left(x \log_e \frac{x}{l} + (l-x) \right)$$

Idealised Bit Form considered in calculations on Bit deflection

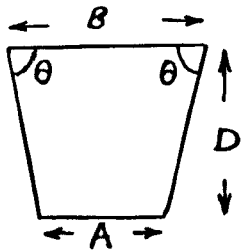


N.B. This form is not actually realisable but involves very little error.



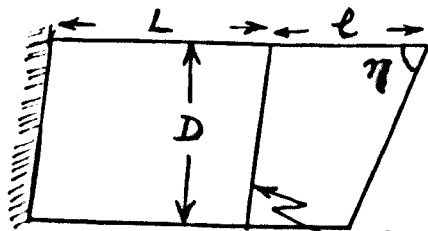
[Tip must be a trapezium]

"B"



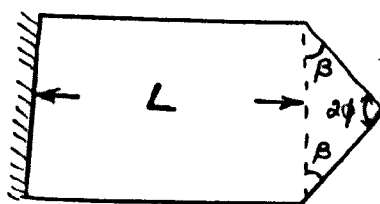
$$A = B - 2D \cot \theta$$

VIEW "A"

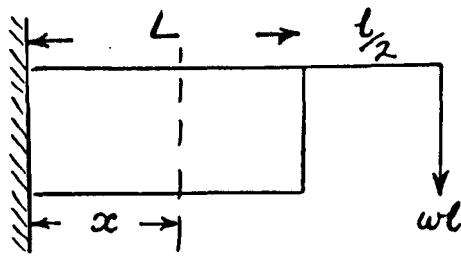


This considered vertical.

VIEW "B"



VIEW "C"



B.M at distance x from rigid section

$$= wl \left(L + \frac{l}{2} - x \right)$$

$$\frac{d^2y}{dx^2} = \frac{wl}{EI} \left(L + \frac{l}{2} - x \right)$$

$$\frac{dy}{dx} = \frac{wl}{EI} \left(Lx + \frac{lx}{2} - \frac{x^2}{2} + A \right)$$

$$\frac{dy}{dx} = 0 \text{ when } x = 0 \therefore A = 0$$

$$y = \frac{wl}{EI} \left(\frac{Lx^2}{2} + \frac{lx^2}{4} - \frac{x^3}{6} + B \right)$$

$$y = 0 \text{ when } x = 0 \therefore B = 0$$

$$y = \frac{wl}{EI} \left(\frac{Lx^2}{2} + \frac{lx^2}{4} - \frac{x^3}{6} \right)$$

Deflection maximum when $x = L$

$$y \text{ max} = \frac{wl}{EI} \left(\frac{L^3}{2} - \frac{L^3}{6} + \frac{L^2l}{4} \right)$$

$$= \frac{wl \cdot L^2}{EI} \left(\frac{4L + 3l}{12} \right) = \frac{3wl \cdot L^2}{E \cdot \mu d^3} (4L + 3l)$$

TOTAL DEFLECTION

$$y_1 = \frac{18w \cot^3 \eta}{E \mu} \left\{ x \log_e \frac{x}{l} + (l - x) \right\}$$

$$y_2 = \frac{3w l L^2}{E \mu d^3} (4L + 3l)$$

$$\underline{L = nl}$$

$$= \frac{3w \cdot n^2 l^3}{E \mu d^3} (4L + 3l)$$

$$= \frac{3wn^2 \cot^3 \eta}{E \mu} (4L + 3l)$$

$$y_t = y_1 + y_2$$

$$y_t = \frac{w \cot^3 \eta}{E \mu} 18 \left\{ x \log_e \frac{x}{l} + (l-x) \right\} + 3n^2(4L + 3l)$$

In above formula:-

y_t = deflection of tip

x = distance from actual tip to "point" (i.e. imaginary junction of two faces)

l = $\frac{1}{2} B \tan \beta$ (See View C) = $2 B \cot \theta$

L = length of straight side

n = Ratio L/l

w = loading/unit length (of l)

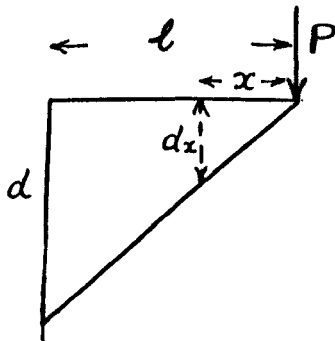
η = wedge angle

μ = $\frac{A^2 + 4AB + B^2}{B + A}$ (See View A)

The above solution would appear to be nearest to the actual conditions in cutting.

Alternative solutions for special cases

CASE 1.



Consider concentrated force P, at extreme tip.

At any point x from tip the bending moment -

$$EI \frac{d^2 y}{dx^2} = Px$$

$$\frac{d^2 y}{dx^2} = \frac{36 P \cot^3 \eta}{E \mu} x^{-2}$$

$$\frac{dy}{dx} = \frac{36 P \cot^3 \eta}{E \mu} (-x^{-1} + A)$$

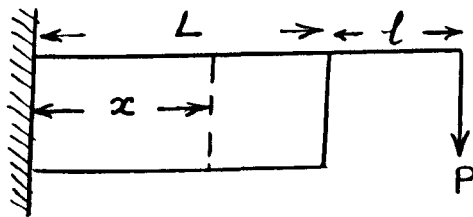
Now $\frac{dy}{dx} = 0$, when $x = 1 \therefore A = 1/l$

$\therefore y = \frac{36 P \cot^3 \eta}{E \mu} (-\log_e x + \frac{x}{l} + B)$

$y = 0$, when $x = l \therefore B = \log_e l - 1$

$\therefore y_1 = \frac{36 P \cot^3 \eta}{E \mu} (\log_e \frac{l}{x} + \frac{x}{l} - 1)$

$y_1 = \frac{36 P \cot^3 \eta}{E \mu} (\frac{x}{l} - 1 - \log \frac{x}{l})$



$\frac{d^2y}{dx^2} = \frac{M}{EI} = \frac{P(L + l - x)}{EI} = \frac{d^2y}{dx^2}$

$\frac{dy}{dx} = \frac{P}{EI} (Lx + lx - \frac{x^2}{2} + A)$

$\frac{dy}{dx} = 0$, when $x = 0 \therefore A = 0$

$y = \frac{P}{EI} (\frac{Lx^2}{2} + \frac{lx^2}{2} - \frac{x^3}{6} + B)$

$y = 0$, when $x = 0 \therefore B = 0$

y_{\max}

$x = L$

$y_2 = \frac{P}{EI} (\frac{L^3}{2} + \frac{L^2 l}{2} - \frac{L^3}{6})$

$= \frac{PL^2}{EI} (\frac{L}{3} + \frac{l}{2})$

$I = \frac{\mu d^3}{36}$

$y_2 = \frac{36 P L^2}{E \mu d^3} (\frac{L}{3} + \frac{l}{2})$

$L = nl$

$y_2 = \frac{36 P n^2 l^3}{E \mu d^3} (\frac{n}{3} + \frac{1}{2})$

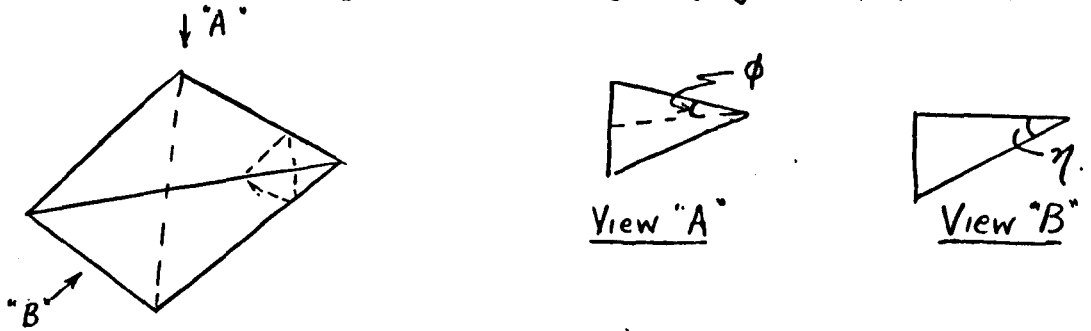
$= \frac{36 P n^2 \cot^3 \eta}{E \mu} (\frac{n}{3} + \frac{1}{2})$

$y_1 + y_2 = y_t = \frac{36 P \cot^3 \eta}{E \mu} (\log_e \frac{l}{x} + \frac{x}{l} - 1 + n^2 (\frac{n}{3} + \frac{1}{2}))$

(vi)

CASE 2.

(C) Tapering width and depth (e.g. at tip points.)



Consider section distance x from tip.
width " b " and depth " d "

$$\text{B.M.} = M_x = E I_x \frac{d^2 y}{dx^2} \quad I_x = \frac{bd^3}{12}$$

$$b = 2x \tan \phi \quad d = x \tan \eta$$

$$\therefore \frac{E \tan \phi \tan^3 \eta}{6} \frac{d^2 y}{dx^2} = Px^{-3}$$

Put $\frac{E \tan \phi \tan^3 \eta}{6} = K$

$$\therefore \frac{d^2 y}{dx^2} = \frac{P}{K} x^{-3}$$

$$\therefore \frac{dy}{dx} = \frac{P}{K} \left(-\frac{x}{2}^{-2} + A \right)$$

Now $\frac{dy}{dx} = 0$, when $x = l$, $\therefore A = 1/2l^2$

$$\frac{dy}{dx} = \frac{P}{2K} (l^{-2} - x^{-2})$$

$$\therefore y = \frac{P}{2K} \left(\frac{x}{l^2} + \frac{1}{x} + B \right)$$

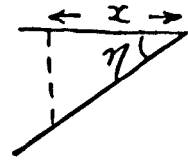
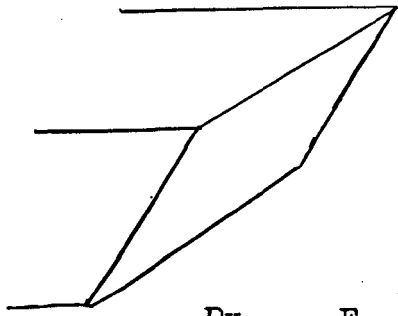
$y = 0$, when $x = l$, $\therefore B = -2/l$

$$y = \frac{P}{2K} \left(\frac{x}{l^2} + \frac{1}{x} - \frac{2}{l} \right)$$

$$= \frac{P}{2K} \frac{(l-x)^2}{l^2 x}$$

$$y = \frac{3 P \cot^3 \eta}{E \tan \mu} \left\{ \frac{(l-x)^2}{l^2 x} \right\}$$

(D) Assuming constant breadth



$$M = EI \frac{d^2 y}{dx^2}$$

$$Px = E \frac{b (x \tan \eta)^3}{12} \cdot \frac{d^2 y}{dx^2}$$

$$\frac{d^2 y}{dx^2} = \frac{12 P}{E b \tan^3 \eta} \cdot x^{-2}$$

$$\frac{dy}{dx} = \frac{12 P}{E b \tan^3 \eta} \left(\frac{x^{-1}}{-1} + A \right) \quad \frac{dy}{dx} = 0 \quad x = l$$

$$A = \frac{1}{l}$$

$$= \frac{12 P}{E b \tan^3 \eta} \left(\frac{1}{l} - \frac{1}{x} \right)$$

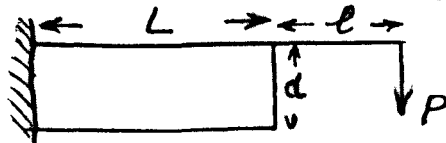
$$y = \frac{12 P}{E b \tan^3 \eta} \left(\frac{x}{l} - \log_e x + B \right) \quad y = 0, \quad x = l$$

$$B = \log_e l - 1$$

$$= \frac{12 P}{E b \tan^3 \eta} \left(\frac{x}{l} - \log_e x + \log_e l - 1 \right)$$

$$= \frac{12 P}{E b \tan^3 \eta} \left(\frac{x}{l} - \log_e \frac{x}{l} - 1 \right)$$

$$y_1 = \frac{12 P}{E b} \cot^3 \eta \left(\frac{x}{l} - \log_e \frac{x}{l} - 1 \right)$$



$$y_2 = \frac{PL^2}{EI} \left(\frac{L}{3} + \frac{l}{2} \right)$$

$$= \frac{12 PL^2 \cot^3 \eta}{E b l^3} \left(\frac{L}{3} + \frac{l}{2} \right)$$

$$= \frac{12 P n^2 \cot^3 \eta}{E b} \left(\frac{n}{3} + \frac{1}{2} \right)$$

$$y_t = \frac{12 P \cot^3 \eta}{E b} \left\{ n^2 \left(\frac{n}{3} + \frac{1}{2} \right) + \frac{x}{l} - \log_e \frac{x}{l} - 1 \right\}$$

Having calculated the deflections under various conditions of loading for various bit types, it is informative to consider the stress conditions at the tip, especially on the front face.

1. Assume constant width tip.

Consider bit with tip of constant width.

Neutral axis OC passes through centroid of individual elements.

$$f_t = \frac{My}{I} \quad \text{where } M \text{ is bending moment at a given section}$$

I - Moment of Inertia of section

$$\text{(about neutral axis)} = \frac{b d^3}{12}$$

f_t - Longitudinal tensile stress at a distance y from neutral axis

Consider a section at distance x from tip where

$$y = \frac{x}{2} \tan \eta \quad \text{and} \quad M = Px$$

$$f_t = \frac{My}{I} = Px \cdot \frac{x \tan \eta}{2} \times \frac{12}{b x^3 \tan^3 \eta}$$

$$\therefore f_t = \frac{6P}{bx \tan^2 \eta}$$

$$\text{i.e. STRESS} \propto \frac{1}{bx \tan^2 \eta}$$

The stress is inversely proportional to $\tan^2 \eta$, distance from tip, and breadth.

$$\text{N.B. Stress} \propto \frac{1}{\text{Breadth}}$$

When considering the bit with point angle = 2ϕ

$$\text{then } f_t = \frac{6P}{2x \tan \phi} \times \tan^2 \eta$$

$$= \frac{3P}{x^2 \tan^2 \eta} \tan \phi.$$

(ix)

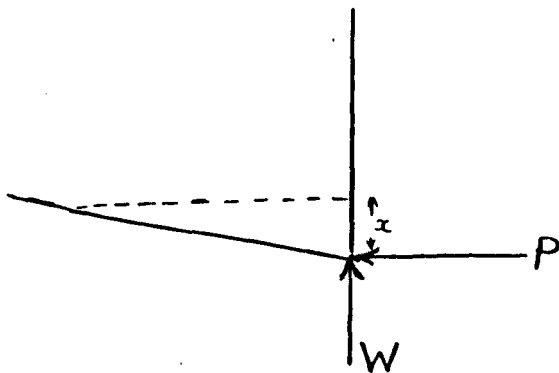
i.e. STRESS $\propto 1/x^2 \tan^2 \eta \tan \phi$

- \therefore Stress reduced by
1. Increasing η
 2. Increasing ϕ .

N.B. tangent of an angle increases rapidly at high values

e.g.	$\tan 70^\circ = 2.7475$	$\tan^2 70^\circ = 7.55$
	$\tan 75^\circ = 3.7321$	$\tan^2 75^\circ = 13.93$
	$\tan 80^\circ = 5.6713$	$\tan^2 80^\circ = 32.2$
	$\tan 85^\circ = 11.43$	$\tan^2 85^\circ = 131.0$
	$\tan 90^\circ = \infty$	

- \therefore Stress can be considerably reduced by increasing $\tan \eta$ and $\tan \phi$.



Consider two components as combination of Bending stress (Force P) and Direct Compressive stress (Force W)

Can consider P constant and Varying W (from $W = P$ say)
 $W = 0$

Consider section distance "x" from tip. Assume constant breadth

Compressive Stress

$$\text{Compressive stress } f_c = W/bx \tan \eta$$

$$\text{Tensile stress } f_t = 6P/bx \tan^2 \eta$$

$$\text{Resultant stress } f_r = \frac{1}{bx \tan \eta} \left(\frac{6P}{\tan \eta} - W \right)$$

(N.B. $f_w \propto \frac{1}{x}$ and $f_t \propto \frac{1}{\tan \eta}$)

Let $\frac{W}{P} = \chi$

$$\text{Resultant Tensile Stress} = \frac{P}{b x \tan^2 \eta} (6 - \chi \tan \eta)$$

From observations by writer χ of order 0.5-1.5

$\tan \eta$ usually of order 1.5-2.5

- \therefore Effect of W is negligible (in reducing stress on front face)

N.B. Any bending effect of W (e.g. with positive rake tools) has been neglected since will not occur in example taken, i.e. zero rake (nor, in fact, with negative rake)

~~Refer to work of~~ }
~~1. Ocker and Pilon~~ }
 2. Archibald }

Impact Velocities

1. By consideration of motion of tip on sudden release of load.
2. By consideration of stored strain energy.

1. Force = Mass x Acceleration

$$wl = \frac{W}{g} \times \frac{d^2y}{dt^2} \quad (i) \quad W = \text{weight of bit}$$

But $wl \propto y$ (previously derived equation)

N.B. $y = \frac{wl \cot^3 \eta}{E\mu} \left\{ 18(t \log_e t + (1-t) + 3n^2(4n+3)) \right\}$ Let $\frac{x}{l} = t$

$\therefore y = Kwl$ (ii) (K is const. = $\frac{\cot^3 \eta}{E\mu} (18(t \log_e \dots))$). $\frac{l}{l} = n$.

Substituting (ii) in (i)

$$\therefore y = \frac{KW}{g} \cdot \frac{d^2y}{dt^2}$$

i.e. Acceleration \propto Displacement

\therefore Motion is Simple Harmonic.

For S.H.M.

$$\frac{d^2x}{dt^2} = -p^2x \quad \therefore p = \sqrt{\frac{g}{KW}}$$

$$\text{Velocity} = \frac{dx}{dt} = p \sqrt{a^2 - x^2} \quad \text{where } a = \text{maximum displacement}$$

$x = \text{displacement at time 't'}$

$$\begin{aligned} \text{Maximum velocity} &= pa \\ &= y \sqrt{\frac{g}{KW}} \\ &= Kwl \sqrt{\frac{g}{KW}} = wl \sqrt{\frac{Kg}{W}} \end{aligned}$$

N.B. This considers only release from deflection caused by static loading.

Strain Energy

Work done by average force $\frac{wl}{2}$ in causing deflection Kwl

$$= \frac{K (wl)^2}{2}$$

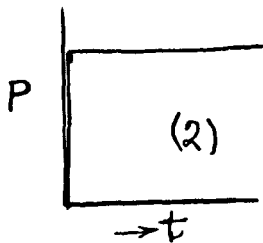
∴ Strain energy stored in beam = $\frac{K (wl)^2}{2}$

At maximum velocity deflection is zero and total strain energy converted to kinetic energy

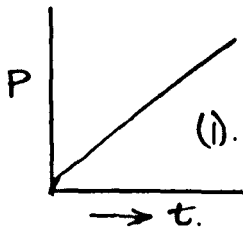
$$\frac{K (wl)^2}{2} = \frac{1}{2} \cdot \frac{W}{g} v^2 \quad v = \text{maximum velocity}$$

$$v = wl \sqrt{\frac{Kg}{W}} \quad (\text{Confirms previous result})$$

If load P applied dynamically without impact,
i.e. Case 2 instead of Case 1



Dynamic Loading



Static Loading

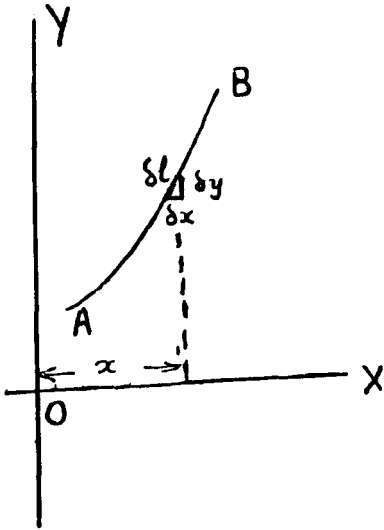
Strain energy
= (2)² x Static strain energy

∴ $v = 2 wl \sqrt{\frac{Kg}{W}}$

APPENDIX 6

Determination of "Ideal" Profile for Cutting Edge of Rotary Drill Bit

The so-called "Ideal" Bit is that which wears uniformly all along the cutting edge.



Let OY be axis of rotation

AB be profile of bit

Consider element " δl " distance
"x" from axis of rotation

Assume wear is proportional to
distance travelled/revolution.

i.e. Wear $\propto (2\pi x)^2 + p^2$
where "p" is penetration/revolution

For uniform wear the length of cutting edge " δl " over given element of cutting path, width " δx " must be proportional to the distance travelled, i.e.

$$\delta l \propto \sqrt{(2\pi x)^2 + p^2}$$

$$\frac{\delta l}{\delta x} \propto \sqrt{(2\pi x)^2 + p^2}$$

$$\delta l^2 = \delta x^2 + \delta y^2 = K^2 \{ (2\pi x)^2 + p^2 \} \cdot \delta x$$

$$\frac{\delta y^2}{\delta x^2} = K^2 \{ (2\pi x)^2 + p^2 \} - 1$$

$$\frac{\delta y}{\delta x} = K \sqrt{(2\pi x)^2 + p^2 - \frac{1}{K^2}}$$

$$dy = K \sqrt{(2\pi x)^2 - \left(\frac{1}{K^2} - p^2\right)} \cdot dx$$

$$= 2\pi K \sqrt{x^2 - \frac{1 - (pK)^2}{4\pi^2 K^2}} \cdot dx$$

Let $a^2 = \frac{1 - (pK)^2}{4\pi^2 K^2}$

$$\therefore dy = 2\pi K \sqrt{x^2 - a^2} \cdot dx$$

$$\int dy = y = 2\pi K \int \sqrt{x^2 - a^2} \cdot dx$$

$$\therefore y = \frac{2\pi K a^2}{2} \left[\frac{x \sqrt{x^2 - a^2}}{a^2} - \cosh^{-1} \frac{x}{a} \right] + C \dots (1)$$

$$x = 0, \text{ when } y = 0 \therefore C = a^2 \pi K$$

$$y = a^2 \pi K \left[\frac{x \sqrt{x^2 - a^2}}{a^2} - \cosh^{-1} \frac{x}{a} + 1 \right] \dots (2)$$

$$\text{As } a = \frac{\sqrt{1 - p^2 K^2}}{2\pi K}$$

$$y = \frac{1 - p^2 K^2}{4\pi K} \left[\frac{4\pi^2 K^2 x \sqrt{\frac{1 - p^2 K^2 x^2 - (1 - p^2 K^2)}{4\pi^2 K^2}}}{1 - p^2 K^2} - \cosh^{-1} \frac{2\pi K x + 1}{1 - p^2 K^2} \right]$$

$$\frac{1 - p^2 K^2}{4\pi K} \left[\frac{2\pi K x \sqrt{(2\pi K x)^2 - (1 - p^2 K^2)}}{1 - p^2 K^2} - \cosh^{-1} \frac{2\pi K x}{1 - p^2 K^2} + 1 \right]$$

$$y = \frac{x}{2} \sqrt{(2\pi K x)^2 - (1 - p^2 K^2)} - \frac{1 - p^2 K^2}{4\pi K} \cdot \frac{\cosh^{-1} 2\pi K x}{\sqrt{1 - p^2 K^2}} + \frac{1 - p^2 K^2}{4\pi K} \dots (3)$$

Alternative solution of Equation 2

$$y = a^2 \pi K \left[\frac{x \sqrt{x^2 - a^2}}{a^2} - \cosh^{-1} \frac{x}{a} + 1 \right] \dots (2)$$

$$\text{But } \cosh^{-1} \frac{x}{a} = \pm \log_e \left(\frac{x}{a} + \sqrt{\frac{x^2}{a^2} - 1} \right) = \pm \log_e \left(\frac{x + \sqrt{x^2 - a^2}}{a} \right)$$

for $x > 0$

$$y = a^2 \pi K \left[\frac{x \sqrt{x^2 - a^2}}{a^2} \pm \left(\log_e \left(x + \sqrt{\frac{4\pi^2 K^2 x^2 - (1 - p^2 K^2)}{4\pi^2 K^2}} \right) - \log_e \frac{\sqrt{1 - p^2 K^2}}{2\pi K} \right) + 1 \right]$$

$$= a^2 \pi K \left[\frac{x \sqrt{x^2 - a^2}}{a^2} \pm \log_e \left(\frac{x + \frac{1}{2\pi K} \sqrt{(2\pi K x)^2 - (1 - p^2 K^2)}}{\frac{\sqrt{1 - p^2 K^2}}{2\pi K}} \right) + 1 \right]$$

$$= a^2 \pi K \left[\frac{x \sqrt{x^2 - a^2}}{a^2} \pm \log_e \left\{ \frac{2\pi Kx}{\sqrt{1-p^2K^2}} + \frac{\sqrt{(2\pi Kx)^2 - (1-p^2K^2)}}{\sqrt{1-p^2K^2}} \right\} + 1 \right]$$

$$= \frac{1-p^2K^2}{4\pi K} \left[\frac{2\pi Kx \sqrt{(2\pi Kx)^2 - (1-p^2K^2)}}{(1-p^2K^2)} \pm \log_e \left\{ \frac{2\pi Kx}{\sqrt{1-p^2K^2}} + \frac{\sqrt{(2\pi Kx)^2 - 1}}{\sqrt{1-p^2K^2}} \right\} + 1 \right]$$

$$y = \frac{x}{2} \sqrt{(2\pi Kx)^2 - (1-pK)^2} \pm \frac{1-p^2K^2}{4\pi K} \log_e \left\{ \frac{2\pi Kx}{\sqrt{1-p^2K^2}} + \frac{\sqrt{(2\pi Kx)^2 - 1}}{\sqrt{1-p^2K^2}} \right\} + \frac{1-p^2K^2}{4\pi K} \dots (4)$$

Minimum Value of Constant K (Dimensions L^{-1} , i.e. units/inch)

$\frac{\delta l}{\delta x}$ has a minimum value = 1 when $x = 0$

$$\therefore \frac{\delta l}{\delta x}_{x=0} = K \sqrt{0 + p^2} = Kp = 1$$

$$\therefore \text{Minimum value of } K = \frac{1}{p}$$

If this value of K is substituted in Equations (3) and (4)

$$y = K \pi x^2 \dots (5)$$

\therefore Ideal profile approximates to a parabola

Example

Let $p = \frac{1}{8}$ /revolution

Then K = 8 units/inch

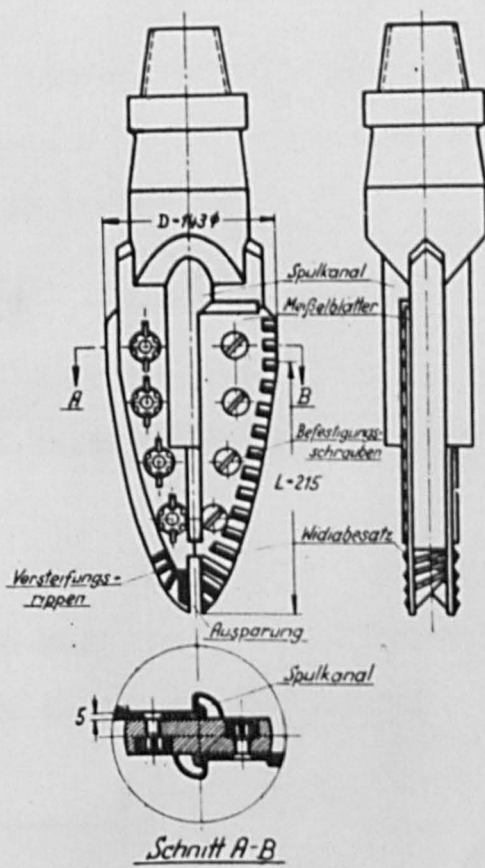
$$\therefore \text{Flattest curve is } y = 8\pi x^2$$

Values of $y = 8\pi x^2$

$x = \frac{1}{4}'' \quad \frac{1}{2}'' \quad \frac{3}{4}'' \quad 1''$

$y = 1.56'' \quad 6.28'' \quad 14.3'' \quad 25.1''$ [i.e. 2" dia. bit would be 25" long.]

Several authorities have described ideal bits and some have attempted to design types. (See overleaf) The above analysis demonstrates that the ideal profile is not practical.



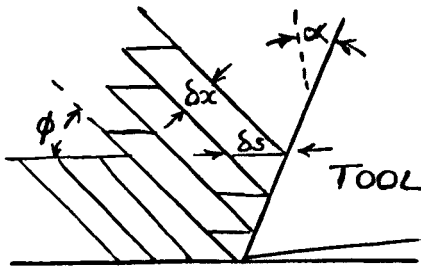
"IDEAL" BIT DESIGNED BY
BESIGK & KÜHNE

APPENDIX 7.

Basic Mechanics of The Metal Cutting Process. M.E. Merchant.
Journal Applied Mechanics A.S.M.E. Vol.66 (1944)
pp. A.168-A.175.

1. Determination of Shear Angle Relationship

Considers idealised model of shearing process.



Shear in "plates" thickness δx .

(In practice $\delta x \rightarrow 0$)

displaced relatively distance δs

From this it is easy to prove

$$\frac{\delta s}{\delta x} = \cot \phi + \tan (\phi - \alpha)$$

$$\frac{d_s}{d_x} = \text{shearing strain (e) undergone by chips.}$$

Considers shear angle to be determined by minimum value of "e" (Called "Minimum Energy Theory")

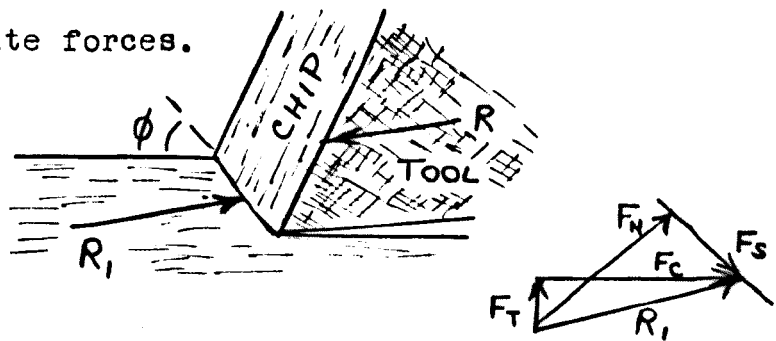
$$\frac{de}{d\phi} = -\operatorname{cosec}^2 \phi + \sec^2 (\phi - \alpha)$$

$$\therefore \phi_{e \min} = \frac{\alpha}{2} + 45^\circ \quad \left(\frac{de}{d\phi} = 0 \right)$$

This represented first expression used for Shear Angle in Metal Cutting.

Force Relationships

The cutting chip must be in equilibrium under the action of equal and opposite forces.



From the above analysis the resultant force may be resolved into

F_c = cutting force - responsible for total work done

F_t = thrust force - does no work

F_n = Normal, compressive force on shear plane

F_s = Shear force - responsible for shearing work

These forces may be represented on a circle diagram as shown. ^{in Fig 17.} Δ
This circle diagram is still accepted as accurate by authorities
on cutting.

Discontinuous Chip Formation (Field & Merchant)

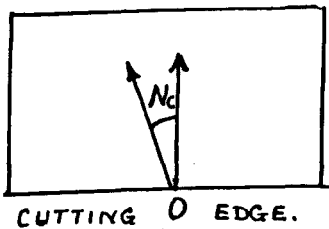
Trans. A.S.M.E. July 1949. Vol.71
pp. 421-430

Authors observed that chip started to shear (without fracture) at a high angle to the previous fracture line. They attempted to derive equations based on the minimum energy principle, relating the initial shear angle to the final fracture angle but found poor agreement with experiments. This paper demonstrates that there appears to be similar ties between this type of cutting and that observed in rock, although the processes are not completely understood.

APPENDIX 8.

Notes on article "The Mechanics of Three-Dimensional Cutting Operations". M.C. Shaw, N.H. Cook and P.A. Smith.
Trans. A.S.M.E. Aug. 1953
pp. 1055-1064

Stabler noted that angle of chip flow up the tool face with oblique tools was not in the direction of maximum slope as would be expected, but along a line inclined at some angle to it. (N_c)



The effective rake angle (α_e) of the cutting tool is determined by the slope of the line of chip flow. Stabler's observations led him to assume that $N_c = \lambda$ where $\lambda =$ Angle of Obliquity

resulting in the Equation

$$\sin \alpha_e = \sin^2 \lambda + \cos^2 \lambda \sin \alpha_a$$

where $\alpha_a =$ rake of tool when is 0 (i.e. orthogonal cutting)

This is shown plotted (from Stabler's paper).

The authors tested the validity of the relationship $N_c = \lambda$ using lubricants.

- Found
1. N_c decreases as rake angle (α_a) is increased.
 2. N_c increases when more efficient lubricant used.
 3. N_c increases as friction characteristics of the metal cut improve.

From these the authors conclude that

Stabler rule ($N_c = \lambda$) is only an approximation which is most nearly true for high friction values.

The above paper demonstrates that the direction of chip flow is considerably altered by oblique tools. Chip flow direction and maximum stress directions are almost collinear and it thus follows that the "directing of stress" effect

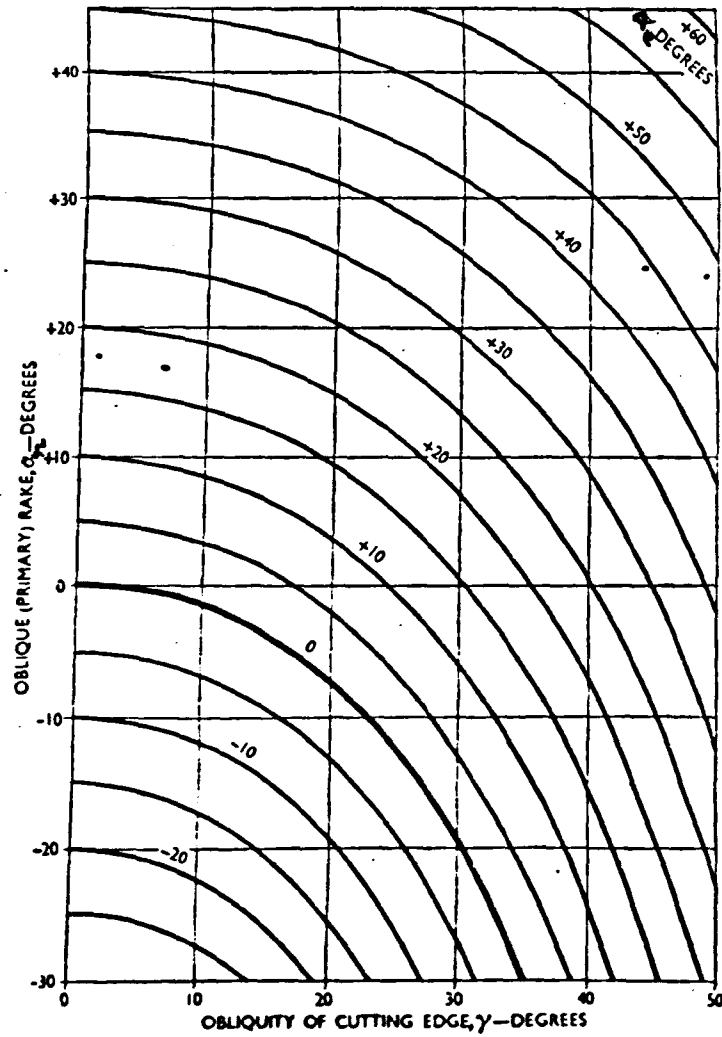


Fig. 7. Curves of Effective Rake α_e

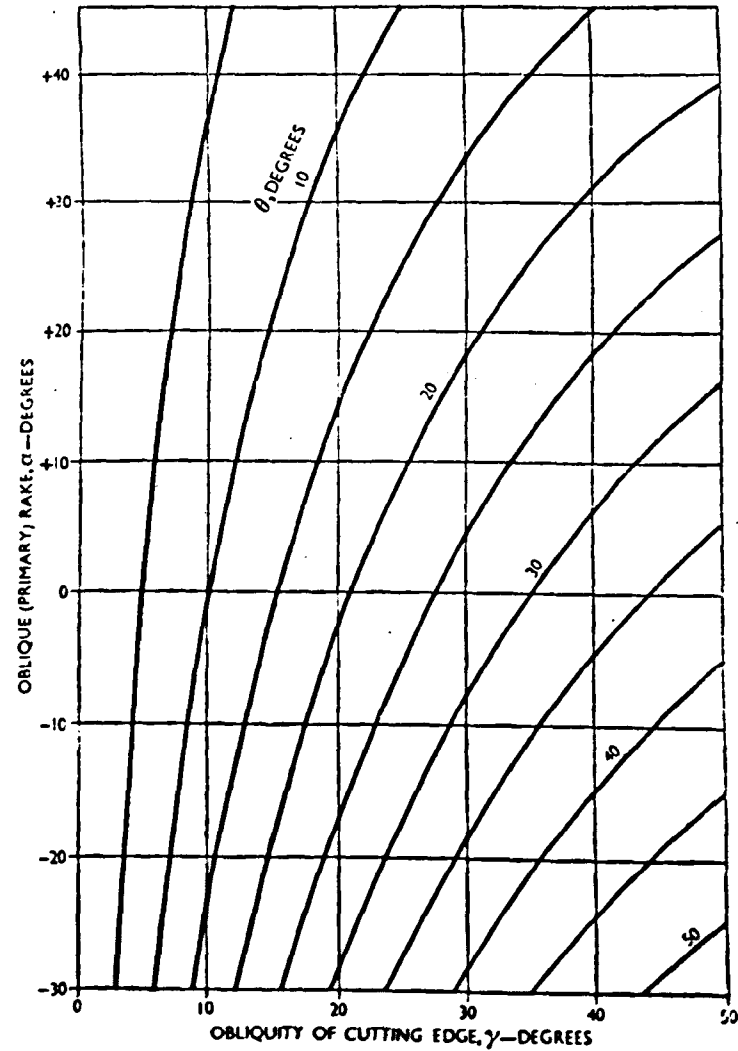
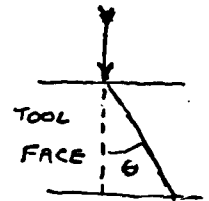


Fig. 8. Curves of θ

θ - Projected angle of deviation of chip flow.



STABLER'S CURVES.

of oblique tools may also be considerable. Since the writer has shown that rock cutting involves high friction forces, it seems possible that the relationship $N_c = \lambda$ is approximately true. This would suggest that oblique tools may prove to be of advantage since the effective rake angle (α_e) predicted by these equations (and curves) may be considerably higher than the apparent rake (α_a).

APPENDIX 9.

Shear-Angle Relationship in Metal Cutting. M.C. Shaw,
N.H. Cook and I. Finnie.
Trans. A.S.M.E. Vol. 75. Feb. 1953.
pp. 273-283

This paper discusses the various assumptions underlying the expressions derived for the Shear Angle value and demonstrates the inadequacy of them, e.g.

1. Minimum Energy Principle
2. Assumption that Coeff. of Friction is independent of Shear Angle
3. The direction of Shear is in the direction of maximum stress

Assumption 1. is not necessarily true and many processes are known where it is not so.

Assumption 2. The authors show that it is possible for the coefficient of friction to be reduced with decreased rake angle by consideration of the "restraint" and "effective hardness" of the wedge shaped area between tool face and shear plane (called restraining surface).

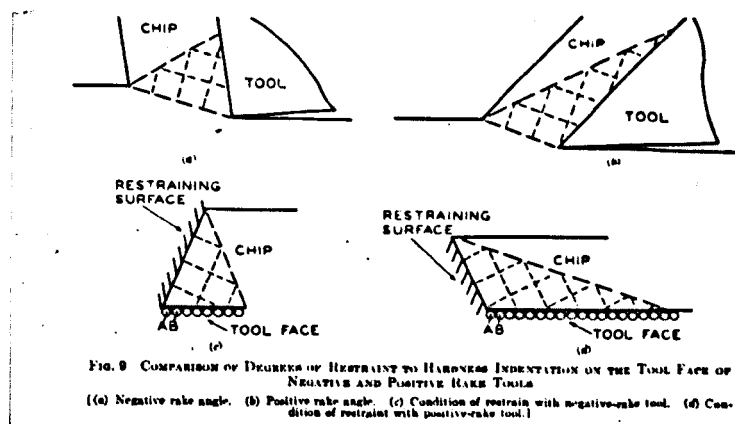


FIG. 9. COMPARISON OF DEGREES OF RESTRAINT TO HARDNESS INDENTATION ON THE TOOL FACE OF NEGATIVE AND POSITIVE RAKE TOOLS
[(a) Negative rake angle. (b) Positive rake angle. (c) Condition of restraint with negative-rake tool. (d) Condition of restraint with positive-rake tool.]

Considers Tool Face as series of small spheres. Material at tool point will resist penetration of sphere A to greater extent in the case of Fig.9(c) than 9(d) owing to relative positions of shearing strains. Metal in front of A must flow predominantly to the right in each case. Metal flowing in front of sphere A will move into the way of sphere B and hence the effect of the restraining surface will be transferred from sphere to sphere to the right. It is evident that the influence of the flow from one sphere to the next will be far greater in

the case of Fig.9(c) than 9(d).

The negative restraint is greater and the effective hardness greater. Thus the authors conclude

1. The coefficient of friction is not independent of the shear angle.
2. In view of the above it follows that the stress field is determined by this friction value and need not be in the direction of Maximum Shear Stress.

By this analysis the authors are able to explain previous conflicting results.

Rock cutting experiments have not allowed verification of this due to the extreme variability of cutting conditions.

APPENDIX 10.

DERIVATION OF BESIGK & KUHNE FORMULA.

- e = Depth of penetration of carbide stamp (in cm)
- K = drilling press. in Kg/cm².
- K_k = critical drilling press. in Kg/cm².
- K₀ = cylinder pressure resistance of rock in Kg/cm².
(infinite loading time)
- Q = total drilling thrust (in Kg).
- S¹ = flake thickness per revolution and one cut. (in cm)
- S = drilling speed cm/min.
- b = Effective thickness of hardmetal insert.
- D = bit. dia. in cm.
- D_k = Core dia. " "
- Z = No. of load changes on borehole face at average bit dia.
- N = Bit R.P.M.
- F = Area of contact between effective hard metal layer and face of bore hole in cm².
- V = Average peripheral velocity in cm/sec.
- a₁ = base of logarithmic curve.
log a₁ 100 with Widia hard metal inserts.
- a₂ = base of exponential curve.
log a₂ = 0.00125
(a₁ and a₂ are values found in experiment)

Basic equation.

$$e = \log_{a_1} \frac{K}{K_k} \dots\dots\dots(9) \text{ (This is from pen/load curve with stamp)}$$

Flake Thickness S¹

$$S^1 = e z \dots\dots\dots(10)$$

No. of load changes.

$$z = \frac{\pi}{2} \frac{D + D_k}{b} \dots\dots\dots(11)$$

Subst. for z in (11)

$$e = \frac{2 S^1 b}{\pi (D + D_k)} \dots\dots\dots(12)$$

Substitute this expression for e in (9)

$$\frac{2 S^1 b}{\pi (D + D_k)} = \log_a \frac{K}{K_k} \dots\dots(13)$$

Substitute $\frac{Q}{F}$ for K

$$\frac{2}{\pi} \frac{s^1 b}{(D + D_k)} = \log_a \frac{Q}{K_k F} \dots\dots\dots (14)$$

Subst. $s^1 = \frac{s}{n}$

$$\frac{2}{\pi} \frac{s}{n} \frac{b}{(D + D_k)} = \log_{a1} \frac{Q}{K_k F} \dots\dots (15)$$

Drilling Speed
cm/min.

$$s = \frac{\pi}{2} n \frac{(D + D_k)}{b} = \log_{a1} \frac{Q}{K_k F} \dots\dots (16)$$

$$s = 0.0157 \frac{\pi}{b} (D + D_k) \log_{a1} \frac{Q}{K_k F} \dots\dots (16a)$$

(N.B. Apparently $\frac{\pi}{2}$ taken as .0157 instead of 1.57

But $K_k = K_o a_2^v \dots\dots\dots (17)$

i.e. $\log \frac{K_k}{K_o} = \log a_2^v = 0.00125 v \dots\dots\dots (17a)$

Also $v = \frac{\pi}{2} \frac{D + D_k}{2} \frac{n}{60}$
 $= 0.0262 n (D + D_k) \dots\dots\dots (18)$

$\log \frac{K_k}{K_o} = 0.00003275 n (D + D_k) \dots\dots\dots (19)$

From this latter formula (19) values of $\frac{K_o}{K_k}$ are plotted for various rotational speeds and a given bit diameter (here 267 mm) and core diameter 30 mm.

Thus if K_o is known then K_k can be calculated and substituted in equation 16(a) from which the drilling rate "s" can be determined.

The authors claim that by this method the drilling rate for any rock may be predicted, although they do not appear to have tested its validity by actual experiments.

This method of calculation of rotary drilling rates has been presented in full since it has been quoted by Sievers & Fellweiss as though valid whilst it is open to several serious objections.

LIST OF REFERENCES.

1. E.W. INETT
High Speed Drifting in the Ruhr Coalfield
with Special Reference to Drilling Techniques.
Trans. I. Min. Engrs. Vol. 114
Jan. 1953.
2. H.S. ALPAN
The Speed of Penetration of Bit in Electric
Rotary Drilling.
Trans. I. Min. Engrs. Vol. 109
Sep. 1950.
3. R. SHEPHERD
Thesis (Sheffield University)
4. R. BERGRAD AND H. SIEVERS
Die Bestimmung Des Bohrwiderstandes
Von Gesteinen Gluckauf 37/38
Sep. 10th, 1950.
5. BESIGK & KUHNE
Oel und Kohle
Sep. 1941 (Exact
reference missing)
6. REHBINDER (Original in Russian)
On the use of Hardness Reducers in Drilling.
Transn. of Melbourne Academy of
Science (Obtainable from Science
Museum, Kensington).
7. R. SHEPHERD
Improving the Efficiency of Rotary Drilling
of Shotholes.
Trans. I. Min. Engrs. Vol. 113
Aug. 1954
9. COEUILLET
Les Outils D'Abatage En Havage Et Foration
Revue De L'Industrie Minerale
Jan. 1954.
10. SHULTZ
Possibilities & Limitations of Rotary Drilling
in Carboniferous Strata.
N.C.B. Information Bulletin.
11. METAL CUTTING SYMPOSIUM, 1913. (Manchester)
Published by Institute of Metals.
12. M.E. MERCHANT
Basic Mechanics of Metal Cutting Process.
J. App. Mechanics.
Amer. Soc. Mech. Engrs. 1944. Vol. 66, pA. 144.

LIST OF REFERENCES, Cont'd

13. PHILLIPS
Tectonics of Mining.
Sheffield University Mining Magazine
1949.
14. SHAW COOK AND FINNIE
Shear Angle Relationship in Metal Cutting.
15. FAIRHURST
Design of Rotary Drill Bits.
Mine & Quarry Engineering, Vol. 20.
June, 1954.
16. STABLER
Fundamental Geometry of Cutting Tools.
Proc. Instn. of Mech. Engrs.
(War Emergency Issues) Vol. 165
P. 14
17. SHAW, COOK AND SMITH
Mechanics of Three Dimensional Cutting
Operations.
Trans. A.S.M.E. Aug. 1952
P. 1055-1064.
18. ELECTRICAL RESISTANCE ^RSTRAIN GAUGES - DOBIE & ISAAC
(Textbook)
19. FAIRHURST, PROCTOR
Some Basic Principles of Rock Drilling.
Sheffield University Mining Magazine
1954. P. 41.

LAUS DEO SEMPER

SECTION V.

TABLES OF RESULTS. .

TABLE NO. 1A

ANALYSIS OF MAJOR FRACTURES OBSERVED IN TWO CAMERA TESTS

In all tests:-

No. of free faces	2
Angle of Obliquity	0°
Speed of Cutting	9"/min.
Width of Cut	0.25" (Nominal)
Depth of Cut	0.100"
State of Wear	Tool Sharp at Start of Each Test.
Dynamometer Tool Setting	1" + 0.050" (\pm 0.005")
Rock	Variable
Rake Angle	Variable

Test Number :- XI 1

Rock	Darley Dale Sandstone (No.5.)
Rake Angle	+ 20°

<u>Fracture No.</u>	<u>Details of Fracture</u>	<u>Direction of Resultant Force</u>	<u>Remarks</u>
1	From Tool Tip + 10° for 0.15" then + 55° for 0.033" then + 13° for 0.166" To Surface.	-51°	
2	From Tool Tip + 55° To Surface	-43°	Rock crystals breaking apart ahead of tool in zone bounded by 55° line:- fracture along this line, then breaking beyond this line before fractured piece removed.
3	From Tool Tip + 25° To Surface	-64°	
3 (a)	From T.T. + 55° To previous fracture line (i.e. 3)		
4	From T.T. + 11° To Surface	-45°	
5	From T.T. + 15° To Surface	-45°	Fracture commenced and then appeared to stop for 3 frames, eventually reaching surface.
6	From T.T. + 30° To Surface	-43°	

<u>Fracture No.</u>	<u>Details of Fracture</u>	<u>Direction of Resultant Force</u>	<u>Remarks</u>
7	From T.T. + 40° To Surface	-55°	
8	From T.T. 0° out of field of view	-43°	Appears to end by piece being lifted and tool face end broken off in bending.

Test Number: XI 2

Rock Darley Dale Sandstone

Rake Angle + 10°

<u>Fracture No.</u>	<u>Details of Fracture</u>	<u>Direction of Resultant Force</u>	<u>Remarks</u>
1	From Tool Tip + 10° To Surface	-40°	
2	From Tool Tip + 10° for 0.233" +45° for 0.133" To Surface	-37°	
3	From Tool Tip + 15° To Surface	-37°	
4	From Tool Tip 0° for 0.150" 45° " 0.133" To Surface	-49°	
5	From Tool Tip -25° for +20° " To Surface	-57°	Fracture developed beyond field of view.

Test Number: XI 3

Rock Darley Dale Sandstone

Rake Angle -10°

<u>Fracture No.</u>	<u>Details of Fracture</u>	<u>Direction of Resultant Force</u>	<u>Remarks</u>
1	From T.T. + 15° To Surface	-33°	
2	From T.T. - 20° for 0.050" + 35° " 0.367" To Surface	-30°	
3	From T.T. - 20° for 0.200" + 10° " 0.233" To Surface	-25°	
4	From T.T. - 20° for 0.067" + 20° " To Surface	-35°	Variable fracture line between + 15° and + 20°

Test Number: XI 4

Rock Darley Dale Sandstone

Rake Angle - 20°

<u>Fracture No.</u>	<u>Details of Fracture</u>	<u>Direction of Resultant Force</u>	<u>Remarks</u>
1	From Tool Tip + 15° To Surface	-26°	
2	From T.T. - 20° Swinging to + 20° To Surface	-45°	
3	From T.T. + 10° To Surface	-34°	
4	From T.T. + 15° To Surface	-35°	
5	From T.T. + 5° +20° just on reaching surface To Surface	-40°	

Test Number: XI 5

Rock Darley Dale Sandstone

Rake Angle 0°

<u>Fracture No.</u>	<u>Details of Fracture</u>	<u>Direction of Resultant Force</u>	<u>Remarks</u>
1	From T.T. + 10° To Surface	-19°	
2	From T.T. + 10° To Surface	-34°	
3	From T.T. -40° * for .016" 0° for 0.133" +10° for 0.133" Swinging to -10° Out of field of view	-9°	* Very approximate values
4	From T.T. 15° for .200" 70° for small dist. Then almost horiz.	-17°	

Test Number: XI 6

Rock Hard White Limestone

Rake Angle 0°

<u>Fracture No.</u>	<u>Details of Fracture</u>	<u>Direction of Resultant Force</u>	<u>Remarks</u>
1	From Tool Tip Initially around grain boundary. 0.033" - 10° for 0.200" + 35° To inclined surface.	-11°	Inclined surface at end of fracture appears to be line of weakness in rock.

Test Number XI 6 Cont'd.

<u>Fracture No.</u>	<u>Details of Fracture</u>	<u>Direction of Resultant Force</u>	<u>Remarks</u>
2	From T.T. + 25° 0.233 To Surface	-21°	
3	From T.T. -10° 0.233" +35° 0.083" 0° 0.033" 30° 0.067" To Surface	-33°	When fracture at 35° starts it appears to go across grains then seemingly in tension (0°) then again in shear.
4	From T.T. 30° To Surface	-32°	
5	From T.T. + 25° 0.100" - 20° 0.100" + 0° transition + 10° out of field of view.	-28°	
6	From T.T. + 10° 0.167" 50°-55° 0.117" To Surface	-29°	
7	From T.T. + 10° for 0.067" - 20° " 0.050" + 23° " 0.167" To Surface	-27°	
8	From T.T. 0° for 0.200" +40° " 0.050" To Surface.	-35°	

Test Number: XI 7

Rock Hard White Limestone. Fossiliferous (2)
 Rake Angle + 10°

<u>Fracture No.</u>	<u>Details of Fracture</u>	<u>Direction of Resultant Force</u>	<u>Remarks</u>
1	From T.T. + 15° for 0.084" + 65° " 0.100" To Surface	-54°	
2	From T.T. - 10° for 0.084" 35° " 0.050" 0° " 0.050" 75° " 0.033" 10° " 0.133" To Surface	-39°	Very irregular fracture (75° appears to be around grain boundary)
3	From T.T. 0° for 0.016" 55° " 0.067" To Surface	-25°	
4	From T.T. 10° To Surface	-40°	Actually swings up steeper at surface.

Test Number XI 7 Cont'd.

<u>Fracture No.</u>	<u>Details of Fracture</u>	<u>Direction of Resultant Force</u>	<u>Remarks</u>
5	From T.T. - 15° for 0.050" + 35° " 0.200" To Surface	-36°	Interesting, clear fracture.
6	From T.T. + 30° for 0.016" + 15°-20° " 0.167" 0° " 0.133" 25°-30° " 0.116" To Surface	-45°	Very interesting. Various small fractures along grain boundaries etc. well shown.
7	From T.T. + 5° out of field of view	-45°	Fracture "undulating". Value given is overall value.
8	From T.T. 0° out of field of view	-25°	Fracture "undulating". value given is overall value.

Test Number XI 8

Rock Hard White Limestone, Fossiliferous (2)

Rake Angle + 20°

<u>Fracture No.</u>	<u>Details of Fracture</u>	<u>Direction of Resultant Force</u>	<u>Remarks</u>
1	From T.T. 0° (v. small distance) +45° To Surface	-32°	Very good Tension - Shear Fracture.
2	From T.T. +10° for 0.100" -90° " 0.033" -15° " 0.116" +55° " 0.116" To Surface	-25°	
3	From T.T. -15° for 0.100" +40° " 0.200" To Surface	-22°	
4	From T.T. -20° for 0.050" +40° " 0.233" To Surface	-25°	
5	From T.T. +15° for 0.384" To Surface	-25°	
6	From T.T. + 5° for 0.233" +35° " 0.233" To Surface	-27°	Overall inclination approx. + 15°
7	From T.T. 0° for 0.367" then Around grain boundaries. To Surface	+23°	Shows path around grain boundaries very well.

Test Number XI 9

Rock Hard White Limestone. Fossiliferous (2)

rake Angle -10°

<u>Fracture No.</u>	<u>Details of Fracture</u>	<u>Direction of Resultant Force</u>	<u>Remarks</u>
1	From T.T. $+20^{\circ}$ for 0.300" To Surface	-15°	Very good, well defined fracture.
2	From T.T. $+17^{\circ}$ for 0.333" To Surface	-18°	
3	From T.T. $+25^{\circ}$ for 0.184" 0° " 0.067" $+20^{\circ}$ " 0.116" To Surface	-49°	
4	From T.T. $+10^{\circ}$ for 0.184" 0° " 0.216" Rising up at end To Surface	-55°	
5	From T.T. $+10^{\circ}$ To Surface	-38°	Fracture starts initially from crushed grain.
6	From T.T. -25° for 0.050" $+5^{\circ}$ " 0.100" $+35^{\circ}$ to Previous Fracture line ($+10^{\circ}$)	-20°	

Test Number XI 10

Rock Durham Post (Perpendicular to Bedding)

rake Angle -20°

<u>Fracture No.</u>	<u>Details of Fracture</u>	<u>Direction of Resultant Force</u>	<u>Remarks</u>
1	From T.T. -20° for 0.050" $+30^{\circ}$ " 0.233" To Surface	-48°	Fracture started behind Tool Tip.
2	From behind T.T. $+10^{\circ}$ To Surface	-30°	
3	From T.T. -20° for 0.100" 0° " 0.100" $25-30^{\circ}$ " 0.067" 0°* " 0.200" $+50^{\circ}$ To Surface	-43°	* 0° around grain
4	Approx. .06" below Surface on tool face. $+5^{\circ}$ for 0.200" To Surface	-52°	Tool had reached inclined (50°) surface.
5	From T.T. -10° for 0.167" $+35^{\circ}$ " 0.151" 0° Out of field of view.	-34°	Very definite line of fracture.

Test Number XI 11

Rock Durham Post (Perpendicular to Bedding)
 Rake Angle +20°

<u>Fracture No.</u>	<u>Details of Fracture</u>	<u>Direction of Resultant Force</u>	<u>Remarks</u>
1	Small "Tension-Shear Fracture" to inclined surface.	-33°	No details given of fracture angles.
2	From inclined surface +15° To Surface, i.e. from A.	-39°	
3	From T.T. 0° for 0.067" 30° " 0.184" To Surface	-34°	
4	From T.T. 25° for 0.267" To Surface	-29°	
5	Tool Tip 0° for 0.100" 38° " 0.200" To Surface	-32°	(Almost 0°)
6	From T.T. 15° To Surface	-30°	
7	From T.T. (i) -20° for 0.267" (ii) +25° " 0.200" To Surface	-30°	(i) to (ii) :- Swinging in 0.100" Note: Would be interesting to observe few frames after to note fall of force.
8	From T.T. 25° To Surface	-30°	

Test Number XI 12

Rock Durham Post (Perpendicular to Bedding)
 Rake Angle +10°

<u>Fracture No.</u>	<u>Details of Fracture</u>	<u>Direction of Resultant Force</u>	<u>Remarks</u>
1	From T.T. -17° for 0.100" +30° " 0.267" To Surface	-62°	Good Tension Shear Fracture
2	From T.T. -15° for 0.233" +30° " 0.133" To Surface	-34°	
3	From T.T. 23° for 0.267" To Surface	-25°	

Test Number XI 13

Rock Durham Post (Perpendicular to Bedding)
 Rake Angle 0°

<u>Fracture No.</u>	<u>Details of Fracture</u>	<u>Direction of Resultant Force</u>	<u>Remarks</u>
	From T.T. -5° for 0.050" +40° " 0.200" To Surface		This fracture omitted in Force Analysis. Actually H = 7 divs V = 4 divs
	From T.T. +13° To Surface		
2	From T.T. +15° for 0.300" To Surface	-31°	Very good surface
3	From T.T. + 12° for 0.333" To Surface	-47°	
4	From T.T. -20° for 0.067" +30° " 0.033" 0° " Out of field of view	-22°	
5	From T.T. 0° Swinging up to approx. 45° at surface. To Surface	-29°	

Test Number XI 14

Rock Durham Post (Perpendicular to Bedding)
 Rake Angle -10°
 Actual Tool Width

<u>Fracture No.</u>	<u>Details of Fracture</u>	<u>Direction of Resultant Force</u>	<u>Remarks</u>
1	From T.T. +20° for 0.067" -20° " 0.067" 0° " 0.033" +45° " 0.017" + 5° Out of field of view.	-27°	Long, low inclination fracture overall +5° but varying from small Tension - shear fracture.
2	From T.T. -20° for 0.050" 0° " 0.067" +25° " 0.067" To Surface	-41°	
3	From T.T. +25° for 0.200" To Surface	-25°	
4	From T.T. -20° for 0.167" +25° " 0.233" To Surface	-23°	
5	From T.T. +18° To Surface	-43°	Appeared to commence as - 20 for 0.050" and then +18° for 0.333" but next frame -20° crack still there and appear to be + 18° from tip.

Test Number XI 14 Cont'd.

<u>Fracture No.</u>	<u>Details of Fracture</u>	<u>Direction of Resultant Force</u>	<u>Remarks</u>
6	From T.T. +15° for 0.350" To Surface	-34°	
7	From T.T. +15° for 0.350" To Surface	-30°	
8	From T.T. +13° for 0.300" To Surface (overall)	-35°	

Test Number XI 15

Rock Durham Fost (Perpendicular to Bedding)
 Strike Angle -20°

<u>Fracture No.</u>	<u>Details of Fracture</u>	<u>Direction of Resultant Force</u>	<u>Remarks</u>
1	From T.T. 6° Out of field of view	-23°	Overall horizontal: Broke off at 90° approx:- In Bending.
2	From T.T. +8° for 0.567" To Surface	-32°	
3	From T.T. +9° for 0.334" +25° " 0.016" -18° " Out of field of view	-39°	This fracture apparently travelled to edge of rock and therefore should be ignored.

TABLE NO. 1 B

Analysis of Force Systems in "Two-Cameral" Tests.

TEST NUMBER	FRACTURE NUMBER	DIAL READINGS		TIEWIST FORCE	CUTTING FORCE	$\frac{V}{H}$	$\tan^{-1} \frac{V}{H}$
		V	H	V	H		°
		Dial Divisions	Dial Divisions	lb.	lb.		
XI 1	1	4	1½	25	20	1.25	-51°
	2	3	4	50	53.5	0.935	-43°
	3	9	2	56	27	2.07	-64°
	4	10	4½	62.5	60	1.04	-45°
	5	9	4	56	53.5	1.05	-45°
	6	10	5	62.5	66.5	0.94	-43°
	7	9	3	56	40	1.40	-55°
	8	10	5	62.5	66.5	0.94	-43°
XI 2	1	9	5	56	66.5	0.84	-40°
	2	9	5½	56	73.5	0.76	-37°
	3	8	5	50	66.5	0.75	-37°
	4	12	5	75	66.5	1.13	-49°
	5	10	3	62.5	40	1.56	-57°
XI 3	1	17	12	106	160	0.66	-33°
	2	10	8	62.5	107	0.584	-30°
	3	8	8	50	107	0.467	-25°
	4	7½	5	47	66.5	0.705	-35°
	5	6	3	37.5	40	0.937	-43°
XI 4	1	13	13	83	173	0.48	-26°
	2	12	10	75	75	1.00	-45°
	3	10	7	62.5	93.5	0.67	-34°
	4	13½	9	84.5	120	0.705	-35°
	5	14	8	87.5	107	0.82	-40°
	6	15	9	94	120	0.784	-38°
XI 5	1	4	5½	25	73.5	0.34	-19°
	2	5	3½	31	46	0.675	-34°
	3	2½	7	16	93.5	0.171	-9°
	4	3	4½	19	60	0.316	-17°

TEST NUMBER	FRACTURE NUMBER	DIAL READINGS		THRUST FORCE	CUTTING FORCE	V H	$\tan^{-1} \frac{V}{H}$
		V	H	V	H		
		Dial Divisions	Dial Divisions	lb.	lb.		°
XI 6	1	2	5	12.5	66.5	0.183	-11°
	2	5	6	31	80	0.333	-21°
	3	5½	4	34.5	53.5	0.645	-33°
	4	4	3	25	40	0.625	-32°
	5	4	3½	25	46.5	0.533	-28°
	6	6	5	37.5	66.5	0.565	-29°
	7	7	6½	44	86.5	0.510	-27°
	8	6	4	37.5	53.5	0.700	-35°
XI 7	1	6	2	37.5	27	1.39	-54°
	2	14	8	37.5	107	0.318	-39°
	3	4	4	25	53.5	0.467	-25°
	4	16	9	100	120	0.834	-40°
	5	14	9	37.5	120	0.730	-36°
	6	16	7½	100	100	1.000	-45°
	7	15	7	94	93.5	1.005	-45°
	8	6	6	37.5	80	0.470	-25°
XI 8	1	6	4½	37.5	60	0.625	-32°
	2	8	8	50	107	0.467	-25°
	3	7	8	44	107	0.410	-22°
	4	5½	5½	34.5	73.5	0.470	-25°
	5	7	7	44	93.5	0.470	-25°
	6	6	5½	37.5	73.5	0.510	-27°
	7	6	6½	37.5	86.5	0.434	-23°
XI 9	1	11½	20	72	266	0.271	-15°
	2	5	7	31	93.5	0.331	-18°
	3	14	10	37.5	75	1.167	-49°
	4	17	10	106	75	1.415	-55°
	5	10	6	62.5	80	0.780	-38°
	6	10	13	62.5	173	0.361	-20°

TEST NUMBER	FRACTURE NUMBER	DIAL READINGS		THRUST FORCE	CUTTING FORCE	$\frac{Y}{H}$	$\tan^{-1} \frac{Y}{H}$
		V	H	V	H		
		Dial Divisions	Dial Divisions	lb.	lb.		°
XI 10	1	14	6	87.5	80	1.093	-48°
	2	17	15	106	200	0.530	-30°
	3	23	14	175	187	0.935	-43°
	4	16	6	100	80	1.250	-52°
	5	19	13	119	173	0.688	-34°
XI 11	1	5½	4	34.5	53.5	0.645	-33°
	2	6	3½	37.5	46.5	0.807	-39°
	3	5	3½	31	46.5	0.667	-34°
	4	7	6	44	80	0.550	-29°
	5	8	6	50	80	0.625	-32°
	6	5	4	31	53.5	0.580	-30°
	7	8½	7	53	93.5	0.567	-30°
	8	6	5	37.5	66.5	0.565	-30°
XI 12	1	10	2½	62.5	33	1.89	-62°
	2	10	7	62.5	93.5	0.67	-34°
	3	3	3	19	40	0.475	-25°
XI 13	1	17	4	106	53.5	1.960	-63°
	2	9	7	56.5	93.5	0.605	-31°
	3	9	4	56.5	53.5	1.06	-47°
	4	7	8	44	107	0.411	-22°
	5	7	6	44	80	0.550	-29°
XI 14	1	14½	14	96.5	187	0.516	-27°
	2	9	5	56.5	65.5	0.861	-41°
	3	7	7	44	93.5	0.470	-25°
	4	8	7	50	93.5	0.535	-28°
	5	11	10	70	75	0.934	-43°
	6	10	7	62.5	93.5	0.669	-34°
	7	10	8	62.5	107	0.585	-30°
	8	9	6	56.5	80	0.706	-35°

TEST NUMBER	FRACTURE NUMBER	DIAL READINGS		THRUST FORCE	CUTTING FORCE	$\frac{V}{H}$	$\tan^{-1} \frac{V}{H}$
		V	H	V	H		
		Dial Divisions	Dial Divisions	lb.	lb.		°
XI 15	1	8	7	50	93.5	0.535	-28°
	2	8	6	50	30	0.625	-32°
	3	11½	7	76.5	93.5	0.819	-39°

TABLE NO. 2.

Test Series VII

To determine Effect of Variation of Tool Rake Angle on Force System.

Depth of Cut	0.075"
Speed of Cutting	9"/min.
Width of Cut	0.250" (Nominal)
No. of Free Faces	1
Obliquity	0°

Test No.	Rake Angle	Rock	No. of Readings	ΣF_V Dial divs.	ΣF_H Dial divs.	\bar{F}_V Dial divs.	\bar{F}_H Dial divs.	\bar{F}_V lbs.	\bar{F}_H lbs.	Remarks
VII 1	+ 10°	1	110	462	403	4.20	3.71	26.2	49.5	Tool Width:- 0.250"
2	"	3A	91	137	213	1.51	2.34	9.4	31.0	
3	"	4	114	1491	411	13.08	3.61	61.3	43.0	
4	"	5	106	2135	404	20.14	3.81	126.0	51.0	.023" wear *
5	- 10°	1	109	1644	707	25.03	6.42	157.0	66.5	Width:- 0.249"
6	"	3A	142	1193	669	8.40	4.71	52.5	63.0	
7	"	4	97	1410	433	14.50	4.93	90.5	66.5	
8	"	5	100	2173	524	21.73	5.24	135.7	70.0	.025" wear
9	0°	1	103	631	451	6.13	4.33	39.4	53.5	Width:- 0.237"
10	"	3A	57	393	313	6.95	2.09	43.5	28.0	
11	"	4	43	413	127	9.72	2.95	61.0	39.5	
12	"	5	83	1392	365	21.50	4.14	134.0	55.0	.013" wear
13	+ 20°	1	123	649	605	5.23	4.92	33.0	65.5	Width:- 0.230"
14	"	3A	83	62	270	0.71	3.07	4.5	41.0	
15	"	4	99	1063	394	10.30	3.97	67.5	53.0	
16	"	5	82	1449	321	17.66	3.91	110.5	52.0	Width:- 0.224"
17	- 20°	1	47	1143	456	24.35	9.7	152.0	129.0	
18	"	3A	51	331	130	6.49	3.53	40.5	47.0	
19	"	4	65	742	301	11.40	4.63	71.0	61.5	
20	"	5	97	1336	569	19.42	5.87	121.5	73.5	

* 'Wear' is width of flat on underface of tool at end of tests.

TABLE NO. 3.

Test Series V & V Ex.

To determine effect of Variation in Depth of Cutting.

Width of Cut 0.237"

Tool Rake Angle: + 20°

No. of Free Faces 1.

Speed Cutting 14.4"/min.

Test No.	Depth of Cut (in.)	No. of Dial Readings	ΣF_V Dial divs.	ΣF_H Dial divs.	\bar{F}_V Dial divs.	\bar{F}_H Dial divs.	\bar{F}_V lbs.	\bar{F}_H lbs.	Rock No.	Remarks
V 1	0.050	260	861	573	3.20	2.20	20.0	29.5	1	
2	0.075	276	1782	1510	6.46	5.47	40.5	73.0	1	
3	0.100	265	2075	3012	7.82	11.37	49.0	152.0	1	
4	0.050	277	1705	1057	6.11	3.79	37.0	50.5	1	
5	0.075	230	1739	1131	6.21	4.04	33.0	54.0	1	
6	0.100	274	2109	1303	7.70	6.53	43.0	63.0	1	
7	0.025	131	391	171	2.98	1.31	13.6	17.5	1	
28	0.050	239	4545	940	19.02	3.93	119.0	52.5	4	
29	0.025	222	2329	491	12.74	2.21	79.5	29.5	4	
30	0.100	176	3354	733	21.89	4.45	137.0	59.5	5	
31	0.075	266	6326	1136	23.73	4.46	149.0	59.5	5	
32	0.050	275	6197	972	22.53	3.53	140.5	47.0	5	
33	0.025	109	2435	359	22.30	3.29	143.0	44.0	5	
33A		103	2235	316	21.15	2.93	132.0	39.0		
35	0.050	265	7506	851	28.32	3.21	176.0	43.0	6	
36	0.025	270	7119	735	26.37	2.72	164.7	26.0	6	
37	0.075	274	7352	1137	26.83	4.15	163.0	55.5	6	
38B	0.100	233	5637	760	24.41	3.26	153.0	43.5	6	
V Ex 8	0.050	73	136	163	2.33	2.09	14.5	23.0	2	
9	0.025	75	201	150	4.01	2.00	25.0	27.0	2	
10	0.100	73	424	460	5.81	6.30	36.5	34.0	2	
11	0.075	50	323	300	6.46	6.00	40.5	30.0	2	
12	0.050	36	632	229	7.35	2.66	46.5	35.5	2	
13	0.075	31	695	550	3.53	6.79	53.5	90.5	2	
14	0.100	135	1267	2223	9.39	16.50	53.5	220.0	2	
15	0.050	33	10	40	0.20	1.21	2.0	16.0	3	
16	0.100	39	40	139	1.03	3.56	6.5	47.5	3	
18	0.050	67	916	241	13.67	3.60	35.5	43.0	4	
19	0.075	100	1443	203	14.43	3.03	90.5	40.5	4	
19A	0.075	77	1421	269	18.45	3.49	115.5	46.5	4	
20	0.100	75	1526	359	20.35	4.79	127.0	64.0	4	
21	0.050	50	762	146	15.24	2.92	95.5	39.0	4	
22	0.100	50	897	192	17.94	3.94	112.0	52.5	4	

TABLE NO. 4.

Test Series VI

To determine Effect of Variation of Width of Cutting Tool.

Tool Rake Angle 0°
 Speed of Cutting 9.0"/min.
 No. of Free Faces 1
 Obliquity 0°

Test No.	Width of Cut .in.	Depth of Cut .in.	Rock	No. of Dial Readings	ΣF_V Dial divs.	ΣF_H Dial divs.	\bar{F}_V Dial divs.	\bar{F}_H Dial divs.	\bar{F}_V lbs.	\bar{F}_H lbs.	Wear of Tool	Remarks
VI 1	0.375"	0.050	1	113	1096	623	9.70	5.51	60.5	73.5		
2	"	0.050	1	131	1199	563	9.15	4.34	57.0	53.0		
3	"	0.050	1	140	1305	575	9.32	4.11	53.5	55.0		
4	"	0.050	1	87	1167	434	13.41	5.56	64.0	74.0		
5	"	0.075	1	134	2391	1246	17.84	9.30	111.5	124.0		
6	"	0.100	1	151	3166	1621	20.96	12.06	129.0	170.0		
7	"	0.050	2	64	1305	502	15.54	5.96	97.0	60.0		
11	"	0.050	4	134	2253	537	16.81	4.01	105.0	53.5		
12	"	0.075	4	126	2700	634	22.06	6.62	133.0	63.0		
13	"	0.100	4	123	2361	699	19.36	5.68	121.0	75.5		
14	0.193"	0.050	1	116	1391	617	16.03	6.92	100.5	92.5		
15	"	0.075	1	153	3446	2166	22.53	14.30	141.0	190.5		Attempted .100" Motor stalled
16	"	0.050	2	103	2045	2037	18.93	18.36	113.5	251.0		
17	"	0.075	2	119	3142	1550	26.40	13.03	165.0	174.0		
18	"	0.050	4	97	1921	530	19.80	5.36	124.0	71.5		
19	"	0.075	4	95	2050	553	21.57	5.82	134.5	77.5		
20	0.744	0.050	1	151	3303	1961	21.87	13.12	137.0	175.0		
21	"	0.075	1	121	4250	2919	35.12	24.12	219.5	321.5		
22	"	0.050	2	130	3329	1727	25.61	13.29	160.5	177.0		
23	"	0.075	2	151	3323	2237	25.35	14.81	153.5	197.5		
24	"	0.050	4	100	3461	1000	34.61	10.00	217.5	133.5		
25	"	0.075	4	46	1574	537	34.22	12.76	214.0	170.0		
26	"	0.075	4	77	3193	1039	41.46	13.49	259.5	100.0		More reliable than 25.
27	0.240	0.050	1	98	734	453	8.00	4.67	50.0	62.0		
28	"	0.075	1	125	1353	1136	10.86	9.09	68.0	121.0		
29	"	0.050	2	123	1066	364	8.33	2.84	52.0	38.0		
30	"	0.075	2	129	1093	1630	8.51	12.64	53.0	168.5		To be inverted begin to cut deeper
31	"	0.050	4	92	1092	351	11.87	3.82	74.0	51.0		With 3 Free Faces
32	"	0.075	4	107	1354	473	12.65	4.47	79.0	59.5		

TABLE NO. 5.

Test Series VIII To determine Effect of Variation of Number of Free Faces.

Tool Rake Angle 0°
 Speed of Cutting 9.0"/min.
 Obliquity 0°

Test No.	Rock No.	No. of Free Faces	Width of Cut (in)	Depth of Cut (in)	No. of Dial Readings	ΣF_V Dial divns.	ΣF_H Dial divns.	$\overline{F_V}$ Dial divns.	$\overline{F_H}$ Dial divns.	$\overline{F_V}$ lbs.	$\overline{F_H}$ lbs.
VIII 1	1A	3	0.490	0.100	81	681	280	8.41	3.46	52.5	46.0
2		2	"	0.100	134	2325	941	17.35	7.02	108.5	93.5
3		1	"	0.100	33	713	442	21.76	11.47	136.0	153.0
4		3	"	0.050	77	957	360	12.43	4.67	77.0	62.5
5		2	"	0.050	67	1213	387	18.10	5.78	113.0	77.0
6		1	"	0.050	61	1105	371	18.11	6.08	113.0	81.0
7	5		"	0.050	83	1309	294	15.77	3.54	98.0	47.0
8		3	"	0.050	61	1717	343	28.14	5.70	175.0	76.0
9		2	"	0.050	54	1849	367	34.24	6.80	214.0	90.5
10		1	"	0.050	76	2757	532	36.27	7.00	226.0	93.0
11		3	"	0.075	69	2353	522	41.42	7.57	259.0	100.5
12		2	"	0.075	45	1502	284	33.33	6.31	203.5	84.0
13		1	"	0.075	131	6413	1350	48.95	10.31	306.0	137.5
14	1	2	0.235	0.100	43	243	85	5.76	1.98	36.0	26.5
15		3	"	0.075	65	152	74	2.34	1.14	14.5	15.0
16		2	"	0.075	67	485	167	7.23	2.49	45.0	33.0
17		3	"	0.050	63	304	95	4.47	1.40	23.0	13.5
18		2	"	0.050	91	626	197	6.87	2.16	43.0	29.0
19	5	3	"	0.075	61	309	135	13.26	2.21		29.5
20		2	"	0.075	45	1222	206	27.16	4.58	169.5	61.0
21		1	"	0.075	81	2257	439	27.86	5.42	174.0	72.0
22		3	"	0.050	62	938	151	15.13	2.44	94.5	32.5
23		2	"	0.050	54	7012	166	12.99	3.07	81.0	41.0
24		1	"	0.050							

Film overexposed - could not be read.

TABLE NO. 6.

Test Series K To determine Effect of Variation of Obliquity Angle.

Tool Rake Angle 0°
 Speed of Cutting $9.0''/\text{min.}$
 No. of Free Faces 1
 Width of Cut $0.375''$

Test No.	Obliquity (Degrees)	Depth of Cut (in)	Rock No.	No. of Dial Readings	ΣF_V Dial divs.	ΣF_H Dial divs.	\bar{F}_V Dial divs.	\bar{F}_H Dial divs.	\bar{F}_V lbs.	\bar{F}_H lbs.	Wear of Tool	Remarks		
X 1	40°	0.050	1	162	2066	674	12.75	4.16	79.5	55.5	Sharp			
2		0.075	1	157	2410	1345	15.35	8.57	96.0	114.0				
3		0.100	1	No results recorded on film - by accident										
4		0.050	5	135	6771	1256	37.63	6.73	236.0	90.5				
5		0.075	5	103	4251	933	39.36	8.64	246.0	115.0				
6		0.100	5	92	4063	1122	44.22	12.19	276.0	162.0				
7	60°	0.050	1	164	2556	1455	15.59	8.87	97.5	113.0	Sharp			
8		0.075	1	102	2079	1443	20.33	14.15	127.5	133.0				
9		0.100	1	163	3472	2703	21.30	16.61	133.0	221.5				
10		0.050	5	No results recorded on film - by accident										
11		0.050	5	113	6623	1569	53.65	13.33	367.0	135.0				
12		0.075	5	116	6391	1333	59.41	15.34	371.0	211.0				
13		0.100	5	47	2399	800	61.60	17.02	335.5	220.5				
14	20°	0.050	1	102	1111	433	10.39	4.73	63.0	63.5	Sharp			
15		0.075	1	105	1534	774	15.03	7.37	93.5	93.0				
16		0.100	1	95	2134	1007	22.93	10.60	144.0	141.0				
17		0.050	5	34	1324	302	21.71	4.54	136.0	60.5		Trial run only		
18		0.050	5	92	2329	521	25.32	5.66	153.0	75.5				
19		0.075	5	103	3541	743	32.73	6.93	204.5	92.5				
20		0.100	5	33	3767	933	45.39	11.24	283.5	150.5				
21	0°	0.050	1	65	360	263	5.50	4.05	34.5	54.0	Sharp			
22		0.075	1	96	1150	357	11.93	3.93	75.0	119.0				
23		0.100	1	96	1631	1465	16.99	15.26	106.0	203.5				
24		0.050	5	77	1961	410	25.47	5.32	153.0	71.0				
25		0.075	5	75	2354	425	31.39	6.60	196.0	33.0				
26		0.100	5	92	2549	1362	27.71	14.30	173.0	197.0				
27	60°	0.050	1	37	513	283	5.90	3.25	37.0	43.5	Sharp			
28	"	0.100	5	35	1075	344	16.54	5.37	107.0	70.5				

TABLE NO. 7.

Test Series III & IV To determine effect of Variation in Speed of Cutting.

Width of Cut: 0.250"
 No of Free Faces: 1
 Depth of Cut: 0.050"
 Obliquity: 0°

(a) Rake Angle: - 20°

Test No.	Cutting Speed in/min.	Rock No.	No. of Dial Readings	ΣF_V Dial divs.	ΣF_H Dial divs.	\bar{F}_V Dial divs.	\bar{F}_H Dial divs.	\bar{F}_V lbs.	\bar{F}_H lbs.	Remarks
III 1	5.5	1								
2	9.0	1	103	1921	726	17.79	6.72	111.0	39.5	
3	14.4	1	123	2630	1033	21.33	8.44	133.5	112.0	
4	5.5	2	111	2270	791	20.45	7.13	123.0	95.0	
5	9.0	2	120	2316	771	19.30	6.43	120.0	86.0	
5A	9.0	2	13	162	43	9.00	2.67	51.0	35.5	
6	14.4	2	255	3526	1067	13.83	4.13	86.5	55.5	
7	5.5	3	110	739	261	7.17	2.37	45.0	31.5	
8	9.0	3	161	1071	437	6.65	3.02	41.5	40.0	
9	14.4	3	264	2533	633	9.59	3.36	60.0	45.0	
10	5.5	4	90	613	269	9.09	2.99	56.5	40.0	
11	9.0	4	134	1514	476	11.20	3.55	70.5	47.5	
12	14.4	4	124	1507	410	12.15	3.31	76.0	44.5	
12A	14.4	4	92	1171	322	12.73	3.50	79.5	46.5	
13	5.5	4	59	944	239	16.00	4.05	100.0	54.0	
14	9.0	4	129	2559	621	19.84	4.81	123.0	64.0	
15	14.4	4	206	3731	1001	13.35	4.86	114.5	65.0	
16	5.5	5	83	2213	496	26.72	5.98	137.0	80.0	
17	9.0	5	129	2945	618	22.83	4.79	143.0	64.0	
18	14.4	5	228	5512	1026	24.18	4.50	151.0	60.0	
19	5.5	6	109	2563	502	23.51	4.61	147.0	61.5	
20	9.0	6	192	6962	1402	36.26	7.30	226.5	97.0	
21	14.4	6	137	3395	517	24.73	3.77	155.0	50.5	
22	5.5	7	40	2036	409	52.15	10.23	Invalid		} Drive } Motor } Stalled
22A	9.0	7	30	1594	277	53.15	9.23	"		
22B	14.4	7	156	7293	997	46.73	6.39	"		

(b) Rake Angle: 0°

IV 11	24.0	2								Tool Sharp
12	13.0	2	171	1311	614	10.59	4.76	66.0	63.5	
13	10.0	2	152	1345	437	8.85	3.20	55.5	42.5	
14	14.4	2	79	509	221	6.44	2.30	40.0	37.5	
15	5.5	2	271	2274		8.39		52.5		
16	24.0	6	94	2453	215	26.14	2.29	163.0	30.5	Wear 0.020"
17	13.0	6	155	3607	353	23.27	2.31	145.5	31.0	
18	10.0	6	136	3273	366	24.07	2.34	150.5	23.5	
19	14.4	6	97	2253	225	23.27	2.32	145.5	31.0	
20	5.5	6	249	5034	533	20.22	2.16	121.5	29.0	
21	24.0	6	113	3035	393	26.85	3.52	163.0	47.0	Wear 0.040

TABLE 8 - PROGRESS OF WEAR OF $\frac{1}{2}$ IN. WIDE TOOL OF HIGH SPEED STEEL
AND EFFECT OF WEAR ON CUTTING FORCE SYSTEM.

Leg Rake, 0° ; Clearance, 7° ; Depth of Cut, $\frac{1}{20}$ in.; Rock, Darley Dale Sandstone.

No. of Run	Distance cut (in.)	Mean Width of Flat (in.)	Mean Force Readings	
			Thrust Force (lb)	Cutting Force (lb)
1	1.90	0.0110	127.9	62.7
2	3.93	0.0144		
3	5.95	0.0233	185.3	74.4
4	7.97	0.0220		
5	10.00	0.0254	227.1	83.3
6	12.02	0.0244		
7	14.03	0.0266		
8	16.05	0.0269	273.1	89.6
9	18.08	0.0271		
10	20.09	0.0232		
11	22.10	0.0230		
12	24.12	0.0233	272.1	85.3
13	26.16	0.0273		

Since a large part of the wear occurred in the first 2 in. of travel the tool was re-sharpened and a further run made to determine the initial rate of development of wear, measurements being made at frequent intervals throughout the cut. The results are shown below.

TABLE 8(a) - INITIAL RATE OF DEVELOPMENT OF WEAR.

Distance Cut (in.)	Mean Wear (in.)
0.102	0.0014
0.502	0.0059
1.013	0.0071
1.503	0.0093
1.943	0.0110

TABLE NO. 2.

BRAKE CHARACTERISTICS OF 1 1/2 H.P. DRILL MOTOR

TESTS USING NOMINAL DRILL SPEED 500 R.P.M.

Wattmeter Readings		INPUT				OUTPUT						Remarks			
W ₁ watts x 20	W ₂ watts x 20	W watts x 20	Power watts	I amps	V volts	Balance Reading lb. oz.		Correction lb. oz.		Corrected Reading lb. oz.			Torque lb. ft.	Speed R.P.M.	
66	-9	57	1140	11.3	139	6	9	4	3	2	1	3	25	515	Correction to balance readings includes weight of brake and arm etc. and zero error of balance
74	4	73	1560	11.0	139	7	14	"	"	3	6	13	50	510	
81	12	93	1360	12.5	139	8	8	"	"	4	0	16	00	498	
95	32	127	2540	13.9	139	10	4	"	"	5	10	22	50	469	
103	43	156	3120	15.5	133	11	10	"	"	7	2	23	50	431	
114	59	173	3460	16.7	135	12	10	"	"	8	2	32	50	409	
2nd TEST															
69	-4	65	1300	11.5	139	7	1	4	3	2	9	10	25	510	Brake arm radius in all cases = 4 ft.
71	3	74	1400	11.6	139	7	3	"	"	3	0	12	00	502	
74	7	81	1620	11.7	139	7	14	"	"	3	6	13	50	496	
76	11	87	1740	11.8	139	8	4	"	"	3	10	14	50	439	
84	22	106	2120	12.4	137	9	4	"	"	4	10	13	50	470	
83	30	113	2360	13.0	133	10	0	"	"	5	3	22	00	460	
94	33	132	2640	13.3	137	10	11	"	"	6	3	25	00	442	
100	46	146	2920	14.6	136	11	3	"	"	6	11	26	75	423	
104	51	155	3100	15.1	135	11	8	"	"	7	0	23	00	402	
117	67	134	3630	17.5	133	13	2	"	"	8	10	34	50	345	
3rd TEST															
64	-21	43	360	12.4	140	5	10	4	3	1	2	4	5	531	
67	-14	53	1060	12.1	140	6	3	"	"	1	11	6	75	518	
74	+2	76	1520	12.0	140	-	-	"	"	Not given		-	-	512	
66	-12	54	1000	12.0	140	7	2	"	"	2	10	10	5	513	
74	+2	76	1520	11.9	140	7	10	"	"	3	2	12	5	510	
82	15	97	1940	12.3	140	8	13	"	"	4	5	17	25	494	
83	26	114	2200	13.0	139	9	13	"	"	5	5	21	25	475	
97	39	136	2720	14.0	133	10	12	"	"	6	4	25	0	452	
4th TEST															
63	-12	56	1120	12.0	140	6	11	4	3	2	3	8	75	523	
70	-7	63	1260	12.0	140	6	12	"	"	2	4	9	00	519	
73	+8	86	1720	12.1	140	8	5	"	"	3	13	15	25	501	
84	13	102	2040	12.5	140	8	12	"	"	4	4	17	00	486	
82	13	95	1900	12.3	140	8	12	"	"	4	4	17	00	492	
90	26	116	2320	13.0	140	9	11	"	"	5	3	20	75	472	
100	40	140	2800	14.3	139	10	12	"	"	6	4	25	0	449	

Similar tests were carried out for nominal rotary speeds of 600 R.P.M., 430 R.P.M., 320 R.P.M.

TABLE NO. 10.

Brake Test on 5 H.P. Handrick Track Motor.

Carried out on rotor shaft i.e. no reduction gearing used.

The gear ratio for the 62.5 R.F.M. gear was 23.5 :1

Rotor Speed R.P.M.	Power Watts x 3	Total Power K.W.	Line Voltage volts.	Line Current Amps.	Balance Reading lb. oz.	Corrected Reading lb. oz.	Rotor Torque lb.ft.	Drill Chuck Speed	Drilling Torque lb. ft.	Remarks
-	-				1 3	0 0	0	0	0	
1490	25(x5)	0.375	411	2.75	1 3	0 0	0	63.4	0	Wattmeter Scale Multiplier (x5)
	25 "	0.420		-	2 0	0 13	1.03	-	25.4	
	45 "	0.675		3.05	3 0	1 13	2.41	-	56.6	
1430	63 "	0.945		3.20	4 0	2 13	3.74	63.0	33.0	
1473	79 "	1.135		3.50	5 0	3 13	5.07	62.3	119.0	
1465	94 "	1.410		3.80	6 0	4 13	6.40	62.4	150.5	
1461	113 "	1.695		4.03	7 0	5 13	7.73	62.2	181.3	
1460	130 "	1.950		4.40	8 0	6 13	9.06	62.2	212.6	
1450	147 "	2.205		4.70	9 0	7 13	10.39	61.6	244.0	
1442	160 "	2.400		5.00	10 0	8 13	11.72	61.4	275.6	
1440	185 "	2.775		5.55	11 0	9 13	13.05	61.3	306.4	
1430	200 "	3.000		5.33	12 0	10 13	14.38	60.9	335.5	
1412	223 "	3.245		6.40	13 0	11 13	15.71	60.2	369.5	
1410	240 "	3.600		6.58	14 0	12 13	17.04	60.0	400.0	
1410	48(x20)	2.630		6.63	14 0	12 13	17.04	60.0	400.0	Wattmeter Scale Multiplier (x20)
1402	51 "	3.060		7.10	15 0	13 13	18.37	59.7	431.0	
1400	53 "	3.180		7.35	15 3	14 5	19.04	59.6	447.0	
1393	57 "	3.420		7.70	16 0	14 13	19.70	59.5	463.0	
1395	60 "	3.600		8.17	17 0	15 13	21.03	59.4	495.0	
1390	65 "	3.900		8.60	18 0	16 13	22.36	59.2	525.0	
1335	70 "	4.200	407	9.03	19 0	17 13	23.69	59.0	556.0	

N.B. There is an obvious error in the x20 scale multiplier which reads low in comparison to the x5 multiplier. This did not introduce error in the drill tests since the readings were all in the x5 range, the same "wattmeter" being used when drilling as when ~~calibrating the motor.~~

TABLE

Test No.	Purpose of Test	Bit Type	Rock	Thrust lb.	Power Input K.W.	Torque lb.ft.	Rotary Speed R.F.M.	Drilling Rate in/min.	Rod Details	Duration of Test secs.	Remarks
1(a)	To determine torque and drilling rates.	Standard U Concentric (1)	Laminated Shale	600	0.575	46.0	63.1	15.6	Scroll	20	Bit Sharp; Undamaged at end of test.
(b)		"	"	1200	1.200	119.0	62.7	17.3	"	40	No visible wear. Undamaged at end of test.
(c)		"	"	1680	1.455	150.0	62.5	27.0	"	10	Both legs failed:- by bending inwards.
2(a)	To determine torque and drilling rates	Spearhead Bit (2)	"	600	0.412	25.3	63.3	9.0	"	30	Bit Sharp; Undamaged at end of test.
(b)		"	"	1200	0.650	55.0	63.2	13.1	"	60	No visible wear " " " " "
(c)		"	"	1800	0.975	92.5	62.9	18.5	"	40	" " " " " " " "
(d)		"	"	2400	1.125	110.5	62.8	19.2	"	50	" " " Speed fell towards end of test.
3(a)	To compare oblique bits with standard bits.	Oblique bit (A)	"	3000	1.900	204.0	62.1	19.5	"	30	Carbide badly flaked.
(b)		(B)	"	900	0.800	72.5	63.1	20.6	"	40	Loading leg failed: by bending.
4(a)	To determine torque and drilling rates.	Spearhead Bit (2)	Parkgate Sands	600	0.615	50.5	63.2	11.3	"	90	" " " " "
(b)		"	"	1200	0.638	54.0	63.2	0.67	"	50	Bit Sharp; Undamaged at end of test.
(c)		"	"	1800	0.975	92.5	62.9	2.10	"	70	Slightly worn " " " " "
(d)		"	"	2400	1.140	113.0	62.7	4.45	"	90	" " " " " " " "
(e)		"	"	3000	1.425	146.0	62.5	5.5	"	65	Wear easily visible; Undamaged at end of test.
(f)		"	"	3600	-	-	-	6.95	"	100	
(g)		"	"	4200	-	-	-	7.9	"	50	Slight flaking at tips.
(h)		"	"	4300	-	-	-	9.5	"	70	Tips badly flaked.
5(a)	To test Alloy Body Bit for leg Strength	Alloy Body 13A (Concentric)	"	4300	-	-	-	7.2	"	80	Worn bit (Similar to other Spearhead)
(b)		"	"	720	-	-	-	12.5/	"	70	Drilling rate fell continuously during test.
(c)		"	"	1200	-	-	-	6.4	"	50	
		"	"	1800	-	-	-	15.7	"	40	Carbide badly flaked (but legs undamaged) due to collaring hole too small.
6(a)	To determine Torque and drilling rates.	Standard U Eccentric Bit)	"	600	0.525	40.0	63.3	8.3	"	50	Test successfully completed.
(b)		"	"	1200	-	-	-	-	"		Legs "folded up" at start of test.
7(a)	To check results of Tests 5.	Alloy body 13A	"	600	0.435	30.0	63.3	-	"	80	-
(b)		"	"	1200	0.705	62.0	63.1	-	"	50	-
(c)		"	"	1800	1.565	162.5	62.4	-	"	30	Backing was "blued" through heat.
(d)		"	"	2400	2.520	276.0	61.4	-	"	35	Carbide completely removed from one leg but legs still intact.
8(a)	To determine torque and drilling rates.	Improved Design (1) (-20° Rake)	Hard Limestone	1800	0.937	82.0	63.0	7.3	Plain Round	150	
(b)		"	"	3000	1.305	133.0	62.6	12.6	"	110	
(c)		"	"	3600	1.912	205.0	62.1	18.3	"	150	Driving lug of rod sheared off.
9(a)	(As 8)	-5° Rake	"	1800	1.125	110.0	62.8	12.8	"		
(b)		"	"	2400	-	-	-	-	"		Water supply blocked immediately at start. Caused binding and shear of thread.
10(a)	(As 8)	-17° Narrow Core	"	1800	0.960	91.0	62.9	-	"		
(b)		"	"	2400	1.170	113.0	62.8	12.5	"		Screw thread sheared.
11(a)	(As 8)	-10° Narrow Core	"	1800	0.340	77.6	63.0	7.6	"	110	Bit Sharp. Using 2% Ni Cr Mo Alloy stud.
(b)		"	"	2400	0.945	89.3	62.9	9.8	"	70	Torque value appears low.
(c)		"	"	3000	1.290	129.3	62.6	13.8	"	60	
(d)		"	"	3600	1.650	171.6	62.3	18.8	"	60	
(e)		"	"	4200	1.935	206.8	62.0	19.5	"	25	Stopped due to lack of water.
(f)		"	"	4800	2.460	270.3	61.4	19.3	"	50	Vibration much more pronounced. Power readings very variable. Fracture (crack) between legs. Carbide undamaged.

TABLE NO. 12.

SIEVE ANALYSIS OF CUTTINGS' SAMPLES.

Sieve Size	Proportion by weight (gn)				Percentage of Total Weight in Various Sizes				Weight of 50 particles of various sizes			
	Sample (a)	Sample (b)	Sample (c)	Sample (d)	(a)	(b)	(c)	(d)	(a)	(b)	(c)	(d)
On 1/2" B.S.S.	0	0	0	0	0%	0%	0%	0%	-	-	-	-
" 7/16 "	0	0	11.0	7.5	0	0	0.9	1.3	-	-	55.0	62.500
" 3/8 "	4.6	14.1	23.0	20.0	0.4	1.6	1.9	3.5	32.36	37.11	41.07	47.61
" 5/16 "	14.3	15.0	34.6	25.3	1.3	1.7	2.9	4.4	24.66	25.00	29.32	33.29
" 1/4 "	23.2	45.7	69.9	29.2	2.6	5.1	5.9	5.1	14.93	14.65	17.362	20.00
" 3/16 "	72.5	66.1	139.0	62.2	6.6	7.3	11.3	14.3	3.183	7.713	7.862	11.663
" 1/8 "	336.3	197.1	300.0	103.5	30.3	30.3	25.4	13.3	1.745	2.124	2.422	3.125
" 5 I.M.M. Sieve	23.0	22.3	29.0	26.7	2.1	2.5	2.5	4.6	1.274	1.491	1.503	1.600
" 8 " "	133.5	132.3	145.3	75.4	12.7	14.6	12.3	13.1	0.460	0.593	0.618	0.630
" 10 " "	50.3	43.9	50.7	22.6	4.6	5.4	4.3	3.9	0.173	0.133	0.220	0.234
" 12 " "	43.5	37.8	43.9	19.9	4.0	4.2	3.7	3.5	0.100	0.105	0.110	0.121
Thro' 12 I.M.M. Sieve	331.7	320.5	335.9	153.2	34.9	35.9	23.4	27.5	-	-	-	-
TOTAL	1093.4	900.3		575.5	100.0%	100.0%	100.0%	100.0%				

Flush Water Flow Tests

1. Comparison of Gauges.

Gauge 3 had previously been calibrated by a Bourdon Pressure Gauge calibrating unit and found to be accurate. It is therefore used as Standard in the following tests.

Gauge 2 lb/sq.in.	12.0	5.5	71.5	54.3	44.5	36.0	23.7	30.0	32.8
" 3 " " "	10.8	3.5	69.5	52.2	42.8	34.0	21.0	27.5	30.2
Gauge 2 " " "	35.3	41.0	53.0	56.0	15.8	9.7	20.8	31.5	38.2
" 3 " " "	33.0	39.0	51.0	53.6	11.8	6.5	18.0	29.0	36.2
Gauge 2 " " "	50.0	53.0	57.0	62.0	66.3	71.0	71.6	69.5	43.0
" 3 " " "	47.5	51.0	55.0	60.0	64.3	69.2	69.7	67.5	46.0
Gauge 2 " " "	33.7	32.2	14.0	23.7					
" 3 " " "	36.7	30.2	11.0	21.5					

A Calibration chart was then drawn up and all indicated values of Gauge 2 reduced to the standard values. All pressure readings given below are reduced values.

2. Tests to determine Water Flow Resistance of Wet Drilling Attachment.

(a) Standard Wet Attachment

Gauge 3 measures water pressures at entry to the wet attachment.

Gauge 2 " " " " exit from the wet attachment.

Water Pressure. lb/sq.in.		Press Drop lb/sq. in.	Rate of Flow galls/min.
Gauge 3	Gauge 2	Gauge 3 - Gauge 2	
48.0	13.5	29.5	3.0
37.0	13.5	23.5	3.33
32.0	11.5	20.5	2.66
20.0	7.0	13.0	2.24
35.0	12.5	22.5	2.80
14.5	4.0	10.5	1.90
21.8	7.5	14.3	2.04
30.5	11.0	19.5	2.60
40.5	15.0	25.5	2.84
44.0	16.5	27.5	3.16
49.5	19.0	30.5	3.06

Resistance was determined by plotting values of 'Pressure Drop' against values of (Rate of Flow) ² and noting the gradient of the straight line through the points.

Resistance of Standard Wet Drilling Attachment

$$= 2.95 \text{ (in units of } \frac{\text{lb.} - \text{min}^2}{\text{in}^2 \cdot \text{gall}^2} \text{)}$$

(b) Modified Wet Attachment.

Water Pressure lb/sq.in.		Pressure drop lb/sq.in.	Rate of Flow
Gauge 3	Gauge 2	Gauge 3 - Gauge 2	Galls/min.
14	9.5	4.5	2.23
4.5	1.5	3.0	1.10
17.5	12.2	5.3	2.03
23.5	17.2	6.3	2.40
29.0	20.3	8.2	2.62
35.5	26.0	9.5	2.70
39.0	28.3	10.7	3.07
46.0	33.0	13.0	3.33
50.0	36.0	14.0	3.45
55.0	40.0	15.0	3.65
56.5	40.5	15.0	3.67

Resistance was determined in the same manner as previously.

Resistance of Modified Wet Drilling Attachment

$$= 1.20$$

3. TESTS TO DETERMINE WATER FLOW RESISTANCE OF INTERNAL BORE (1/4" DIAMETER) OF 1" DIAMETER ROUND DRILL ROD.

Using 1/4" bore steel plug in place of bit.

Gauge 1. measured water pressure on supply tank.

Gauge 2. " " " at drive end of drill rod.

Gauge 3. " " " at bit end " " "

Distance between Gauge 2 and Gauge 3 = 3'6"

Water Pressures lb/sq.in.			Pressure drop lb/sq.in.	Rate of Flow galls/min.
Gauge 1	Gauge 2	Gauge 3	Gauge 2-Gauge 3	
86.5	14.1	7.8	6.5	2.29
"	17.5	10.0	7.5	2.35
86.0	26.7	15.5	11.2	3.03
"	31.7	13.3	13.4	3.31
"	36.2	21.5	14.7	3.41
87.0	41.5	24.5	17.0	3.69
"	8.3	4.2	4.6	1.77
"	14.6	7.5	7.1	2.17
"	21.0	11.7	9.3	2.63
87.0	23.5	13.5	10.0	2.79
"	30.6	17.5	13.1	3.19
"	33.3	19.5	13.3	3.19
"	35.3	21.0	14.3	3.42
"	33.5	22.7	16.1	3.54
"	40.3	23.7	16.6	3.64
87.0	10.3	5.3	5.0	2.01
"	15.3	8.3	7.5	2.35
"	22.5	10.5	12.0	2.79
"	29.2	16.5	12.7	3.04
"	34.9	20.1	14.3	3.25
"	40.3	24.0	16.3	3.41

By plotting.

Resistance of Bore of 1" round drill rod 3'6" long

= 1.52 units.

= 0.54 units/foot length.

4. TESTS TO DETERMINE WATER FLOW RESISTANCE OF INTERNAL BORE
($\frac{1}{2}$ " DIAMETER) OF $\frac{1}{2}$ " DIAMETER ROUND DRILL ROD.

(i) Using $\frac{1}{2}$ " bore steel plug in place of bit.

Gauges 1, 2, 3 as in Tests 3.

Water Pressure lb/sq. in.			Pressure drop lb/sq.in.	Rate of Flow galls/min.
Gauge 1	Gauge 2	Gauge 3	Gauge 2 - Gauge 3	
87	16.0	7.0	11.0	2.10
"	26.0	15.0	21.0	3.01
"	39.0	17.5	21.5	3.43
"	39.5	17.5	22.0	4.20
"	31.0	11.0	19.0	2.99
"	31.0	13.0	13.0	3.37
"	17.0	6.0	11.0	2.25
"	23.5	9.3	13.7	2.66
"	29.0	12.2	16.3	2.71
"	42.5	19.3	23.2	3.55
"	6.0	2.0	6.0	1.57
"	13.5	4.3	3.7	1.98
"	32.0	14.0	13.0	3.08

(11) Using Standard U-bit with 2x side-water holes each 1/4" diameter branching from central hole 3/4" diameter.

Water Pressure lb/sq.in.			Pressure drop lb/sq.in.	Rate of Flow galls/min.
Gauge 1	Gauge 2	Gauge 3	Gauge 2 - Gauge 3	
87	24.0	20.0	4.0	1.33
"	13.5	15.0	4.5	1.29
"	14.0	11.5	2.5	0.97
"	30.0	25.5	4.5	1.42
"	34.3	29.7	5.1	1.61
"	41.5	35.0	6.5	1.63
"	43.3	41.0	7.3	1.99
"	54.0	45.5	3.5	1.92
"	64.0	53.0	11.0	2.26
"	64.0	53.0	11.0	2.24
86	63.0	50.0	13.0	2.74
87	51.0	41.0	10.0	2.12
"	36.0	30.0	6.0	1.70
"	24.0	21.5	2.5	1.32
"	18.0	16.0	2.0	1.22
"	11.0	10.0	1.0	1.12
"	18.5	16.5	2.0	1.16

Cont'd

Water Pressure lb/sq.in.			Pressure drop lb/sq.in.	Rate of Flow galls/min.
Gauge 1	Gauge 2	Gauge 3	Gauge 2-Gauge 3	
Cont'd				
37	23.0	20.5	2.5	1.33
"	29.0	25.3	3.7	1.50
"	33.3	33.0	3.3	1.52
"	45.0	33.0	7.0	2.00
"	50.0	41.0	9.0	1.93
"	64.0	52.5	11.5	2.24
"	54.0	45.0	9.0	2.20
"	6.0	5.5	0.5	0.73
"	10.0	9.0	1.0	0.93
"	17.5	15.5	2.0	1.03
"	20.0	13.0	2.0	1.30
"	26.0	23.0	3.0	1.72
"	28.8	25.0	3.3	1.54
"	35.5	31.0	4.5	1.76
"	42.2	36.2	6.0	1.92
"	51.0	43.0	8.0	2.03
"	56.0	46.5	9.5	2.13
"	62.0	51.0	11.0	2.43

By plotting, Resistance of bore of 3/4" drill rod 3'6" long.

= 1.30 units.

= 0.37 units/foot length.

5. TESTS TO DETERMINE WATER FLOW RESISTANCE OF U-BIT WITH 2 SIDE WATER HOLES EACH 1/2" DIAMETER BRANCHING FROM CENTRAL HOLE ALSO 1/2" DIAMETER.

Gauge 1 - on tank

Gauge 2 - measures water pressure at exit from wet attachment (i.e. drive end of drill rod).

Drill Rod - 1" diameter round (as tested).

Water Pressure lb/sq. in.		Rate of Flow galls/min.
Gauge 1	Gauge 2	
87	21.0	2.96
"	11.5	2.44
"	15.0	2.60
"	5.0	1.90
"	2.0	1.40
"	18.5	2.84
"	22.5	2.84
"	16.5	2.64
"	12.0	2.20
"	8.0	1.84
"	2.5	1.56
"	28.5	3.24

With 3" enlargement

With no enlargement

By plotting Total Resistance of Rod and Bit

= 2.6 units (for both with and without enlargement)

Resistance of Rod = 1.90 units

∴ Resistance of Bit = 0.70 units

Similarly by plotting values of Gauge 2 against (Rate of Flow)² for results of Tests 4(ii) the water flow resistance of the Standard U-bit may be determined.

N.B. The water pressure on Gauge 2 is measured at a point where the bore Diameter is $\frac{1}{4}$ " . Since the bit has $\frac{1}{8}$ " diameter holes there is an increase in Velocity Pressure. (This is not so for the bit of Tests 5.) which must be considered.

e.g. Velocity pressure of jet at exit from bit ($\frac{1}{8}$ in dia.) for flow of 1 gallon/minute (0.1604 cu.ft/min.) i.e. $\frac{1}{4}$ gallon/minute through each hole:

$$\begin{aligned} \text{Velocity at exit from bit} &= \frac{0.1604}{2 \times 60} \div \left(\frac{\pi}{4} \left(\frac{1}{8} \right)^2 \frac{1}{144} \right) \text{ ft/sec.} \\ &= 15.7 \text{ ft/sec.} \end{aligned}$$

$$\text{Velocity Pressure} = \frac{15.7^2}{2g} \times 0.0434 = \underline{1.67 \text{ lb/sq.in.}}$$

Similarly Velocity pressure for 1 gallon/minute through $\frac{1}{4}$ " diameter hole (entry to wet attachment)
 $= 0.42 \text{ lb/sq.in.}$

Gain in Velocity pressure for 1 gallon/minute = 1.25 lb/sq.in.
 For x gallons: Gain in Velocity Pressure = $1.25x^2 \text{ lb/sq.in.}$

Water Pressure lb/sq.in. Gauge 2.	Rate of Flow galls/min.	Gain in Velocity Pressure lb/sq.in.	Drop in Total Pressure lb/sq.in.
24.0	1.33	2.21	21.79
13.5	1.29	2.06	16.42
14.0	0.97	1.18	12.82
30.0	1.42	2.52	27.43
34.3	1.61	3.24	31.56
41.5	1.68	3.53	37.97
etc.	etc.	etc.	etc.

By plotting Drop in Total Pressure against (Rate of Flow)²

Resistance of U-bit with $\frac{3}{8}$ " holes together
 with $\frac{7}{8}$ " diameter drill rod.
 $= 5.8 \text{ units}$

Resistance of Rod = 1.30 units

Resistance of Standard U-bit with $\frac{3}{8}$ " diameter holes
 $= \underline{\underline{7.5 \text{ units}}}$

Resistances (Units $\frac{\text{lb}}{\text{in}^2} \left(\frac{\text{min}}{\text{gall}}\right)^2$)

Standard wet attachment :- 2.95

Modified " " :- 1.20

$\frac{7}{8}$ " drill rod :- 0.37 units/foot *

1" " " :- 0.54 " / foot *

Standard bit with $\frac{3}{8}$ " dia. water holes:- 7.50 units

Screw bit with $\frac{1}{2}$ " dia. water holes :- 0.70 units

* Discrepancy between values is due to non-circularity of water bores.

Note on Chezy Formula for Pipe Flow.

Modified Chezy Formula for pipe running full

$$h_f = \frac{4 f l v^2}{2gd}$$

where f = experimentally determined constant

l = length of pipe in feet

v = velocity of water in ft/sec.

g = acceleration due to gravity (ft/sec²)

d = diameter of pipe bore (in feet)

h_f = head lost in friction in feet of water

or

$$h_f = \frac{4 f l Q^2}{d^5 2g}$$

where Q = quantity of water in cu.ft/sec.

This reduces to

$$p = \frac{f l Q^2}{166 d^5}$$

where p = pressure loss in lb/sq.in.

l = length of pipe in feet

Q = quantity of water in galls/min.

d = diameter of pipe in inches

f = experimentally determined constant.

By comparison with $p = R Q^2$

$$\underline{\underline{R \propto \frac{1}{d^5}}}$$

Thus increase of bore diameter from $\frac{1''}{4}$ to $\frac{5''}{16}$

will reduce resistance $\left(\frac{5^5}{4}\right) = 3.07$ times.

Thus $\frac{7''}{8}$ drill rod $\frac{5''}{16}$ bore will have

$$\underline{\underline{\text{resistance}}} \quad 0.37 \times \frac{1}{3.07} = \underline{\underline{0.12 \text{ units/foot length}}}$$

ROCKS USED IN PLANING TESTS.

- ROCK 1. Soft White Limestone. A heterogeneous
oolitic limestone, weakly bonded. Non-abrasive.
- ROCK 2. Hard White Limestone. Similar to Rock 1
but more strongly bonded; contain occasional
large shell inclusions. Non-abrasive.
- ROCK 3. Soft Green Ironstone. Fine grained
weak rock with shell inclusions. Non-abrasive.
- ROCK 4. Durham Post. Fine grained, Micaceous,
Bedded Sandstone. Moderately abrasive.
4 i :- cut taken perpendicular to the bedding
4 ii :- cut " parallel with the bedding
- ROCK 5. Darley Dale Sandstone. Medium grained,
homogeneous, abrasive sandstone, moderate hardness.
- ROCK 6. "Gritstone" (Quartz Conglomerate). Very
heterogeneous rock containing large quartz crystals.
Very abrasive.
- ROCK 7. "Syenite". Very hard, heterogeneous rock
with free feldspar.

LIST OF REFERENCES.

1. E.W. INETT

High Speed Drifting in the Ruhr Coalfield
with Special Reference to Drilling Techniques.

Trans. I. Min. Engrs. Vol. 114
Jan. 1953.

2. H.S. ALPAN

The Speed of Penetration of Bit in Electric
Rotary Drilling.

Trans. I. Min. Engrs. Vol. 109
Sep. 1950.

3. R. SHEPHERD

Thesis (Sheffield University)

4. R. BERGRAD AND H. SIEVERS

Die Bestimmung Des Bohrwiderstandes
Von Gesteinen Gluckauf 37/38

Sep. 10th, 1950.

5. BESICK & KUHNE

Oil und Kohle

Sep. 1941 (Exact
reference missing)

6. REIBINDER (Original in Russian)

On the use of Hardness Reducers in Drilling.

Transn. of Melbourne Academy of
Science (Obtainable from Science
Museum, Kensington).

7. R. SHEPHERD

Improving the Efficiency of Rotary Drilling
of Shotholes.

Trans. I. Min. Engrs. Vol. 113
Aug. 1954

9. COEUILLET

Les Outils D'Abatage En Havage Et Foration

Revue De L'Industrie Minerale

Jan. 1954.

10. SHULTZ

Possibilities & Limitations of Rotary Drilling
in Carboniferous Strata.

N.C.B. Information Bulletin.

11. METAL CUTTING SYMPOSIUM, 1913. (Manchester)

Published by Institute of Metals.

12. M.E. MERCHANT

Basic Mechanics of Metal Cutting Process.

J. App. Mechanics.

Amer. Soc. Mech. Engrs. 1944. Vol. 66, p.A. 144.

LIST OF REFERENCES, Cont'd

13. PHILLIPS
Tectonics of Mining.
Sheffield University Mining Magazine
1949.
14. SHAW COOK AND FINNIE
Shear Angle Relationship in Metal Cutting.
15. FAIRHURST
Design of Rotary Drill Bits.
Mine & Quarry Engineering, Vol. 20.
June, 1954.
16. STABLER
Fundamental Geometry of Cutting Tools.
Proc. Instn. of Mech. Engrs.
(War Emergency Issues) Vol. 165
P. 14
17. SHAW, COOK AND SMITH
Mechanics of Three Dimensional Cutting
Operations.
Trans. A.S.M.E. Aug. 1952
P.1055-1064.
18. ELECTRICAL RESISTANCE STAIN GAUGES - DOBIE & ISAAC
(Textbook)
19. FAIRHURST, PROCTOR
Some Basic Principles of Rock Drilling.
Sheffield University Mining Magazine
1954. P.41.